The Pennsylvania State University

The Graduate School

College of Engineering

THE ROLE OF VASCULAR SMOOTH MUSCLE CELLS AND ADVENTITIAL FIBROBLASTS IN FLOW-MEDIATED MECHANISMS OF INTIMAL HYPERPLASIA AND ARTERIALIZATION

A Thesis in

Bioengineering

by

Jeffrey Stock Garanich

Submitted in Partial Fulfillment
of the Requirements
for the Degree of

Doctor of Philosophy

May 2006

The thesis of Jeffrey Stock Garanich was reviewed and approved* by the following:

Peter J. Butler
Assistant Professor of Bioengineering
Thesis Advisor
Co-Chair of Committee

John M. Tarbell
Distinguished Professor of Biomedical Engineering
City College of New York/CUNY
Special Member
Co-Chair of Committee

Herbert H. Lipowsky
Professor of Bioengineering
Head of the Department of Bioengineering

David A. Antonetti
Associate Professor of Cellular and Molecular Physiology

Michael J. Eppihimer
Associate Professor of Bioengineering

*Signatures are on file in the Graduate School

ABSTRACT

Vascular smooth muscle cells (SMCs) reside in the medial layer of blood vessels and under physiological conditions, maintain a quiescent phenotype through which they carry out their primary function: regulation of the systemic blood pressure via control of vessel dilation and contraction. In regions of vascular injury, such as at the site of vessel repair by angioplasty and at the anastomoses of a vascular graft with the native artery, SMCs transform to a proliferative phenotype, resulting in abnormal proliferation in the media and subsequent migration to the intima. The contribution of hemodynamics to the regulation of this intimal hyperplasia (IH; accumulation of cells and matrix in the intimal layer) has received considerable attention. The conventional view of mechanical forces on SMCs is that due to the presence of the endothelium, SMCs are shielded from direct blood flow and its subsequent shear stress (SS) and are primarily exposed to circumferential stress and strain associated with the pulsatility of blood flow. However, recent modeling studies have shown that medial SMCs in an intact vessel are subjected to physiologically relevant shear stresses through their exposure to transmural interstitial flow driven by the transmural pressure gradient (arterial pressure – tissue pressure) that are near the order of magnitude of those experienced by the endothelium due to luminal blood flow. In fact, due to the funneling of transmural flow through the pores of the internal elastic lamina (IEL), the most superficial layer of SMCs is exposed to SS much greater in magnitude than the underlying layers. This, accompanied by the fact that SMCs are directly subjected to blood flow SS in cases of vascular injury (endothelial

denudation and IEL damage), necessitates an understanding of the role of SS in the control of SMC migration and proliferation.

There is considerable *in vivo* evidence suggesting that IH progression is attenuated in regions of elevated blood flow and, conversely, that IH is enhanced in low flow areas. *In vitro* studies have supported this notion by reporting inhibition of SMC proliferation in response to SS, but similar studies to evaluate the role of SS on SMC migration have yet to be conducted. We therefore seeded rat aortic SMCs on porous cell culture inserts coated with Matrigel (a representative basement membrane matrix) and quantified their migratory activity toward platelet-derived growth factor (PDGF)-BB when exposed to 1, 10, or 20 dyn/cm^2 SS for 1-4 h with a rotating disk apparatus.

Four h of either 10 or 20 dyn/cm^2 SS significantly inhibited SMC migration through the Matrigel layer to the underside of the insert. This inhibition was associated with downregulation of SMC matrix metalloproteinase (MMP)-2 activation in response to SS. Four h of 10 dyn/cm^2 markedly increased the SMC production of nitric oxide (NO). Addition of a NO synthase inhibitor (N^G-nitro-L-arginine methyl ester; 100 μM) to cells abolished the shear-mediated increase in NO production as well as the inhibition of SMC migration and MMP-2 activity. Through the use of a NO donor (S-nitroso-N-acetylpenicillamine; 500 μM), it was shown that NO acts to suppress SMC migration via the reduction of both total (proenzyme + active) and active MMP-2 levels. Addition of 50 ng/ml exogenous active MMP-2 to inserts significantly elevated SMC migration levels whereas addition of 10 μM MMP-2 Inhibitor I to inserts significantly reduced SMC migration levels, lending further support to the role of MMP-2 in SMC migration.

Western blots showed no effect of 4 h of 20 dyn/cm^2 SS on SMC production of PDGF-AA, another chemical known to suppress SMC migration. Thus, it appears that SS inhibits SMC migration by upregulating the cellular production of NO which subsequently downregulates MMP-2 activity.

Vascular fibroblasts (FBs) are primarily contained in the outer adventitial layer of blood vessels, which has historically been considered a supporting tissue. Recent *in vivo* work, however, suggests that, along with SMCs, FBs also contribute to intimal lesion formation and that this involvement is at least in part mediated by their acquisition of the smooth muscle (SM)-specific phenotypic marker, SM α-actin, and differentiation to smooth muscle-like cells, the myofibroblasts (myoFBs). FBs are sparsely populated in the adventitia and come into closer contact with other FBs and medial SMCs as they migrate to the intima following injury. We hypothesize that the proximity of FBs to neighboring cells plays a role in modulating their conversion to myoFBs through the expression of SM α-actin. As described above for SMCs, FBs are exposed to transmural interstitial flow (SS) driven by the transmural pressure gradient.

Other studies conducted on the microcirculatory level have shown that interstitial FBs are involved in the arterialization of capillaries that connect two high pressure arteriolar trees, allowing for improved regulation of local blood flow to tissues during processes such as exercise hypertrophy and wound healing. The expression of SM α-actin by interstitial FBs as they approach the arterializing vessel and come into closer contact with neighboring cells suggests that the degree of confluence of FBs may affect their expression of SM-specific phenotypic markers. The recruitment of FBs to

arterializing vessels has been suggested to be regulated in part by local hemodynamic conditions, namely elevated circumferential stresses in the arterializing vessel due to elevated luminal pressure compared to surrounding capillaries. We suggest that the elevated luminal pressure in the arterializing vessel drives enhanced interstitial flow that subjects nearby FBs to enhanced levels of fluid SS, and that this force directly recruits these cells to the vicinity of the vessel.

The involvement of FBs and myoFBs in physiologic and pathologic processes on both the macrocirculatory and microcirculatory levels accompanied by the lack of existing studies of the effects of mechanical and chemical stimulation on their function motivated the present study. Rat adventitial FBs were isolated and maintained at either subconfluent (30-50% confluence in culture) or confluent (100% confluence in culture) culture conditions. Both cell populations were analyzed for their expression of two SM-specific phenotype markers: SM α-actin and SM myosin heavy chain (MHC), a marker of mature, fully differentiated SMCs. Cells maintained at subconfluent culture conditions expressed a modest amount of SM α-actin and virtually no SM-MHC whereas confluent cells expressed a large amount of SM α-actin and modest SM-MHC. Based on these results, subconfluent cells were labeled “fibroblasts” and confluent cells were termed “myofibroblasts” according to literature convention. Each cell population was seeded on Matrigel-coated porous cell culture inserts in the presence of PDGF-BB and exposed to 4 h of 20 dyn/cm^2 SS in experiments similar to those conducted using SMCs above. The contractile responses of serum-starved FBs and myoFBs to an interstitial fluid solute (serum) were also determined. In stark contrast to the SMC migratory response to SS and

contractile response to serum, FBs enhanced their migration upon exposure to shear and did not contract when re-exposed to serum. MyoFBs, on the other hand, displayed SM-like responses by inhibiting their migratory activity when exposed to SS and significantly contracting within 2 min of re-exposure to serum. These data suggest that modulation of FB phenotype appears to be one way to regulate their involvement in both physiologic and pathologic processes.

TABLE OF CONTENTS

LIST OF FIGURES

LIST OF TABLES

ACKNOWLEDGEMENTS

I would like to extend the utmost thanks and gratitude to my research mentor, Dr. John M. Tarbell, for his extraordinary amount of academic guidance and support throughout my graduate study. He has provided me with the means to grow significantly on both professional and personal levels and for that, I am grateful. I would like to thank the members of my Ph.D. committee: Dr. David A. Antonetti, Dr. Peter J. Butler, Dr. Michael J. Eppihimer, and Dr. Herbert H. Lipowsky for their technical expertise as well as their patience and understanding during what has been a unique graduate research experience.

I would also like recognize my lab mates at both Penn State and the City College of New York for their friendship and support: Kristy Ainslie, Danielle Berardi, Limary Cancel, Mete Civelek, Michael Dancu, Lucas DeMaio, Andrew Fitting, Dr. Mechteld Hillsley, Jason Kosky, Sunitha Lakshminarayanan, Veronica Lopez, Manolis Pahakis, Zhengyu Pang, and Zhong-Dong Shi. I thoroughly enjoyed the time we spent together and hope that we have all formed friendships that will continue beyond our graduate study. I would like to acknowledge Mete Civelek for teaching me all cell culture techniques and experimental protocols required for my research when I began my graduate study. I would like to thank Mike Dancu for countless technical discussions that led to significant progress in my research. Over the course of my Ph.D. study, I have had the opportunity to work with some extremely talented undergraduate researchers: Jeffry Florian, Rishi Mathura, and Blair Urish. They were each a pleasure to work with and I would like to wish them the best in the future. Rishi Mathura contributed his original

artwork to several figures included in this thesis. I would like to acknowledge the faculty, staff, and students in the Department of Biomedical Engineering at City College for their friendship and support following our lab's move there.

On a personal level, I would like to extend unending thanks and gratitude to my parents, Ronald and Genevieve Garanich, for their unconditional love, support, and guidance, not only throughout my graduate study, but throughout my entire life. Along with them, I would like to dedicate this thesis to my grandparents, Michael and Anna Garanich and Walter and Helen Stock, who instilled in me the belief in higher education and the values of hard work and perseverance necessary to achieve my goals in life.

Chapter 1

INTRODUCTION AND BACKGROUND

1.1 General blood vessel structure

Arteries, arterioles, capillaries, venules, and veins form a closed system of blood vessels that transport blood from the heart to the tissues of the body and back to the heart. Arteries, which carry blood from the heart to the tissues, are comprised of three layers that surround the hollow lumen through which blood flows (Fig. 1-1) (135). The innermost layer, the tunica intima, is composed of a monolayer of endothelial cells (ECs) that come in to direct contact with the flowing blood, an underlying basement membrane, and a porous, elastic layer - the internal elastic lamina (IEL). The middle layer, the tunica media, contains arrays of elongated smooth muscle cells (SMCs) embedded in an extracellular matrix composed of collagen and glycosaminoglycans. SMCs are oriented with their long axis directed circumferentially around the vessel (19) and due to their contractile nature are primarily responsible for the arterial regulation of blood flow and pressure. The external elastic lamina (EEL) separates the tunica media from the outermost layer, the tunica adventitia, which contains fibroblasts (FBs) as well as collagenous and elastic fibers.

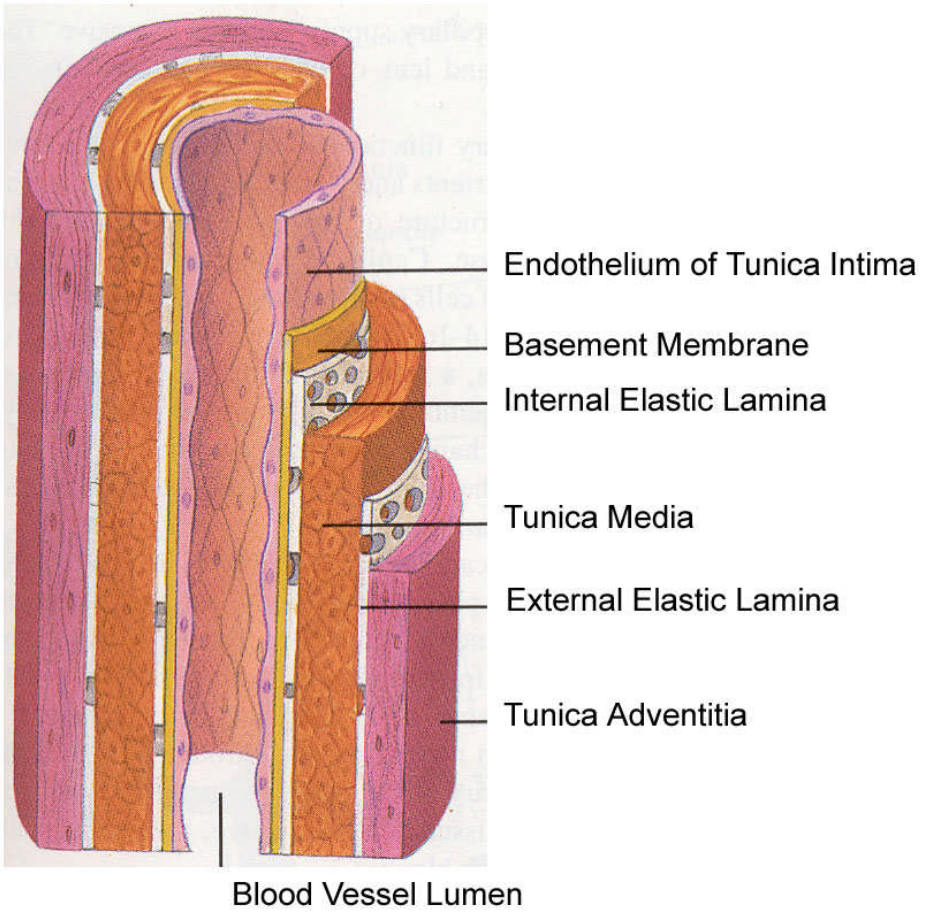

Figure 1-1: Structure of an arterial wall. The arterial wall is composed of three layers: the tunica intima, tunica media, and tunica adventitia. The tunica intima contains the endothelium, a monolayer of endothelial cells that come into direct contact with the flowing blood, a basement membrane, and the porous internal elastic lamina. The tunica media is comprised of smooth muscle cells which are embedded in an extracellular matrix of collagen and glycosaminoglycans and are oriented with their long axis directed longitudinally around the vessel. The external elastic lamina separates the tunica media from the tunica adventitia, which contains fibroblasts and elastic and collagenous fibers. Figure modified from (135).

As arteries become smaller, they divide into arterioles, which are classified as very small arteries that deliver blood to the capillaries (135). Arterioles that branch from arteries contain all three layers discussed above, but as they approach the capillaries are

comprised of only an EC layer surrounded by a sparse layer of SMCs. These SMCs are also contractile in nature and play a major role in the arteriolar control of blood flow. Arterioles connect to capillaries whose primary function is regulation of exchange of nutrients and waste between blood cells and the surrounding tissue. Capillary walls are comprised of a single EC layer about 1 μm thick (32) and do not contain a tunica media or tunica adventitia. As blood flows through the capillaries, it is collected in the venules. The venules nearest the capillaries contain an endothelium and a tunica adventitia. As they approach the veins, venules also contain a tunica media. Blood returns to the heart through the veins, which are comprised of a tunica intima (thinner than the arterial intima), a tunica media (thinner than the arterial media), and a tunica adventitia (thicker than the arterial adventitia).

The work presented in this thesis focuses on the role of mechanical and chemical stimulation on the involvement of SMCs and FBs in physiologic and pathologic processes on both the macrocirculatory (intimal hyperplasia (IH)) and microcirculatory (capillary arterialization) levels.

1.2 Smooth muscle cell exposure to mechanical forces

The conventional view of vascular cell exposure to mechanical forces has been that the endothelium is subjected to the direct fluid shearing forces of blood flow as well as the solid mechanical circumferential stress and strain (stretch) associated with the pulsatile nature of blood flow while the underlying medial SMCs and adventitial FBs are exposed primarily to circumferential stress and strain (84, 133). However, at the location

of surgical intervention, such as the anastomoses of a vascular graft with the native artery or the region of a vessel repaired by balloon angioplasty (55, 70, 104), the endothelium is injured (denuded) and the IEL is torn. Fibrin deposition and platelet adhesion may occur within minutes following vessel injury. However, anti-coagulation (i.e. heparin and coumadin) and anti-platelet (i.e. aspirin and plavix) agents are commonly administered clinically following vascular procedures to prevent fibrin deposition and platelet adhesion, respectively. In this case, the underlying, most superficial, layer of SMCs is exposed directly to blood flow shear stress (SS; Fig. 1-2). Animal models of atherosclerosis and intimal hyperplasia (IH) have shown that luminal SMCs are present for days to months after injury (20, 34).

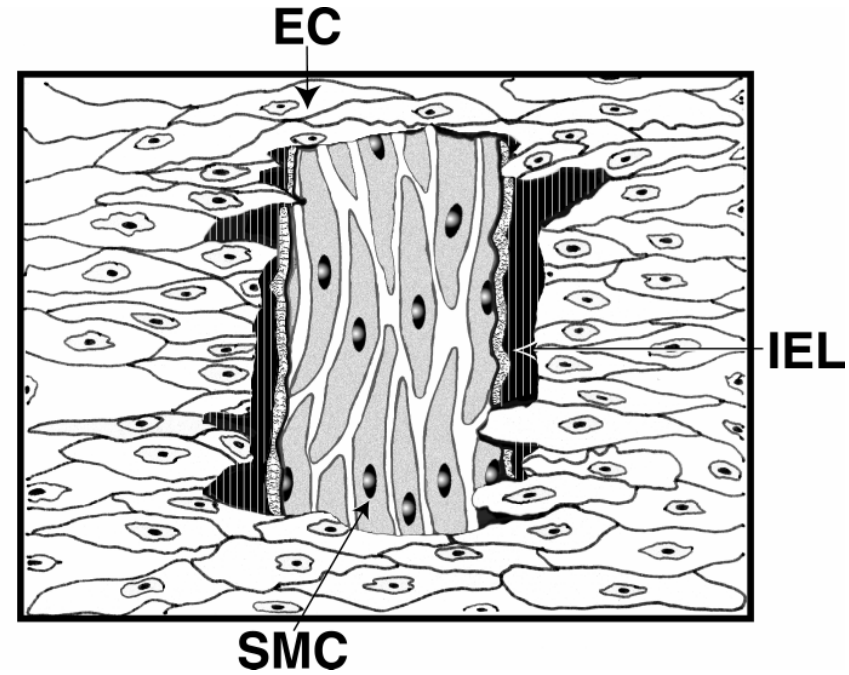

Figure 1-2: Smooth muscle cell exposure to blood flow shear stress in an injured vessel. In cases of vascular injury when endothelial cells (ECs) are denuded and the internal elastic lamina (IEL) is torn, SMCs are directly subjected to the shearing forces of blood flow. The magnitude of this shear stress can be assumed to be on the same order that the endothelium is exposed to in a healthy vessel (10 dyn/cm^2) (68).

Superficial SMCs exposed to blood flow as a result of vascular injury are assumed to be subjected to SS levels of the same order of magnitude as those experienced by ECs in an intact vessel. Lipowsky (68) estimated the mean (time average) wall SS (τ_w) in straight vessel sections using Eq. 1-1 along with measured values of the blood volumetric flow rate (Q), inner vessel radius (a), pressure drop (ΔP) over vessel length (L), and estimates for blood viscosity (μ) in different regions of the circulation. Using this technique, the mean τ_w in larger arteries and veins was estimated to be approximately 10 dyn/cm^2.

$$\tau_w = \frac{4\mu Q}{\pi a^3} = \frac{\Delta P a}{2L} \qquad \text{(Eq. 1-1)}$$

1.2.1 Smooth muscle cell exposure to interstitial flow shear stress

Although they are shielded from direct blood flow by the endothelium in an intact vessel, SMCs are still exposed to fluid SS via transmural interstitial flow driven by the transmural pressure differential (arterial pressure – tissue pressure; Fig. 1-3). While the magnitude of the superficial velocity of this flow (transmural flow rate divided by vessel surface area) is very small (on the order of 10^{-5} to 10^{-6} cm/s; approximately 4 to 8 orders of magnitude lower than average velocities throughout the circulation), the interstitial spaces in the extracellular matrix are also very small (on the order of nanometers) and the SS on SMCs can be significant.

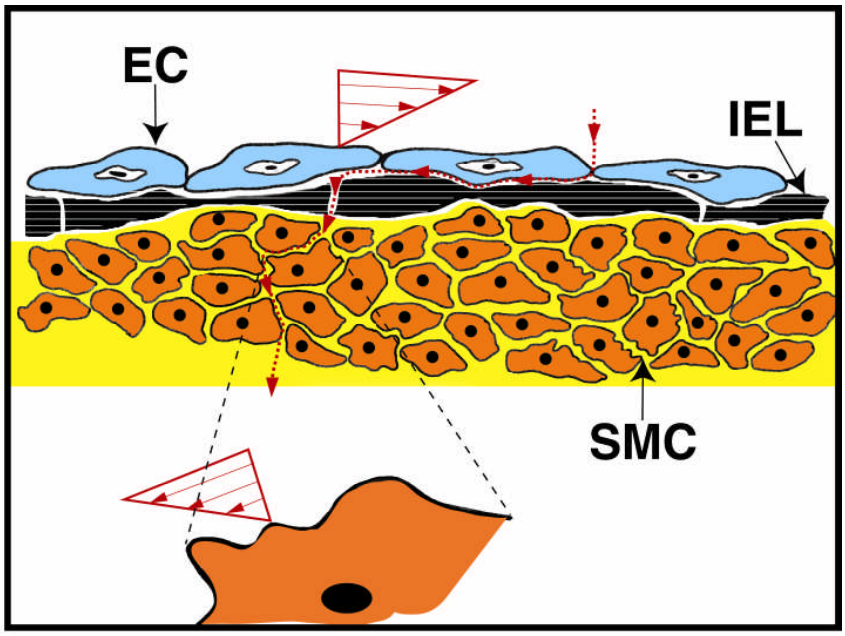

Figure 1-3: Smooth muscle cell exposure to interstitial flow shear stress in an intact vessel. In a healthy vessel, medial SMCs are subjected to fluid SS through their exposure to transmural interstitial flow driven by the transmural pressure differential (arterial pressure – tissue pressure). Computational studies have shown that, due to the funneling of flow through the pores of the internal elastic lamina (IEL), the most superficial layer of SMCs is exposed to SS levels many times higher (132) than those experienced by underlying layers (order of 1 dyn/cm^2) (140).

Tarbell et al. provide a detailed description of the theoretical analysis used to quantify the magnitude of the interstitial SS on SMCs. (133). A summary is included here. A SMC with a fixed boundary that is impermeable to water flow and satisfies a no slip boundary condition is embedded in an interstitial matrix of protein and glycoprotein fibers characterized by a Darcy permeability coefficient, K_p. The superficial velocity of transmural flow, which far away from the cell surface is U^{∞}, satisfies the Debye-Brinkman modification of Darcy's Law (Eq. 1-2) (13).

$$\frac{dP}{dx} = -\frac{\mu U}{K_p} + \mu \frac{d^2 U}{dy^2} \qquad \text{(Eq. 1-2)}$$

Note that this modification of Darcy's Law is required to satisfy the no slip boundary condition at the cell surface. In Eq. 1-2, dP/dx is the pressure gradient in the direction of flow, μ is the interstitial fluid viscosity, U is the interstitial flow superficial velocity, and y is the perpendicular distance from the cell surface. The velocity profile that results from solving Eq. 1-2 subject to the boundary conditions U = 0 at y = 0 and U = U^{∞} at y = ∞ is given in Eq. 1-3.

$$U = U^{\infty}[1 - \exp(\frac{-y}{\sqrt{K_p}})] \qquad \text{(Eq. 1-3)}$$

The expression that results from substituting Eq. 1-3 into Newton's equation for wall SS (Eq. 1-4) is given in Eq. 1-5.

$$\tau_w = \mu \frac{dU}{dy}\Big|_{y=0} \qquad \text{(Eq. 1-4)}$$

$$\tau_w = \mu \frac{U^{\infty}}{\sqrt{K_p}} \qquad \text{(Eq. 1-5)}$$

Wang and Tarbell (140) extended this analysis of flow over a flat surface to account for the distribution of SMCs in the interstitial matrix. By modeling medial SMCs as an array of cylinders embedded in a uniform matrix and taking the volume fraction of cells in the matrix into account, they estimated interstitial SS on SMCs to be approximately 1 dyn/cm^2, which is near the order of SS levels experienced by the endothelium as a result of direct blood flow.

In arteries and arterioles, the layer of SMCs bordering the subendothelial intima is affected by the presence of the porous IEL. Modeling studies have suggested that, because the extracellular matrix contained in the fenestral pores of the IEL is much less dense than the elastin fibers comprising the IEL, transmural flow is funneled through the pores as it enters the media (47, 148). Tada and Tarbell (130-132) expanded on the model described above and showed that, due to this entrance condition, the first layer of SMCs is exposed to shear stresses approximately 30 times greater than those experienced by the underlying layers. These results suggest that the most superficial layer of medial SMCs is subjected to SS comparable or greater in magnitude than that imposed on ECs by luminal blood flow and highlight the importance for furthering our understanding of the role of fluid SS on SMC function in both physiological and pathological conditions.

1.3 The role of fluid shear stress in the regulation of intimal hyperplasia (*in vivo* studies)

The progression of vascular pathologies such as IH (the accumulation of cells and extracellular matrix in the tunica intima) has been attributed to, among other things, hemodynamic conditions at the diseased site. In particular, an inverse relationship between the magnitude of blood flow SS in an area and the amount of intimal lesion development in that region has been well established in vessels subjected to altered flow conditions (9, 34, 55, 56, 60, 72, 78, 114, 120, 143, 155). The effect of SS on intimal thickening is discussed in greater detail below for 3 experimental conditions: (1) native vessels or implanted vascular grafts in which the endothelium is intact, (2) vessels that

have been denuded of their endothelium by balloon catheter injury, and (3) vessels that have been fitted with a collar to inhibit transmural flow.

1.3.1 The effect of fluid shear stress on intimal hyperplasia in endothelialized vessels

A commonly used experimental model used to study the effect of blood flow on intimal lesion development has been the implantation of polytetrafluoroethylene grafts in the baboon arterial circulation (9, 34, 56, 72). Through the creation of arterio-venous fistulas, it is possible to subject both grafts (9, 34, 56, 72) and native vessels (78, 114, 155) to altered hemodynamics. In each case, elevated flow (SS) attenuated IH whereas reduced flow (SS) enhanced intimal thickening progression. Changes in intimal area were attributed to variations in SMC proliferation and/or migration in response to alterations in flow.

One explanation for this flow-mediated inhibition of IH is that ECs responded directly to changes in blood flow (SS) and communicated an anti-migratory and/or anti-proliferative signal to underlying SMCs. However, *in vivo* (62) and *in vitro* (14, 116) studies have both reported elevated EC hydraulic conductivity (L_p) in response to shear exposure. It is, therefore, also possible that enhanced luminal SS led to increased transmural flow SS on underlying SMCs (via modulation of endothelial L_p), which directly inhibited their proliferative and/or migratory activity.

1.3.2 The effect of fluid shear stress on intimal hyperplasia in balloon-injured vessels

In cases of balloon catheter injury, the endothelium is denuded and the underlying SMCs come into contact with the flowing blood and its associated SS (see section 1.2). Intimal thickening is also attenuated upon vessel exposure to elevated flow conditions in this injury model, suggesting that SMCs respond directly to changes in flow (55, 120, 143). Kohler and Jawien (55) did not observe a significant change in SMC proliferation rates upon exposure to elevated flow and concluded that the inhibition of IH development was due to reduced SMC migratory activity in response to heightened SS levels. Ward et al. (143) reported elevated SMC migration in injured vessels subjected to low flow conditions compared to those exposed to high flow.

1.3.3 The effect of reductions in interstitial flow on intimal hyperplasia

Intimal thickening has been accelerated in rabbit carotid arteries following the placement of a silicone collar around the vessel (26). More intimal thickening was observed in vessels whose collar was completely sealed at the ends than those in which the collar was left open with loose endings. The authors hypothesized that the closed collar reduced interstitial flow through the artery, preventing the removal of toxic cytokines and leading to IH progression. In another study, collar-induced intimal thickening was reduced by exposure to elevated flow conditions and this response was abolished through the use of a nitric oxide (NO) inhibitor (71). The role of NO on the shear-induced inhibition of SMC migration and proliferation will be discussed in greater

detail in subsequent sections. Another interpretation of collar-induced intimal thickening is that reduced SS on SMCs due to lower interstitial flow led to enhanced SMC migration and/or proliferation.

1.4 Effects of fluid shear stress on smooth muscle cell proliferation and migration (*in vitro* studies)

As discussed above, intimal lesion progression is attenuated in regions of elevated flow in animal models both in the presence and absence of an intact endothelium. Since SMC proliferation and migration are two hallmarks of IH, it seems plausible that increased flow (SS) might inhibit these processes. Sterpetti et al. (122, 125, 126) observed that the proliferation rate of bovine aortic SMCs was significantly reduced upon exposure to 24 h of 3, 6, or 9 dyn/cm^2 SS and that the level of inhibition was proportional to the shear magnitude. Cell alignment in the direction of flow and the reorganization of actin, tubulin, and other cytoskeletal microfilaments were also reported (122). Others have observed a decrease in the proliferation rate of human aortic SMCs in response to 24 h of 5 or 25 dyn/cm^2 SS, but no effect of shear on cell orientation was reported in this work (85). Increases in tissue-type plasminogen activator (tPA) and TGF-β1 mRNA and protein levels coincided with decreases in human aortic SMC proliferation in response to 24 h of 14 or 28 dyn/cm^2 SS (138). tPA converts plasminogen to plasmin which is an activator of TGF-β1. TGF-β1 is known to suppress SMC proliferation (38, 44, 99, 100), suggesting a mechanism in which SMCs produce tPA and TGF-β1 in response to shear, which subsequently suppress their proliferation in an autocrine manner.

Enhanced production of NO in both human (87) and rat (37) aortic SMCs as well as increased production of prostaglandins E_2 and I_2 (PGI_2) (3) upon exposure to SS have been observed. Papadaki et al. (86) reported transient increases in protease activated receptor (PAR)-1 expression and decreases in tPA expression in both human and rat aortic SMC in response to low SS (5 dyn/cm^2) while the opposite trends in expression of both biochemicals were observed upon exposure to high SS (25 dyn/cm^2). While SMC proliferation rates were not quantified in these experiments, NO (16, 41, 75), PGI_2 (80), and tPA (through the activation of TGF-β1) (38, 44, 99, 100) have each been shown to inhibit SMC proliferation. Therefore, these studies suggest additional potential autocrine mechanisms through which SMCs can modulate their proliferation rate.

The direct effect of SS on SMC migratory activity has not been as well studied. In one investigation, the effect of SS on human aortic SMC spreading activity, which takes into account both proliferation and migration, was quantified (113). In the only *in vitro* study, to our knowledge, that examined the effect of SS exclusively on SMC migration (83), bovine aortic SMCs were subjected to SS in culture. Cells were then trypsinized and incorporated into a variation of the Boyden chamber assay to quantify their migratory activity. Three h of 12 dyn/cm^2 SS did not affect SMC migration levels whereas 15 h of 12 dyn/cm^2 SS significantly inhibited SMC migration. Although this study provided valuable initial insight into the role of SS on SMC migration, the cells were not sheared directly while migrating and were subjected to harsh, nonphysiological treatment (trypsinization) during the experiment. Therefore, it is important to conduct quantifiable experiments in which SMCs are subjected to SS directly while migrating through a representative extracellular matrix.

1.5 Biomolecules important in smooth muscle cell migration

Numerous biomolecules have been proposed to play a role in the regulation of SMC migration and proliferation. The work presented in this thesis focused on the effects of SS on the SMC production of 3 in particular: matrix metalloproteinase (MMP)-2, NO, and platelet-derived growth factor (PDGF)-AA. Also, PDGF-BB served as a chemoattractant in migration experiments presented here. Existing knowledge of involvement of each of these biomolecules in the regulation of SMC migratory activity is discussed below.

1.5.1 Matrix metalloproteinase-2

The MMPs, a family of endopeptidases with the ability to degrade extracellular matrix molecules (31), are generally considered to play a key role in cell migration. MMPs are divided into the following subgroups based on their structure and substrate specificity: collagenases, gelatinases, membrane-type (MT)-MMPs, stromelysins, stromelysin-like MMPs, and other MMPs (98). The importance of MMPs in SMC migration has been highlighted through the use of general MMP inhibitors that attenuated SMC migratory activity in balloon-injured rat carotid arteries (7, 8, 152), baboon aortic medial explants (51, 54), and an *in vitro* model of SMC migration through a reconstituted basement membrane preparation (Matrigel) (152).

The gelatinases, MMP-2 (72-kD type IV collagenase (gelatinase); gelatinase A) and MMP-9 (92-kDa type IV collagenase (gelatinase); gelatinase B) in particular play a key role in SMC intimal migration due to their ability to degrade the basement membrane

(primary components: type IV collagen, laminin, and heparan sulfate proteoglycans) that surrounds medial SMCs (53, 144, 151). MMP-2 activity was required for rat aortic SMC migration through Matrigel in *in vitro* experiments similar to those conducted in this thesis (90) and PDGF-BB-stimulated SMC migration was dependent on MMP-2 (53). Inhibition of MMP-2 production and activity reduced rat aortic SMC migration levels in a Boyden chamber assay (97). Therefore, the work presented here will focus on the effects of SS on SMC production and activation of MMP-2.

1.5.1.1 Regulation of MMP-2 activity

MMP-2 is secreted in an inactive zymogen form (pro-MMP-2) and is activated through removal of its pro-domain via interaction with MT-MMPs on the cell surface (76, 106). MT-MMP-1 and, to a lesser extent, MT-MMP-3, converted MMP-2 to its active form (MW ~ 62 kDa) (115). MT-MMP-1 levels were elevated in both rat carotid arteries (50) and rabbit aortas (141) following balloon injury and these increases correlated with enhancement of MMP-2 activity in the developing neointima.

1.5.1.2 The role of hemodynamics on MMP-2 production and activation by smooth muscle cells

In the only other study we are aware of that investigated the effects of SS on SMC migration (see section 1.4), Palumbo et al. (83) concluded that the shear-mediated inhibition of bovine aortic SMC migration that they observed was due to reductions in MMP-2 levels. Significant inhibition of both pro- and active MMP-2 was reported in

response to 15 h of 12 dyn/cm^2 SS, but MMP-9 levels were unaffected. Reductions in mRNA and protein for MT-MMP were also observed. Others have also reported attenuation of MMP levels in response to SS (134). Both MMP-2 and MMP-9 levels were downregulated in porcine thoracic aortic organ samples in this study. Bassiouny et al. (6) observed drastic increases in MMP-2 mRNA in balloon-injured rabbit carotid arteries upon exposure to low flow conditions and elevations in MMP-2 mRNA following injury were lessened in vessels subjected to high flow conditions. Expression of TGF-β1, which has been shown to suppress MMP-2 and MMP-9 levels (22), was elevated in balloon-injured rabbit carotid arteries exposed to increased flow (SS) conditions (120). It seems plausible that the flow-induced regulation of MMP-2 reported by Bassiouny et al. (6) was mediated at least in part by TGF-β1. Kenagy and colleagues (52) reported modest increases in both pro-MMP-2 and active MMP-2 in implanted baboon grafts after exposure to elevated flow levels. Total MMP-2 and MMP-9 levels in porcine carotid arteries were upregulated when vessels were subjected to elevations in transmural pressure but were unaffected by changes in luminal SS (17). Stimulation of human aortic SMCs seeded in collagen constructs by cyclic strain resulted in increases in the production of pro-MMP-2 and its enzymatic conversion to the active form (108).

1.5.2 Nitric oxide

NO is a low molecular weight, free radical gas formed from its precursor L-arginine through the enzymatic action of a family of enzymes termed nitric oxide synthases (NOS), which is comprised of endothelial NOS (eNOS), inducible NOS

(iNOS), which is found in macrophages, hepatocytes, and SMCs, and neuronal NOS (nNOS). Because of its short half-life (order of seconds), NO acts primarily on cells neighboring the site where it is produced. Primary functions of NO in the vasculature include the regulation of regional blood flow through the stimulation of SMC relaxation (vasodilation), the inhibition of platelet adherence and aggregation, the inhibition of leukocyte adhesion and infiltration, and the prevention of the oxidative modification of low-density lipoprotein (24).

1.5.2.1 The role of hemodynamics on nitric oxide production by smooth muscle cells

SS has stimulated both NO (79, 87) and iNOS (37, 79) expression in SMCs. This, accompanied by reports that NO regulates SMC migration (35, 42, 102) and proliferation (4, 16, 41, 61, 75, 88, 101, 107), suggests a role for NO in the regulation of IH. Marano et al. (71) induced intimal thickening in rabbit carotid arteries via the placement of a nonconstrictive, soft silicone collar around the vessels. Increased flow significantly inhibited IH and this effect was reversed through the administration of a NOS inhibitor, N^G-nitro-L-arginine methyl ester (L-NAME). Others have linked NO production in a vessel to MMP activity in that vessel (136), suggesting a biomolecular mechanism for flow-mediated alterations in MMP levels (section 1.5.1.2). As discussed in section 1.3.1, it is plausible that elevations in luminal flow led to increased endothelial L_p, which resulted in enhanced interstitial flow (SS) on SMCs, directly stimulating their NO production and attenuating IH.

1.5.3 Platelet-derived growth factor

The platelet-derived growth factor family consists of 4 polypeptide chains: PDGF-A, -B, -C, and -D that form disulphide-bonded homodimers (PDGF-AA, -BB, -CC, and -DD) or a PDGF-AB heterodimer (29). Total PDGF levels vary significantly among species, ranging from approximately 1 ng/ml in rat serum to approximately 13 ng/ml in human serum (12). PDGF-BB comprises 15% of the total PDGF found in human serum whereas a vast majority of PDGF in rat serum is the BB isoform (12). PDGF was recognized as a chemoattractant for SMCs more than 20 years ago (39, 40) and acts by activating two structurally related protein tyrosine kinase receptors, PDGFR-α and PDGFR-β, on the target cell (45, 48). Because PDGF isoforms are dimers, the receptors are dimerized upon binding to two PDGF chains simultaneously (45). The $\alpha\alpha$ receptor binds to PDGF-AA, -AB, -BB, and –CC, the $\alpha\beta$ receptor binds to PDGF-AB and –BB, and the $\beta\beta$ receptor binds to PDGF-BB and –DD (82). PDGF-BB is widely accepted as a chemoattractant for SMCs (49, 51, 53, 57, 77, 128) whereas PDGF-AA has been shown to have very little, if any, chemoattractive activity for SMCs by itself (21, 53, 58), and actually inhibits SMC migration when used together with PDGF-BB, compared to PDGF-BB used alone (57). The chemotactic effects of the other PDGF isoforms are much less studied.

1.5.3.1 The role of hemodynamics on platelet-derived growth factor production by smooth muscle cells

Sterpetti et al. (123-125) demonstrated that SS modulates the production of a PDGF-like substance by bovine arterials SMCs. This increase in growth factor production appears to contradict the notion that shear stimulates anti-proliferative and potentially anti-migratory mechanisms in SMCs. However, in these studies, the authors did not specify which isoform of PDGF was upregulated by SS. They did observe that conditioned media from sheared SMCs elevated tritiated thymidine uptake by Swiss 3T3 fibroblasts, which have been shown to be chemoattracted by PDGF-AA (46). This data, accompanied by reports that SMCs primarily produce PDGF-AA (5) and that only 1.6% of SMCs cultured from normal medial tissue express PDGF-BB mRNA (67), suggests that the PDGF production observed by Sterpetti and colleagues was PDGF-AA, which as discussed above, does not act as a chemoattractant for SMCs (21, 53, 57, 58). Both elevated (137) and reduced (59) flow conditions (SS) *in vivo* have been associated with increased SMC PDGF-AA mRNA expression. Along with inhibition of migratory activity and MMP-2 production and activation, Palumbo et al. (83) also observed downregulation of bovine arterial SMC PDGFR-β levels in response to SS, which, accompanied by reports that PDGFR-β is required for flow-induced neointimal formation (23), suggests a manner in which blood flow regulates IH progression.

1.6 The role of adventitial fibroblasts in intimal hyperplasia

Studies examining the contribution of vascular cells to the progression of intimal thickening have focused predominantly on SMCs (reviewed in Section 1.3) while vascular FBs have received significantly less attention due to their location in the tunica adventitia, which is widely considered a supporting tissue (73, 103). Porcine coronary artery balloon overstretch injury models, however, have suggested, via bromo-deoxyuridine (BrDU) labeling, that the adventitia is the first major site of cell proliferation following balloon overstretch injury and that proliferating adventitial cells synthesize growth factors and localize to the intima of the injured vessel (105, 112, 145). No proliferating cells were observed in the adventitia of uninjured vessels. In each study, expression of SM α-actin, the most reliable marker of myoFB differentiation (30, 109), was enhanced in BrDU-positive cells, indicating their transition to a myofibroblast phenotype. MyoFBs, through their acquisition of SM α-actin and its contractile properties, are also thought to participate in late lumen loss following vascular injury by inducing vessel constriction in a process that has been compared to the contraction of healing skin wounds (105, 127, 149). Although these studies suggest that adventitial cells contribute to intimal thickening following vascular injury, the results are inconclusive due to the fact that BrDU could label a small population of medial SMC clones as they proliferate and migrate to the intima (150).

More direct evidence for the involvement of adventitial FBs in IH was provided by Li et al. (63), who transfected rat carotid artery FBs with retroviral particles encoding β-galactosidase (LacZ) and injected them into the adventitia of rat carotid arteries

immediately following balloon injury. LacZ expression was detected in both the media and intima post-injury and was localized to the adventitia in uninjured arteries. Siow and colleagues (117) directly labeled adventitial cells of rat carotid arteries with LacZ prior to balloon catheter injury. LacZ remained in the adventitia of uninjured vessels but was observed in both the media and intima of injured vessels and cells expressing LacZ stained positive for SM α-actin, indicating their conversion to myoFBs.

1.6.1 Adventitial fibroblast exposure to shear stress in large vessels

As discussed in detail above for SMCs (Section 1.2.1), FBs in an intact vessel are exposed to interstitial flow (SS) driven by the transmural pressure gradient. It seems plausible that this SS is approximately equal to the magnitude of that experienced by underlying layers of SMCs in the media (order of 1 dyn/cm^2) (140). In cases of vessel injury, FBs are exposed to elevated levels of interstitial flow and its associated SS due to the removal of the hydraulic resistance of the endothelium. Thus, in both intact and injured vessels, FBs are subjected to SS magnitudes near the order of those experienced by ECs and SMCs. However, the role of SS on FB migration, a contributing factor to IH, has not been determined. Therefore, in this thesis, the effect of SS applied directly to FBs as they migrate in a quantifiable assay is evaluated and implications for intimal lesion progression are discussed.

1.7 The role of interstitial fibroblasts in capillary arterialization

Regulation of arteriolar development is critical in processes such as wound healing, the stimulation of collateral vessel growth in infarcted myocardium, and exercise hypertrophy. New arterioles are required to deliver adequate flow, as capillaries alone are insufficient to provide the reduction in local flow resistance required to sufficiently perfuse the tissue (119). The source of contractile cells involved in the arterialization process has received considerable attention recently. Skalak and Price (118) proposed three scenarios for arterialization. First, SMCs from terminal arterioles may proliferate and migrate to the arterializing capillary. Second, pericytes or FBs already attached to the abluminal surface of the capillary may differentiate to a SM phenotype. Third, undifferentiated interstitial cells, presumably FBs, may proliferate, migrate to the arterializing vessel, and differentiate to a SM phenotype. Evidence supporting the final hypothesis was obtained through the use of the α_1 adrenergic blocker prazosin (93). Prazosin, a vasodilator, resulted in increases in both the number of developing terminal arterioles and the number of arteriolar arcade segments in rat skeletal muscle. In a follow-up study, prazosin treatment resulted in a drastic increase in the density of proliferating FBs surrounding transverse arteriolar trees (96). *In vitro* experiments showed that prazosin had no direct effect on FB proliferation, indicating that the enhancement of FB proliferation was due to elevations in hemodynamic stress resulting from vasodilation. The authors hypothesized that the stimulus responsible for elevated levels of FB proliferation was either increased capillary wall SS or enhanced capillary circumferential wall stress (CWS).

Through the use of a computer model, Price and Skalak (94) further elucidated a role for mechanical stresses in arterialization. Arteriolar input pressure was elevated by 25% and arterioles were dilated by 50% to simulate vasodilation and capillaries were permitted to arterialize in two manners. First, a capillary reaching a threshold CWS was arterialized and second, a capillary reaching a threshold wall SS was arterialized. Elevations in CWS resulted in new arcade arteriolar loops whereas elevations in wall SS produced only arterio-venous shunts, which were never observed experimentally. Experimental evidence also supports a role for enhanced CWS in arterialization. Capillaries that participate in arcade arteriole development connect two high-pressure arteriolar trees and are exposed to significant CWS due to enhanced luminal pressure compared to surrounding capillaries. Capillaries exposed to the highest SS in the capillary network connect a high-pressure arteriolar tree to a low-pressure venular tree and do not appear to be involved in the development of arcade arterioles (92). The authors hypothesize that elevations in CWS lead to enhanced production of growth factors by ECs of the capillary wall, which recruit FBs to the arterializing vessel. An alternate hypothesis as to the role of hemodynamics in arterialization is that elevations in luminal pressure result in increased interstitial flow (SS), which directly recruits FBs to the arterializing capillary.

1.7.1 Fibroblast exposure to shear stress in the microcirculation

Detailed calculations of this SS, to our knowledge, have not been performed and thus, an order of magnitude calculation is presented here. Capillary hydraulic

conductivity in the frog mesentery was reported to be in the range 0.7 – 96.8 x 10^{-7} cm/s/cmH_2O at a pressure of 30 cmH_20 (146). Tissue K_p is estimated to be in the range 2.16 x 10^{-11} cm^2 to 7.68 x 10^{-14} cm^2 for a fluid viscosity of 1.2 cP based on the data of Guyton et al. for dog subcutaneous tissue (43) and Swabb et al. for rat subcutaneous tissue (129), respectively. Using these values along with Eq. 1-5, interstitial flow SS imposed on FBs surrounding an arterializing capillary is estimated to be in the range 0.01 – 12.6 dyn/cm^2. It should be noted that arterialization is hypothesized to occur in capillaries exposed to elevated luminal pressures with respect to surrounding vessels. In this case, the values presented here should be considered conservative estimates of the SS imposed on interstitial FBs located outside of arterializing capillaries.

1.8 Effects of mechanical and chemical stimulation on adventitial fibroblast function

Studies examining the role of mechanical and/or chemical stimulation on adventitial FB function are extremely limited. Those relevant to the current study are reviewed briefly here. FBs exposed to mechanical stretch *in vitro* upregulated their expression of syndecan-4, which, in separate experiments, elicited a chemotactic response from the cells (66). Ten dyn/cm^2 SS applied for 24 h enhanced FB angiotensin converting enzyme activity (36). Both basic fibroblast growth factor and PDGF stimulated FB migration (69). Growth-arrested FBs enhanced their migratory activity when exposed to norepinephrine (NE). NE and PDGF-BB had an additive effect on FB migration levels and this response was mediated by α_2- and β-adrenoceptors (153). Estrogen has been shown to mediate SMC-mediated FB migration (64) via the inhibition

of SMC osteopontin production (65). Each of the above studies was conducted with rat aortic adventitial FBs.

In summary, *in vivo* studies have shown that FBs participate in both IH and capillary arterialization. Among the factors suggested to play a role in the regulation of FB involvement in these processes is FB differentiation to SM-like cells, myoFBs. FBs and myoFBs in both large vessels and the microcirculation are subjected to interstitial flow and its accompanying mechanical (SS) and chemical (exposure to interstitial solutes such as serum) stimuli. However, existing *in vitro* studies of the role of mechanical and chemical stimulation on FB and myoFB function are limited. Therefore, in this thesis, a cell culture protocol for regulating the differentiation of FBs to myoFBs was established and the effects of both mechanical (SS) and chemical (exposure to serum) stimulation on FB and myoFB migration and contraction, respectively, were evaluated. New views of the contribution of FBs and myoFBs to IH and capillary arterialization are hypothesized.

1.9 Specific aims

Building on the above background, the specific aims of this thesis are:

1. <u>To evaluate the role of fluid shear stress on smooth muscle cell migration.</u> IH progression was discussed for 3 *in vivo* experimental conditions above: (1) native vessels or implanted vascular grafts in which the endothelium remained intact, (2) vessels that have been denuded of their endothelium by balloon catheter injury, and (3) vessels that have been fitted with a collar to inhibit transmural flow. Enhanced SS attenuated intimal lesion development in each of these cases.

Abnormal SMC migration and proliferation are recognized as hallmarks of intimal thickening. Numerous *in vitro* studies have suggested a shear-mediated reduction in SMC proliferation, but experiments determining the direct effect of SS on SMC migratory activity have yet to be conducted. Therefore, we seeded rat aortic SMCs on Matrigel-coated porous cell culture inserts and quantified the effect of directly-applied SS on their migration towards a known chemoattractant (PDGF-BB).

2. To determine the biochemical pathway through which the shear-mediated regulation of SMC migration occurs. Studies reviewed here have shown that SMCs are able to modulate their production of numerous biochemicals (e.g. NO, prostaglandins, tPA, and TGF-β1) in response to direct SS, both *in vivo* (SMCs form inner vessel lining following EC denudation and IEL damage and are directly exposed to blood flow (SS)) and *in vitro* (cells plated on a 2-dimensional surface and subjected to controlled SS levels). Previous work has proposed a role for MMP-2, NO, and PDGF-AA in the control of SMC migratory activity. We therefore determined the role of these 3 biomolecules in the shear-mediated regulation of SMC migration through the application of both mechanical (SS) and chemical stimuli.
3. To characterize two distinct subpopulations of adventitial fibroblasts. FBs are primarily located in the adventitial layer of large blood vessels, which has historically been considered a supporting tissue. Recent work, however, has shown that FBs participate in intimal lesion formation and that this process involves FB differentiation to a smooth muscle-like cell, the myofibroblast. On

the microcirculatory level, FBs play a role in capillary arterialization, a process hypothesized to be mediated by local hemodynamics. *In vitro* studies examining the effects of mechanical and chemical stimulation on FB function are limited. Therefore, we verified our ability to modulate the phenotype of cells obtained from the same rat adventitial layers in primary culture between FBs and myoFBs by evaluating both populations' expression of SM α-actin and SM-MHC. We then determined the effects of mechanical (SS) and chemical (exposure to serum) stimuli on the migratory and contractile properties, respectively, of each population. New roles for FBs and myoFBs in the IH and capillary arterialization processes are proposed.

Chapter 2

MATERIALS AND METHODS

2.1 Chemicals

The following chemicals were obtained from Sigma-Aldrich Chemical Company (St. Louis, MO): bovine serum albumin (BSA; 30% solution), dimethyl sulfoxide (DMSO), Dulbecco's Modified Eagle's Medium Nutrient Mixture F-12 Ham (DMEM/F12), DMEM/F12 without phenol red, matrix metalloproteinase (MMP)-2, mouse monoclonal smooth muscle α-actin antibodies, N^G-nitro-L-arginine methyl ester (L-NAME), penicillin-streptomycin solution containing 100 U/ml penicillin and 100 µg/ml streptomycin (1% P/S), platelet-derived growth factor (PDGF)-AA, PDGF-BB, S-nitroso-N-acetylpenicillamine (SNAP), SIGMA*FAST*™ Fast Red TR/Naphthol AS-MX tablets, sodium bicarbonate, sodium nitrite, Triton X-100, trypsin-EDTA, Tween 20, and 2, 3 diaminonaphthalene. Fetal bovine serum (FBS) was purchased from HyClone Laboratories, Inc. (Logan, UT). Collagenase II, soybean trypsin inhibitor, and elastase were obtained from Worthington Biochemical Corporation (Lakewood, NJ). Hanks' balanced salts solution (HBSS) was obtained from Irvine Scientific (Santa Ana, CA). Sylgard 184 silicone elastomer was purchased from Dow Corning (Midland, MI). The following antibodies were purchased from Santa Cruz Biotechnology, Inc. (Santa Cruz, CA): monoclonal mouse anti-rat MHC antibody, polyclonal human anti-rabbit PDGF-A antibody, and a horseradish peroxidase-labeled anti-rabbit secondary antibody. An Alexa

Fluor 488 goat anti-mouse IgG secondary antibody was purchased from Molecular Probes (Eugene, OR). Fluoromount-G was purchased from Southern Biotechnology Associates, Inc. (Birmingham, AL). Growth factor reduced (GFR) Matrigel basement membrane matrix was obtained from BD Biosciences (Bedford, MA). Dulbecco's phosphate buffered saline (DPBS) was purchased from Mediatech, Inc. (Herndon, VA). DPBS with Ca^{2+} was obtained from CAMBREX Bio Science, Inc. (Walkersville, MD). The Diff-Quik stain set was obtained from Dade Behring (Newark, DE). Ethanol, paraformaldehyde, and sodium hydroxide were obtained from Fisher Scientific (Fair Lawn, NJ). The chemiluminescence ECL Western blotting analysis system and MMP-2 activity assay were obtained from Amersham Biosciences (Piscataway, NJ). MMP-2 Inhibitor I, p-aminophenylmercuric acetate (APMA), and sodium chloride were obtained from Calbiochem (San Diego, CA). Acrylamide/Bis, ammonium persulfate, protein DC assay, sodium dodecyl sulfate (SDS), TEMED, and Tris were obtained from Bio-Rad Laboratories (Hercules, CA).

2.2 Smooth muscle cell and fibroblast isolation and primary culture

SMCs and FBs were enzymatically isolated from the thoracic aortas of male Sprague Dawley rats (weighing approximately 150-200 grams) using a procedure similar to one used previously to obtain SMCs in our laboratory (1-3, 18, 142) and that was approved by both the Pennsylvania State University and City College of New York Institutional Animal Care and Use Committees. For each primary culture, five rats were euthanized via CO_2 asphyxiation and their aortas were removed aseptically. Aortas were

moved to a sterile laminar flow hood where they were placed into a petri dish containing sterile DMEM/F12 + 1% P/S and outer adherent fat and connective tissue layers were removed. Aortas were then transferred to a petri dish containing an enzyme solution (1 mg/ml collagenase II, 1 mg/ml soybean trypsin inhibitor, 0.25 mg/ml elastase, and 1% P/S in HBSS) and placed in a 37^{o}C, 5% CO_2/95% air incubator for 30-35 minutes. Following incubation, aortas were returned to a laminar flow hood where they were rinsed in DMEM/F12 + 1% P/S. The outer adventitial layer was then removed, rinsed in DMEM/F12 + 1% P/S, placed into a fresh quantity of the enzyme solution detailed above, and incubated at 37^{o}C, 5% CO_2/95% air for 2-3 hours, or until the tissue edges became blurry with migrating cells. During this incubation period, the remaining portions of the aortas (intimal and medial layers), maintained in DMEM/F12 + 1% P/S, were cut longitudinally and the intimal layer was gently scraped away with fine-toothed forceps. The remaining medial layers were rinsed in DMEM/F12 + 1% P/S and moved to a petri dish containing a fresh quantity of the enzyme solution outlined above. Medial layers were cut into 0.5-1 mm^2 pieces and incubated at 37^{o}C, 5% CO_2/95% air for 3-4 hours, or until the edges of tissue pieces were blurry with migrating cells. Following the designated incubation period, petri dishes containing either SMCs (medial layer) or FBs (adventitial layer) in enzyme solution were returned to a laminar flow hood and the cell/enzyme solutions were triturated 30-40 times and expelled forcefully through 40 μm cell strainers (BD Biosciences, Bedford, MA) into petri dishes. The solutions were then mixed with a fresh quantity of DMEM/F12 + 20% FBS + 1% P/S and centrifuged a 600g for 10 minutes. Supernatant was discarded and cells were resuspended in 5 ml of DMEM/F12 + 20% FBS + 1% P/S and placed in a 25 cm^2 culture flask. SMCs were

maintained at 80% confluence and FBs were maintained at 30-50% confluence in primary culture. Upon reaching passage 3, cells were gradually frozen down and stored at –196^{o}C in liquid nitrogen until needed for experiments.

2.3 General cell culture

SMCs were passed at 80% confluence and fibroblasts were passed at either 30-50% confluence (FBs) or 100% confluence (myoFBs). DMEM/F12 + 10% FBS + 1% P/S served as the culture media for all cell populations and was changed every 2-3 days. Passages 3-9 were used for all experiments.

2.4 Characterization of smooth muscle cells and fibroblasts in culture

2.4.1 Smooth muscle cell characterization

SMCs were identified by their characteristic “hill-and valley” morphology in culture and also by their expression of SM-specific α-actin and SM-MHC. The expression of each protein was evaluated in both serum-starved (contractile phenotype) and non-starved (synthetic phenotype) cells. To induce the contractile phenotype, upon reaching 80% confluence in culture flasks, SMCs were serum-starved (maintained in DMEM/F12 + 1% P/S) for two days. Cells were then seeded onto glass slides (75 x 38 mm diameter, 1 mm thick; Corning Glass Works, Corning, NY) glued to 24.5 mm diameter Transwell filter holders (with the filter removed; Costar Corporation, Cambridge, MA) with Sylgard silicone elastomer at a concentration of 27,000 cells/slide.

Cells were maintained in serum-free media for two additional days before experimentation. In other experiments, to maintain the synthetic phenotype, SMCs remained in DMEM/F12 + 10% FBS + 1% P/S throughout culture and upon reaching 80% confluence, were seeded onto glass slides in the same manner described above. Cells were then maintained in DMEM/F12 + 10% FBS + 1% P/S for two additional days before experimentation.

SM-specific α-actin expression was determined using the same procedure in both serum-starved and non-starved cells. Cells were first rinsed in DPBS for 5 minutes and then fixed via exposure to an ethanol gradient (70% for 4 minutes followed by 95% for 20 minutes. SMCs were maintained at -20^{o}C overnight and were then rehydrated in DPBS for 5 minutes. Cells were then incubated at 37^{o}C with a monoclonal anti-α-SM actin clone 1A4 alkaline phosphatase conjugate for 1 hour, followed by a 5 minute rinse with DPBS and a 15 minute room temperature incubation with an alkaline phosphatase substrate (SIGMA*FAST* Fast Red TR/Naphthol AS-MX tablet set).

SM-MHC expression was also evaluated via the same procedure, outlined elsewhere (11), in both serum-starved and non-starved cells. Briefly, SMCs were fixed in paraformaldehyde solution (4% in DPBS) for 10 minutes, permeabilized with Triton X-100 (0.2% in DPBS) for 30 minutes, and incubated with blocking solution (2% BSA in DPBS) for 30 minutes. Cells were then incubated with a monoclonal mouse anti-rat MHC antibody diluted 1:100 in blocking solution for 90 minutes followed by a 60 minute incubation in darkness with an Alexa Fluor 488 goat anti-mouse IgG secondary antibody (100 μg/ml in blocking solution). Cells were rinsed with DPBS for 1 minute between

each step and all incubations were carried out at room temperature. Negative controls (no primary antibody added) were also conducted in all sets of experiments.

For all experiments, following the last incubation step, a drop of Fluoromount-G mounting media was added to slides followed by a glass coverslip. Slides were stored at 4-8^{o}C overnight and were then observed with a 20x objective on a Nikon Eclipse TE2000-E inverted microscope. Cells were counted as "positive" for SM-specific α-actin or SM-MHC if they visually exhibited significantly brighter staining than their respective negative control. For each set of experiments, 4-5 fields of 2-12 cells were counted on each of 3-5 individual slides.

2.4.2 Fibroblast characterization

SM α-actin and SM-MHC expression was evaluated in serum-starved and non-starved FBs using the procedure outlined above for SM-MHC expression in SMCs with one exception. Cells were not serum-starved in culture flasks prior to being seeded on glass slides but instead were plated on slides in the presence of culture media containing 10% FBS and allowed to reach the desired confluence level. Cells were then serum-starved for 4 days prior to experimentation. This was done to ensure that each cell population was at its appropriate confluence level when its phenotypic marker expression was determined. Cells were incubated with either a monoclonal mouse SM α-actin antibody diluted to a final concentration of 10 μg/ml or a monoclonal mouse anti-rat MHC antibody diluted 1:100 in blocking solution for 90 min. In all cases, an Alexa Fluor 488 goat anti-mouse IgG secondary antibody diluted to a final concentration of 10 μg/ml

in blocking solution was used. Slides were analyzed for SM α-actin or SM-MHC expression in the same manner as described above for SMCs.

2.5 Smooth muscle cell and fibroblast migration insert preparation

Cell culture inserts used in both SMC and FB two-dimensional migration experiments were coated using this procedure. Inserts (8.0 μm pore diameter; BD Biosciences) housed in 6-well companion plates (BD Biosciences) were coated with 750 μl GFR Matrigel basement membrane matrix diluted in DPBS to a final concentration of 476 μg/ml. Coated inserts were then incubated at 37^{o}C, 5% CO_2/95% air for 3 hours to provide sufficient time for the Matrigel proteins to gel. Inserts were next moved to a hood that had previously been sterilized via exposure to ultraviolet light and allowed to air dry for 48 hours. Once dry, plates were wrapped in aluminum foil and stored at 4-8^{o}C until needed for experimentation. This protocol reproducibly resulted in a 5-7 μm Matrigel coating thickness near the center of the insert as determined by scanning electron microscopy.

2.6 Smooth muscle cell and fibroblast migration experiments

The traditional Boyden chamber assay, used by others to examine vascular cell migration *in vitro* (57, 90), was used to investigate SMC or FB migration with slight modifications. Inserts previously coated with GFR Matrigel as described above were rehydrated in DPBS for one hour in a 37^{o}C, 5% CO_2/95% air incubator. PDGF-AA or

PDGF-BB was then diluted in DMEM/F12 + 1% P/S to a final concentration of 10 (90, 152) or 100 ng/ml (89) and 2.5 ml of this solution was added to the well of the companion plate to serve as the chemoattractant. SMCs, FBs, or myoFBs were then trypsinized from culture flasks, centrifuged, and resuspended in DMEM/F12 + 10% FBS + 1% P/S, at a concentration of 250,000 cells/ml. DPBS was removed and 2 ml of the cell suspension was added to the insert. Depending on the cell type and experiment, inserts were then incubated for 10-24 hours. In experiments conducted to evaluate the role of NO produced by SMCs on their migration and MMP-2 activation, 100 μM L-NAME was added to inserts 1 h after initial cell seeding. Inserts were then returned to the incubator and exposed to SS as detailed below.

2.6.1 Shear stress or chemical application

Following incubation, inserts to be used in SS experiments were moved to an experimental hood containing a rotating disk apparatus (Fig. 2-1) used previously in our laboratory (3, 116, 142). Cells were maintained at 37^{o}C, 5% CO_2/95% air and exposed to 1, 10, or 20 dyn/cm^2 SS for 1-4 h. SS was calculated using Eq. 2-1:

$$\tau = \frac{\mu \omega r}{h} \qquad \text{(Eq. 2-1)}$$

where τ is the SS, μ is the fluid viscosity (1.2 cP), ω is the rotational velocity of the disk (23.9, 239, or 478 rpm for 1, 10, or 20 dyn/cm^2 SS, respectively), r is the radius of the disk (11.12 mm), and h is the gap distance between the disk and the cell surface (251

μm). All SS magnitudes presented here are maximum values and values ranged from 0 dyn/cm^2 (center of the insert) to the maximum at the edge of the disk (near the edge of the insert), with the average value being 2/3 of the maximum. Total experimental time from initial cell seeding to completion of shear exposure was 10-11 h. For example, if an insert was first incubated for 6 h, it was then subjected to SS for 4 h. This time course was determined to be optimal through an initial set of experiments in which it was observed that after 6-7 h cells had attached to the GFR Matrigel coating firmly enough to withstand shear exposure but none had yet migrated to the underside of the insert. Under control conditions, inserts were housed in the experimental hood with a rotating disk in place, but the disk remained stationary throughout the completion of the experiment.

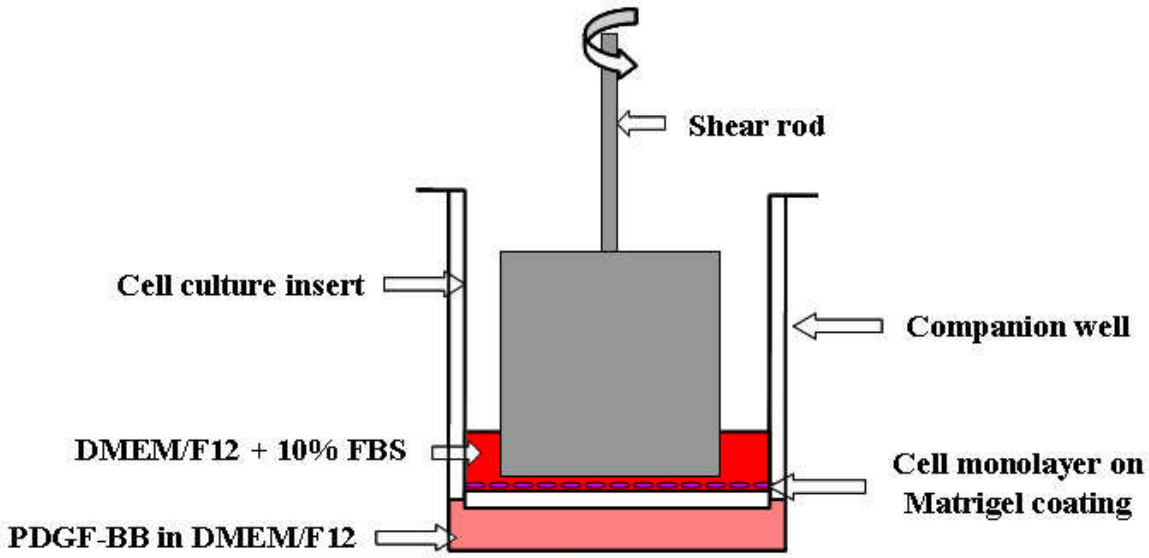

Figure 2-1: Experimental configuration used in shear stress experiments. PDGF-BB (10 or 100 ng/ml) was placed in the companion well to serve as the chemoattractant. SMCs, FBs, or myoFBs (250,000 cells/ml) were seeded on 8.0 μm pore cell culture inserts that had previously been coated with 476 μg/ml GFR Matrigel. SS (1, 10, or 20 dyn/cm^2) was applied for 1-4 h via the use of a rotating disk apparatus.

In some SMC migration experiments, SS application was replaced by the addition of an exogenous chemical to culture media at a designated time following cell seeding. Cells were seeded onto Matrigel-coated cell culture inserts housed in 6-well companion plates as described in section 2.6 and incubated at 37^{o}C, 5% CO_2/95% air for 6-7 hours. A NO donor (500 μM SNAP), 50 ng/ml active MMP-2, or a MMP-2 inhibitor (10 μM MMP-2 Inhibitor I) was then added to insert culture media and inserts were returned to the incubator for 4 hours. Although the inhibitor chosen for this study has been utilized by others to target MMP-2 (154), inhibitors of specific MMPs should be chosen carefully due to their ability to act on multiple MMPs. This time frame for initial cell seeding and chemical exposure was identical to that used in SS migration experiments. SNAP was diluted in fresh culture media (DMEM/F12 + 10% FBS + 1% P/S) and MMP-2 Inhibitor I was diluted in DMSO (0.5 % (v/v) of the final culture media). ProMMP-2 was first converted to its active form by a two-hour incubation with 0.5 mM APMA. Active MMP-2 was then diluted in fresh culture media and added to inserts. During chemical addition, the same amount of solvent was added to control inserts and inserts to which a chemical was added, but the solvent did not contain the respective chemical in control inserts.

Following experimental completion, inserts were first examined under 100x light microscopy to ensure that the cell monolayer was not compromised during the experiment. Conditioned media on top of the insert was removed and stored at –20^{o}C for use in future assays. In some cases, samples of this media were used to determine the number of cells that became dislodged from the insert as a result of SS or chemical exposure. In all cases, this number was found to be minimal (< 4% of total cells seeded).

Cells that had migrated through the Matrigel to the underside of the insert were fixed and stained with the DiffQuik staining solution while cells remaining on top of the insert and the Matrigel layer itself were mechanically removed with a cotton swab. Migrated cells were then counted in five 100x fields (field diameter = 1.8 mm), four around the edges of the insert and one in the center. The average number of cells counted in these five fields was used to quantify cell migration.

2.7 Determination of smooth muscle cell nitric oxide production in the presence of shear stress

Transwell filter holders (24.5 mm diameter) with the filter removed were glued to glass slides (75 x 38 mm, 1 mm thick) with Sylgard silicone elastomer and sterilized through overnight exposure to ultraviolet light. SMCs were then plated onto the slides and maintained in DMEM/F12 + 10% FBS + 1% P/S until reaching confluence (4-5 days). Two hours prior to an experiment, the media in 3 slides was changed to DMEM/F12 without phenol red + 1% BSA + 1% P/S. A NO synthase inhibitor (100 μM L-NAME) was added to one slide to evaluate its effect on shear-mediated NO production by SMCs. Three slides (control, SS, and SS + L-NAME) were moved to an experimental hood containing the rotating disk apparatus described in section 2.6.1 and cells were exposed to 4 hours of 10 dyn/cm^2 SS in the presence and absence of L-NAME. The rotating disk was in place but remained stationary in control slides. Following shear exposure, 500 μl of conditioned media from each slide was stored at -20^{o}C.

A fluorometric assay described in detail elsewhere (74) that is sensitive to nitrite concentrations as low as 10 nM was later used to quantify nitrite levels in samples.

Others have used changes in nitrite levels to reflect changes in NO production (87). Briefly, sodium nitrite standards, in the range 0-20 μM, were diluted in DMEM/F12 without phenol red + 1% BSA + 1% P/S. 100 μl of standard or sample was added to 100 μl of bi-distilled water in a Microlite flat-bottom white opaque 96-well plate (ThermoLabsystems, Franklin, MA). 40 μl of 2, 3 diaminonaphthalene solution (final mixture concentration 25 μM) was added and the plate was shaken for 10 minutes at room temperature in darkness. 40 μl NaOH (final concentration 0.3 N) was then added to increase the pH of the mixture, thereby stabilizing the fluorescent product 1-(H)-naphthotriazole and maximizing emitted fluorescence. A Synergy HT multi-detection microplate reader (360 nm excitation and 430 nm emission wavelength; Bio-Tek Instruments, Inc., Winoski, VT) was used to determine fluorescent intensity values in all standards and samples. Nitrite concentrations in samples were calculated through the use of a standard curve constructed from fluorescent intensity measurements of standards of known nitrite concentration.

2.8 Determination of total and active smooth muscle cell matrix metalloproteinase-2 activity in the presence of shear stress or exogenous chemical stimulation

Total (proenzyme and active) and active MMP-2 levels in SMC conditioned media following SS or SNAP exposure were quantified through the use of a commercially available ELISA assay used according to the manufacturer's specifications.

2.9 Western blotting

In some experiments, following exposure to SS as described in section 2.6.1, conditioned media was removed and SMCs remaining on the GFR Matrigel layer were washed twice in DPBS with Ca^{2+} and then lysed with the SDS extraction buffer as outlined by DeMaio et al. (25). Lysate was purified from insoluble material by centrifugation at 14,000 g for 10 min, and protein concentrations were determined through the use of a commercially available protein assay. Equal protein levels were then loaded onto 10% SDS-polyacrylamide gels under non-reducing conditions (27). Following electrophoresis, proteins were transferred to Immun-Blot polyvinylidene difluoride membranes (Bio-Rad) and were blocked with 5% milk in Tris-buffered saline containing 0.1% Tween 20 for 1 h. Membranes were then incubated with a polyclonal human anti-rabbit PDGF-A antibody (27) for 2 h at a dilution of 1:200. This was followed by a 1 h incubation with a horseradish peroxidase-labeled anti-rabbit secondary antibody at a dilution of 1:2,000. All incubations were carried out at room temperature. PDGF-AA content on the membrane was then detected through the use of a chemiluminescence ECL Western blotting analysis system, a 2 min exposure to Kodak Biomax Light film, and Scion Image analysis software (Scion Corporation, Frederick, MD).

2.10 Scanning electron microscopy studies

Samples were fixed in 2.5% glutaraldehyde in 0.1 M cacodylate buffer (pH = 7.4) for 2 hours at room temperature and were then washed in 0.1 M cacodylate buffer.

Samples were then dehydrated in a graded series of ethanol solutions, freeze-fractured in liquid N_2, critical-point dried, and sputter-coated with platinum. A JSM 5400 scanning electron microscope (JEOL) was used to examine all samples.

2.11 Fibroblast and myofibroblast serum contraction experiments

FBs or myoFBs were grown to the appropriate confluence level in DMEM/F12 + 10% FBS + 1% P/S in culture flasks. Cells were serum-starved (cultured in DMEM/F12 + 1% P/S not containing FBS) for 2 days and were then trypsinized from flasks and plated on glass slides at a density of 150,000 cells/slide. Cells were then serum-starved for two additional days. This protocol has induced rat aortic SMC transformation to the contractile phenotype *in vitro* (1, 2, 18). Additional experiments were conducted in which FBs or myoFBs were maintained in DMEM/F12 + 10% FBS + 1% P/S in flasks until reaching the desired confluence level and were then plated on glass slides housed in petri dishes without being serum-starved. These cells were maintained in 10% FBS culture media for one additional day prior to experimentation.

Contraction experiments with both serum-starved and non-starved cells were conducted by first removing the surrounding culture media in the petri dish in a laminar flow hood. The dish housing the glass slide was then mounted on the stage of a Nikon Eclipse TE2000-E inverted microscope and a field of view containing 3-8 isolated cells at 20x magnification was chosen. A Photometrics Cascade 650 camera connected to the microscope and the MetaVue version 6.2r2 imaging software was used to capture an image of the field of view before fresh culture media was added. This image served as

the t = 0 min time point for the measurement of individual cell area in subsequent data analysis. Fresh culture media with or without (control) 2% serum was then added slowly to the slide over the course of 30 s to 1 min to prevent cell exposure to significant mechanical stress. Images of the field of view were captured at designated time points following the addition of fresh culture media (1, 2, 3, 4, 5, 10, 15, 20, 25, 30, 40, 50, and 60 min).

Following completion of an experiment, the boundary of each cell in the field of view at each time point was manually traced and the MetaVue software was used to calculate cell area, which has been used previously as a measure of cell contraction (1, 2, 10, 18, 28). To account for differences in initial cell size, cell areas at all time points greater than t = 0 min were normalized with respect to the t = 0 min value.

2.12 Statistical analysis

All data are presented as mean ± SEM. PDGF-AA content and FB and myoFB migration levels in the presence of SS were normalized with respect to companion control (no shear exposure) levels for each experiment. For all SMC, FB, and myoFB migration and SMC PDGF-AA quantification experiments, data sets were analyzed for statistical significance using a Student's t-test with a two-tailed distribution. For FB and myoFB contraction experiments, general linear model ANOVA incorporating the Tukey-Kramer method on a 95% confidence interval was used to make pairwise comparisons at each time point. T-test P-values obtained from regression analysis were used to determine statistical significance. In all cases, $P < 0.05$ was considered statistically

significant. The Bonferroni correction, which gives a conservative significance level of P/m, where m is the number of comparisons to be performed, was used where appropriate. For example, when 3 groups were compared, 0.05 was replaced by 0.05/3 = 0.017 to determine significance.

Chapter 3

RESULTS (PART 1): THE ROLE OF FLUID SHEAR STRESS IN VASCULAR SMOOTH MUSCLE CELL MIGRATION

3.1 Scanning electron microscopy images of smooth muscle cell migration

A scanning electron microscopy (SEM) study was conducted to examine our experimental system visually prior to completing experiments to determine the role of SS on SMC migration. Representative images collected in this work are presented in Fig. 3-1 and Fig. 3-2. In Fig. 3-1, a SMC monolayer was seeded onto a cell culture insert coated with GFR Matrigel. A cell that has digested the Matrigel contained in one of the pores of the insert and has begun to migrate through the pore to the underside of the insert is shown. The lack of cell monolayer confluency in this image that was reproducibly observed via light microscopy prior to conducting all experiments is due to the fixation and dehydration processes involved in SEM sample preparation. The underside of a cell culture insert in shown in Fig. 3-2. A SMC has migrated through the pore of the insert and has attached to its underside and is representative of a cell that would be counted as "migrated" in all data presented in this thesis. The pore diameter in Fig. 3-1 and Fig. 3-2 is 8 μm. The thickness of the GFR Matrigel layer used to coat cell culture inserts in this work was determined to be 5-7 μm. This value is a slight underestimate when the dehydration process involved in sample preparation is taken into account.

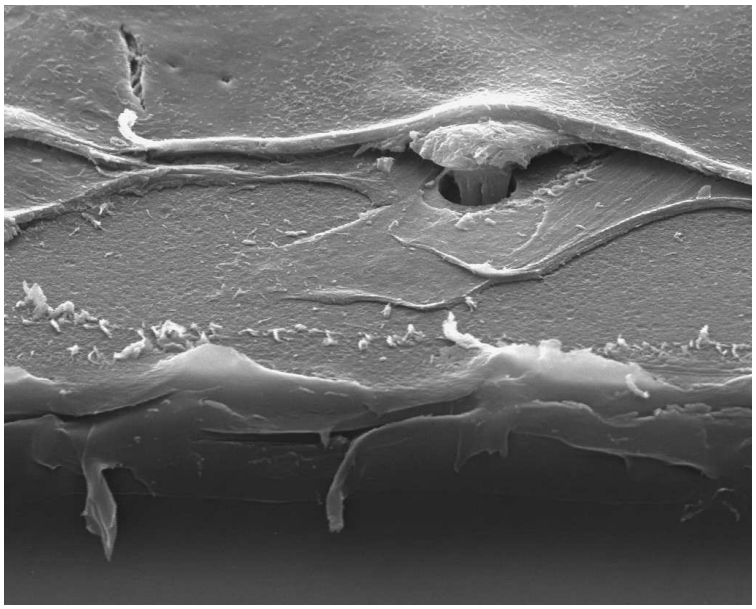

Figure 3-1: SEM image of a SMC that has digested the Matrigel contained in the pore of a cell culture insert and has begun to migrate through the pore to the underside of the insert. Pore diameter is 8 μm.

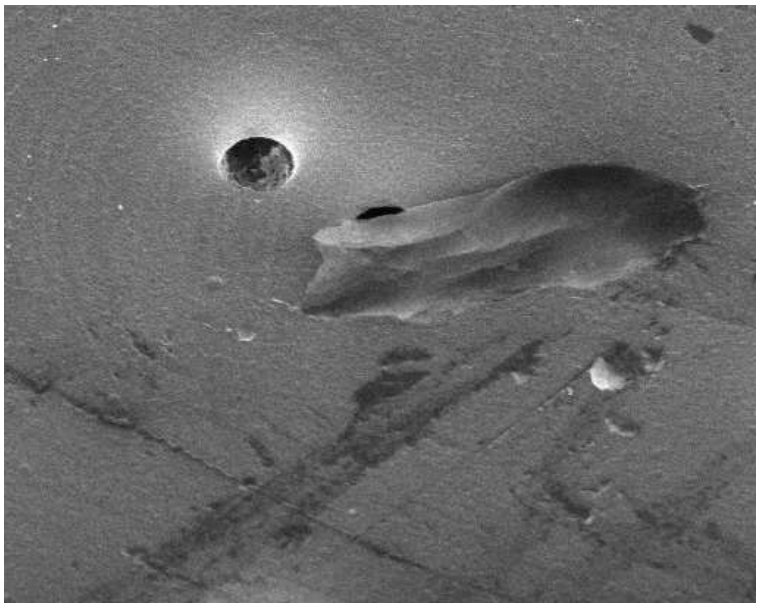

Figure 3-2: SEM image of a SMC that has migrated through one of the pores of a cell culture insert and has attached to its underside. Pore diameter is 8 μm.

3.2 Effects of shear stress on smooth muscle cell migration

The SMC migratory response to 4 hours of 1, 10, or 20 dyn/cm^2 SS is shown in Fig. 3-3. SMCs were seeded onto Matrigel-coated cell culture inserts and placed into a 37^{o}C, 5% CO_2/95% air incubator in the presence of 100 ng/ml PDGF-BB (89) for 6-7 h prior to shear exposure. This time frame was chosen because after 6-7 h, cells were attached to the Matrigel firmly enough to withstand shear exposure, but none had migrated to the underside of the insert. Following the completion of an experiment, inserts were examined microscopically to ensure that a significant number of cells did not detach in response to SS, and then migration levels were quantified. Because control conditions were the same in each experimental group (6-7 h incubation followed by 4-h exposure to a stationary shear rod), all control values are presented together. In Fig. 3-3, 83.0 ± 13.01 cells per 100x field migrated under control conditions (n = 19), 56.5 ± 10.71 cells/field migrated in response to 4 h of 1 dyn/cm^2 SS (n = 6), 30.07 ± 11.99 cells/field migrated upon exposure to 10 dyn/cm^2 SS for 4 h (n = 7), and 9.69 ± 6.22 cells per 100x field migrated in response to 4 h of 20 dyn/cm^2 (n = 6). SMC exposure to both 10 dyn/cm^2 shear ($P < 0.05$) and 20 dyn/cm^2 shear ($P < 0.001$) resulted in a significant inhibition of migratory activity. There was also significantly less migration in inserts subjected to 4 h of 20 dyn/cm^2 SS compared with those exposed to 1 dyn/cm^2 SS for 4 h ($P < 0.05$).

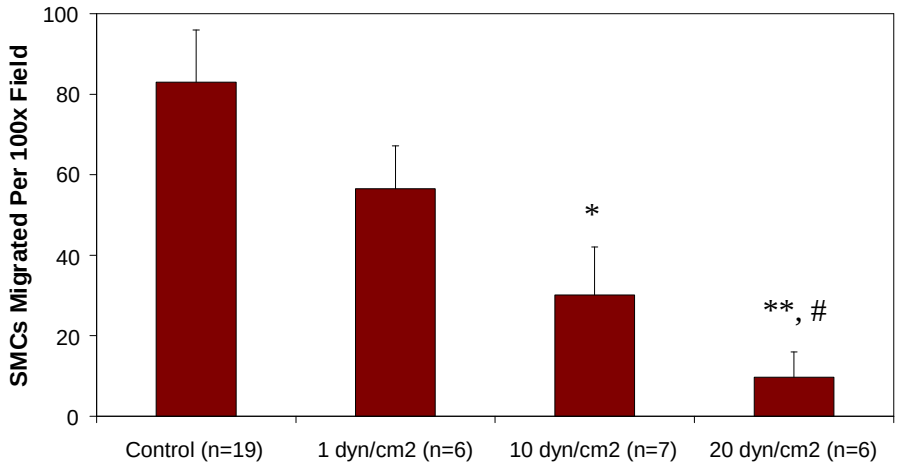

Figure 3-3: Effect of shear stress magnitude on SMC migration. Cells seeded on Matrigel-coated cell culture inserts were exposed to 4 h of 1, 10, or 20 dyn/cm^2 SS following an initial 6-7 h incubation. Control conditions were those in which the shear rod was in place but remained stationary throughout the completion of the experiment. Migratory activity was quantified in both control and shear inserts. n represents the number of times each experimental case was completed. Data are presented as mean ± SEM. * $P < 0.05$ compared to control; ** $P < 0.001$ compared to control; # $P < 0.05$ compared to 1 dyn/cm^2 SS.

The duration of shear exposure required for significant inhibition of SMC migration was also determined (Fig. 3-4). SMCs were seeded on Matrigel-coated cell culture inserts and exposed to 20 dyn/cm^2 SS for 1, 2, 3, or 4 h. If SS was to be applied for 1 h, inserts were first incubated for 9-10 h, a 8-9 hour incubation preceded a 2-h shear exposure, etc., so that total running time for each group of experiments was 10-11 h. Control cases were again the same for each experimental group (10-11 h incubation at 37^{o}C, 5% CO_2/95% air with no shear exposure) and are thus included in one data set. In Fig. 3-4, 52.68 ± 8.99 cells per 100x field migrated under control conditions (n = 23), 41.91 ± 14.19 cells/field migrated in response to 1 h of 20 dyn/cm^2 SS (n = 7), 27.53 ±

8.06 cells/field migrated upon exposure to 20 dyn/cm^2 SS for 2 h (n = 5), 24.33 ± 13.83 cells/field migrated when subjected to 3 h of 20 dyn/cm^2 SS (n = 5), and 9.69 ± 6.22 cells/field migrated in response to 4 h of 20 dyn/cm^2 SS (n = 6). Although there appears to be a decrease in migration levels as shear duration increases, only the 4-h data set is statistically different from control ($P < 0.001$).

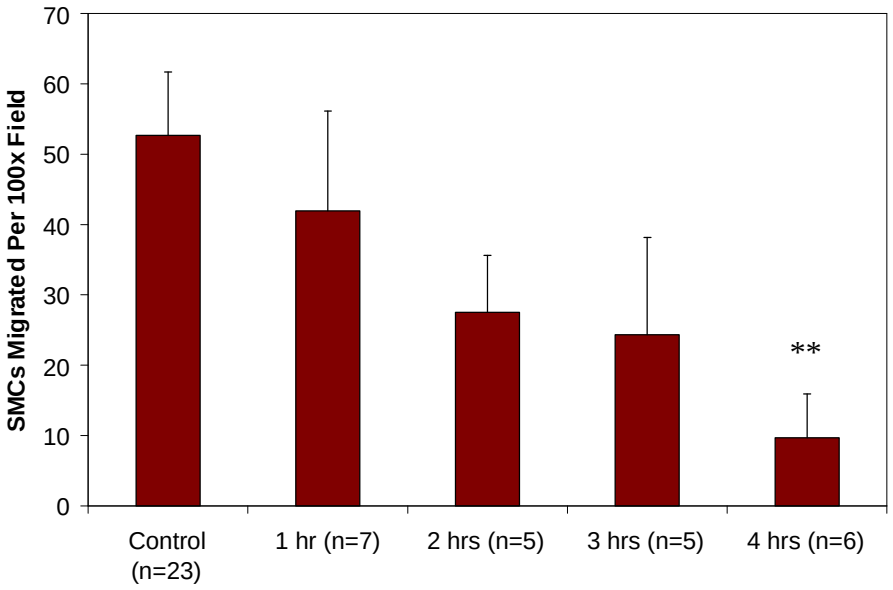

Figure 3-4: Effect of shear stress duration on SMC migration. Cells seeded on Matrigel-coated cell culture inserts were exposed to 20 dyn/cm^2 SS for 1, 2, 3, or 4 h following an initial incubation timed to bring the total experimental time to 10-11 h. Control conditions were those in which the shear rod was in place but remained stationary throughout the completion of the experiment. Migratory activity was quantified in both control and shear inserts. n represents the number of times each experimental case was completed. Data are presented as mean ± SEM. ** $P < 0.001$ compared to control.

SS inhibited SMC migration both in the center of inserts (Fig. 3-5), where shear is relatively small, and the perimeter of inserts (Fig. 3-6), where shear is maximum. In the central area of inserts, 88.32 ± 14.29 cells per 100x field migrated under control

conditions (n = 19) and 17.5 ± 11.95 cells/field migrated in inserts exposed to 4 h of 20/dyn/cm^2 SS (n = 6). The two groups are statistically different (P < 0.01). Examining the perimeter fields of the same inserts, 12.36 ± 3.75 cells/field migrated under control conditions and 1.88 ± 0.61 cells/field migrated in response to 4 h of 20 dyn/cm^2 SS. The difference between the two groups is again statistically significant (P < 0.05).

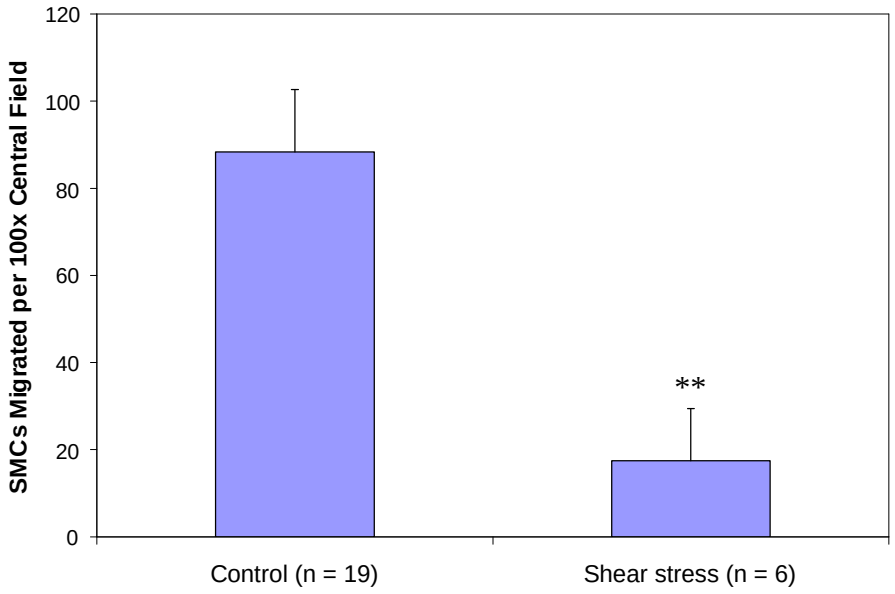

Figure 3-5: Effect of shear stress on SMC migration in the central area of inserts. SMCs were seeded on Matrigel-coated cell culture inserts and exposed to 20 dyn/cm^2 SS for 4 h following a 6-7 h incubation. Control conditions were those in which the shear rod was in place but remained stationary throughout the completion of the experiment. n represents the number of times each experimental case was completed. Data are presented as mean ± SEM. ** P < 0.01 compared to control.

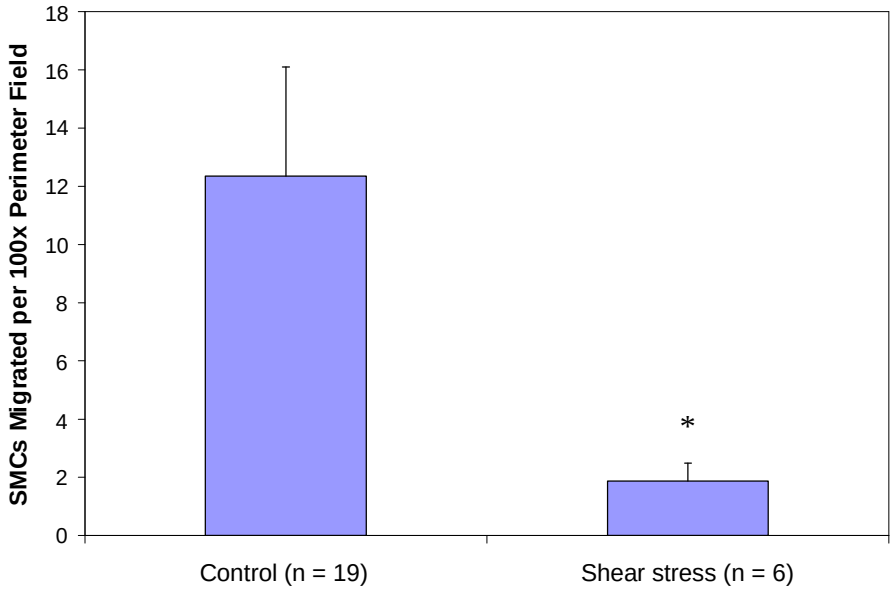

Figure 3-6: Effect of shear stress on SMC migration in the perimeter of inserts. SMCs were seeded on Matrigel-coated cell culture inserts and exposed to 20 dyn/cm^2 SS for 4 h following a 6-7 h incubation. Control conditions were those in which the shear rod was in place but remained stationary throughout the completion of the experiment. n represents the number of times each experimental case was completed. Data are presented as mean ± SEM. * $P < 0.05$ compared to control.

3.3 Effect of shear stress on smooth muscle cell nitric oxide production

The role of SS on SMC production of NO is displayed in Fig. 3-7. Experiments were conducted as described in Section 2.7. SMCs produced 0.517 ± 0.115 nmol NO/10^6 cells in 4 h under control conditions (shear rod in place but stationary throughout duration of experiment with no L-NAME present; n = 5), 1.853 ± 0.371 nmol NO/10^6 cells when exposed to SS (n = 5), and 0.673 ± 0.215 nmol NO/10^6 cells when exposed to SS

following incubation with L-NAME. These values represent NO produced during the 4-h experimental period, as NO levels measured immediately prior to shear exposure were subtracted from values measured after shear exposure. SMC NO production was significantly elevated upon exposure to SS when compared to control conditions ($P < 0.05$), but SMC production of NO when incubated with L-NAME prior to shear exposure was not significantly greater than control levels ($P > 0.05$), suggesting that L-NAME significantly reduced the shear-mediated SMC production of NO.

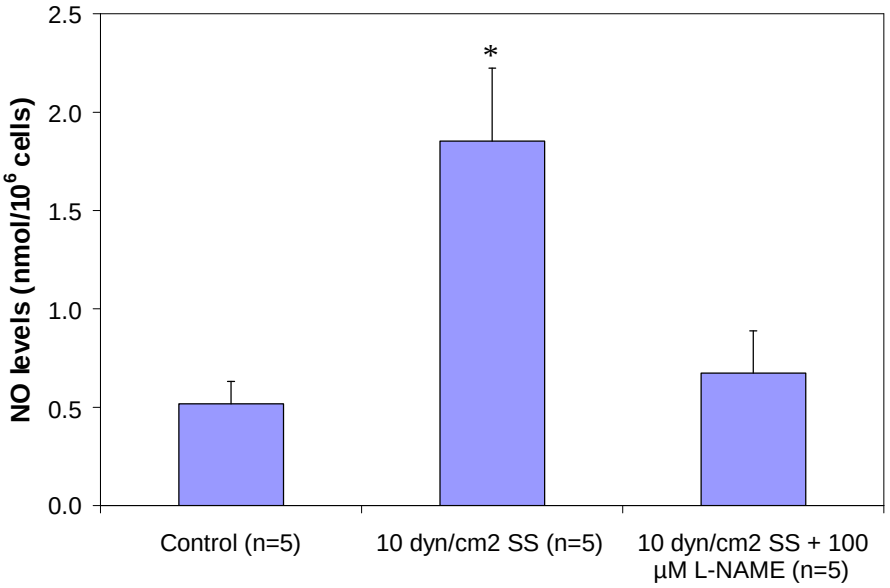

Figure 3-7: Effect of shear stress and N^G-nitro-L-arginine methyl ester (L-NAME) on SMC NO production. In each experiment, one slide was exposed to control conditions (no SS or L-NAME exposure), one was exposed to 4 h of 10 dyn/cm^2 SS, and one was exposed to SS following a 2 h incubation with 100 µM L-NAME. Conditioned media from all 3 slides were collected following experimentation and assayed for NO levels. n represents the number of times each experimental condition was completed. Data are presented as mean ± SEM. * $P < 0.05$ compared to control (no shear or L-NAME exposure). SMC production of NO when incubated with L-NAME prior to shear exposure was not significantly greater than that under control conditions.

3.4 Effect of nitric oxide on smooth muscle cell migratory activity

S-nitroso-N-acetyl-penicillamine (SNAP), a NO donor, was added to inserts in place of SS to evaluate whether increases in NO affected SMC migration. To replicate conditions used in SS experiments, following initial cell seeding, inserts were incubated for 6-7 h following which 500 μM SNAP was added to selected inserts for 4 h. Under control conditions, the same volume of media was removed as in SNAP inserts, but was replaced with an equal volume of fresh media not containing SNAP. SMC migratory activity was quantified following SNAP exposure and the results are presented in Fig. 3-8. SNAP significantly inhibited SMC migration ($P < 0.05$) as 41.11 ± 5.43 cells per 100x field migrated under control conditions ($n = 9$) and 23.64 ± 5.08 cells/field migrated in the presence of SNAP ($n = 10$).

Experiments were also conducted in which 100 μM L-NAME was added to selected inserts 1 h following cell seeding. Inserts were incubated for an additional 5-6 h and were then exposed to 4 h of 20 dyn/cm^2 SS. As with SNAP experiments, control conditions were those in which an equal volume of media was removed as in L-NAME inserts, but was replaced with the same volume of media containing no L-NAME. Inserts incubated with L-NAME were exposed to SS as described in Section 2.6.1. L-NAME abolished the shear-mediated inhibition of SMC migration seen earlier (Fig. 3-3 and Fig. 3-4), as 135.06 ± 16.61 cells/field migrated under control conditions ($n = 4$) and 135.97 ± 23.49 cells/field migrated when subjected to 4 h of 20 dyn/cm^2 SS following incubation with L-NAME ($n = 4$). The two groups are not statistically different ($P > 0.05$; Fig. 3-9).

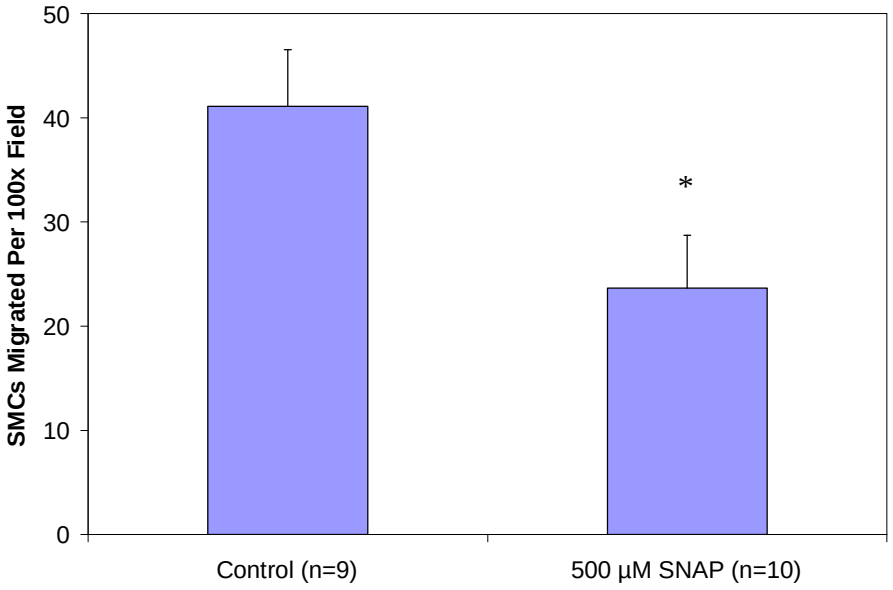

Figure 3-8: Effect of NO donor (S-nitroso-N-acetyl-penicillamine; SNAP) on SMC migration. SNAP (500 µM) was added to selected inserts for 4 h following an initial 6-7 h incubation. Under control conditions, an equal volume of media was removed as in SNAP inserts, but was replaced with fresh culture media not containing SNAP. n represents the number of times each experimental condition was completed. Data are presented as mean ± SEM. * $P < 0.05$ compared to control (no SNAP exposure).

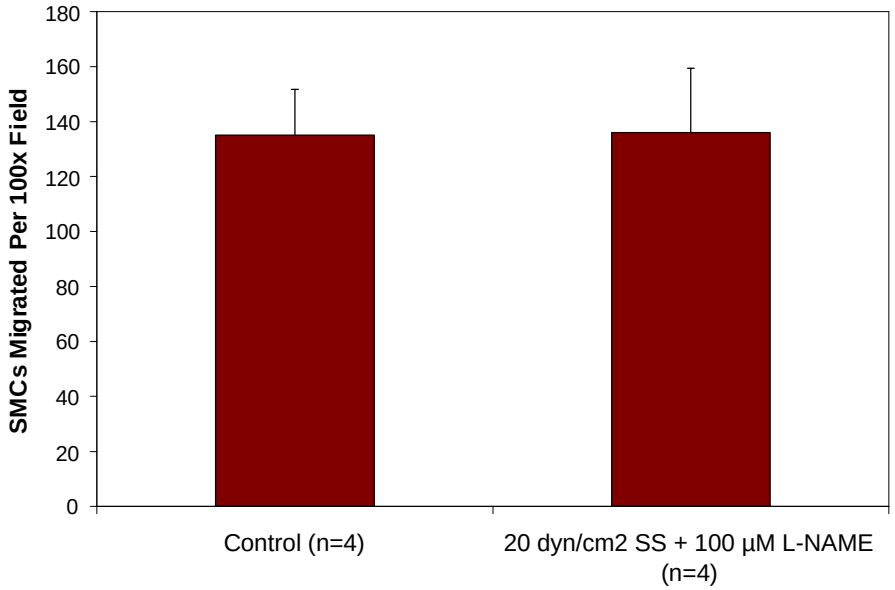

Figure 3-9: Effect of L-NAME on the shear-mediated inhibition of SMC migration. L-NAME (100 µM) was added to inserts to be exposed to SS 1 h following cell seeding. Inserts were incubated for 5-6 h following the addition of L-NAME and were then subjected to 4 h of 20 dyn/cm^2 SS. Control conditions were those in which L-NAME was not added to inserts and the shear rod was in place but remained stationary throughout the duration of the experiment. n represents the number of times each experimental condition was completed. Data are presented as mean ± SEM. Shear exposure had no effect on the migratory activity of cells that had first been incubated with L-NAME.

L-NAME (100 µM) was also added to inserts 1 h following cell seeding in the absence of SS to determine if it had a direct effect on SMC migratory activity. Control conditions were identical to those described for the L-NAME/SS experiments reported above. Following the addition of L-NAME, both control and L-NAME inserts remained in a 37^{o}C, 5% CO_2/95% air incubator for the remainder of the experimental time (9-10 h) and migratory activity was then quantified. In these experiments, 83.5 ± 4.58 cells/field migrated in control inserts (n = 5) and 85.73 ± 3.16 cells/field migrated in the presence of

L-NAME (n=5). L-NAME in the absence of SS had no significant effect on SMC migration levels ($P > 0.05$; Fig. 3-10).

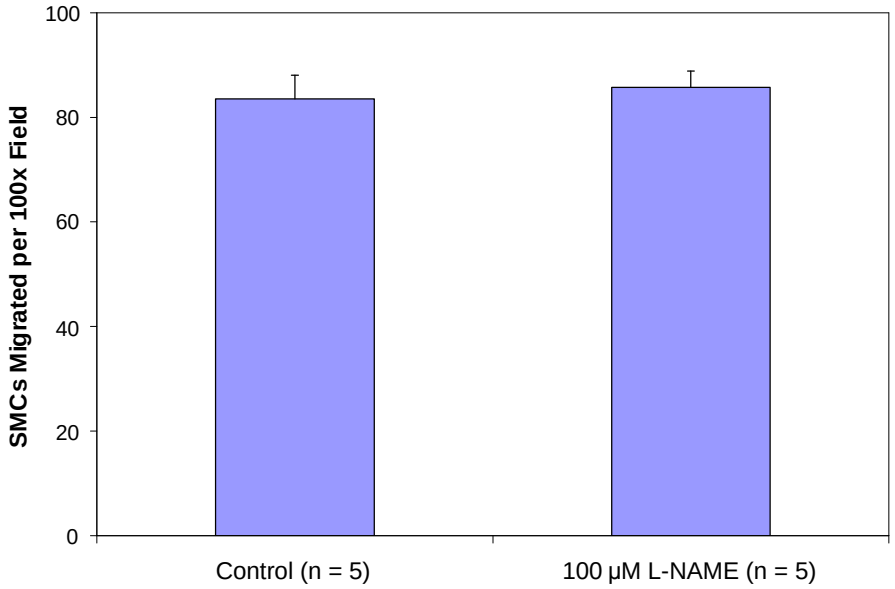

Figure 3-10: Effect of 100 µM L-NAME on SMC migratory activity in the absence of shear stress. L-NAME was added to selected inserts 1 h following cell seeding. Control conditions were those in which the same volume of media was removed as in L-NAME inserts, but was replaced with fresh culture media containing no L-NAME. n represents the number of times each experimental condition was completed. Data are presented as mean ± SEM. In the absence of shear exposure, L-NAME had no significant effect on SMC migration.

3.5 Effect of shear stress on matrix metalloproteinase-2 production and activity

Conditioned media samples from both control (no shear exposure) and sheared inserts were collected immediately following experimentation and both total (proenzyme + active) and active MMP-2 levels were determined in all samples through the use of ELISA. Because 4 h of both 10 and 20 dyn/cm^2 SS significantly inhibited SMC migration (Fig. 3-3), the role of both shear magnitudes on SMC production and activation of MMP-2 was evaluated. The effect of 4 h of 10 dyn/cm^2 SS on SMC total and active MMP-2 levels are presented in Fig. 3-11. Media collected from inserts exposed to 4 h of 10 dyn/cm^2 SS had a total MMP-2 concentration of 13.55 ± 2.93 ng/ml ($n = 4$) and an active MMP-2 concentration of 4.04 ± 0.19 ng/ml ($n = 4$). Media collected from companion control inserts had a total MMP-2 concentration of 14.28 ± 2.84 ng/ml ($n = 4$) and an active MMP-2 concentration of 4.88 ± 0.26 ng/ml ($n = 4$). SS did not have an effect on total MMP-2 levels ($P > 0.05$) but did significantly reduce active MMP-2 levels ($P < 0.05$).

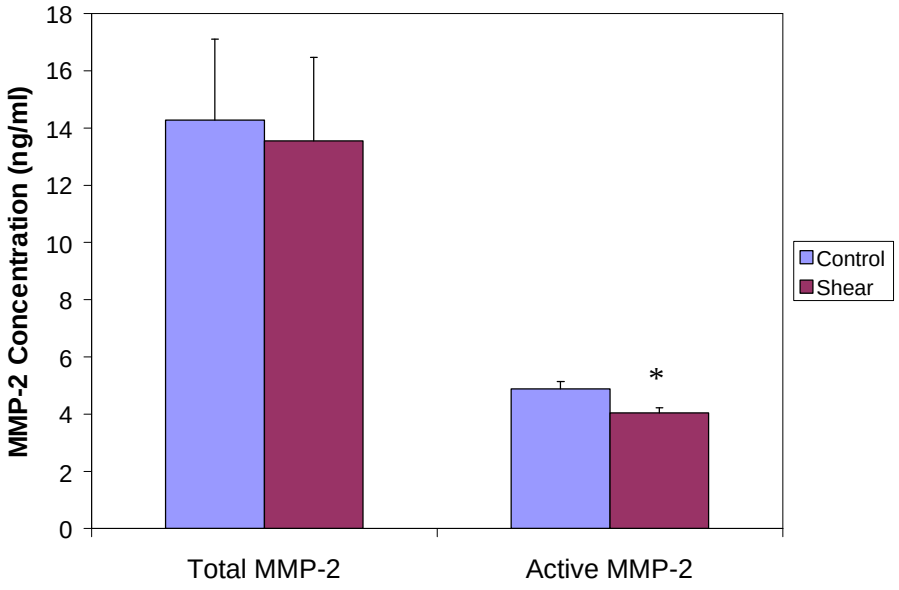

Figure 3-11: Effect of 4 h of 10 dyn/cm^2 shear stress on SMC total and active MMP-2 levels. SMCs were seeded on Matrigel-coated cell culture inserts, exposed to SS, and conditioned media samples from both control and sheared inserts were used in ELISA to determine total (proenzyme + active) and active MMP-2 levels. MMP-2 levels were quantified in n = 4 samples. Data are presented as mean ± SEM. * $P < 0.05$ compared to control (no shear exposure).

The results of ELISA conducted to evaluate the role of 4 h of 20 dyn/cm^2 SS on SMC total and active MMP-2 levels are presented in Fig. 3-12. Four h of 20 dyn/cm^2 SS had no effect on SMC total MMP-2 levels ($P > 0.05$) as media collected from inserts exposed to shear had a total MMP-2 concentration of 11.50 ± 1.95 ng/ml (n = 6) and media from companion control inserts contained 13.76 ± 0.97 ng/ml total MMP-2 (n = 6). As was the case with 4 h of 10 dyn/cm^2 SS (Fig. 3-11), 4 h of 20 dyn/cm^2 SS significantly reduced SMC active MMP-2 levels ($P < 0.05$). Media from sheared inserts had an active MMP-2 concentration of 2.56 ± 0.34 ng/ml (n = 9) whereas media collected

from companion control inserts had an active MMP-2 concentration of 3.74 ± 0.26 ng/ml (n = 9).

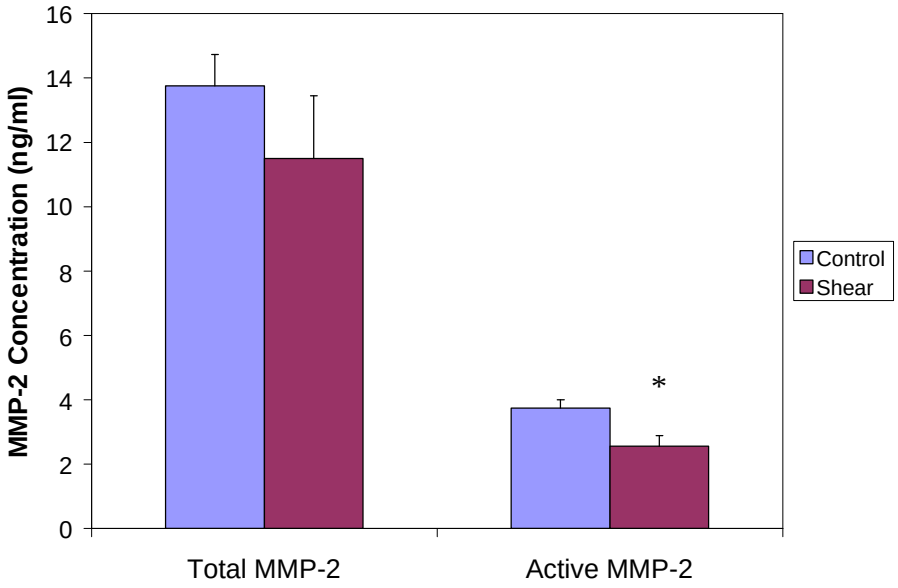

Figure 3-12: Effect of 4 h of 20 dyn/cm^2 shear stress on SMC total and active MMP-2 levels. SMCs were seeded on Matrigel-coated cell culture inserts, exposed to SS, and conditioned media samples from both control and SS inserts were used in ELISA to determine total (proenzyme + active) and active MMP-2 levels. Total MMP-2 levels were quantified in n = 6 samples and active MMP-2 levels were quantified in n = 9 samples. Data are presented as mean ± SEM. * $P < 0.05$ compared to control (no shear exposure).

3.6 Effect of nitric oxide on matrix metalloproteinase-2 production and activity

SS has been shown to inhibit both SMC migration levels (Fig. 3-3 and Fig. 3-4) and MMP-2 activity (Fig. 3-11 and Fig. 3-12). Because SNAP, a NO donor, also inhibited SMC migration (Fig. 3-8), its effect on SMC total and active MMP-2

concentrations was quantified through ELISA. In conditioned media collected from cells exposed to 500 μM SNAP, total MMP-2 levels were 6.32 ± 0.31 ng/ml (n = 5), whereas media collected from cells exposed to control conditions was 11.51 ± 0.77 ng/ml (n = 5). The difference between the two groups was statistically significant ($P < 0.001$; Fig. 3-13). Conditioned media from cells exposed to SNAP had an active MMP-2 concentration of 1.44 ± 0.16 ng/ml (n = 5) and media collected from control cells had an active MMP-2 concentration of 2.07 ± 0.09 ng/ml (n = 5). The difference between the two groups was again statistically significant ($P < 0.01$; Fig. 3-14).

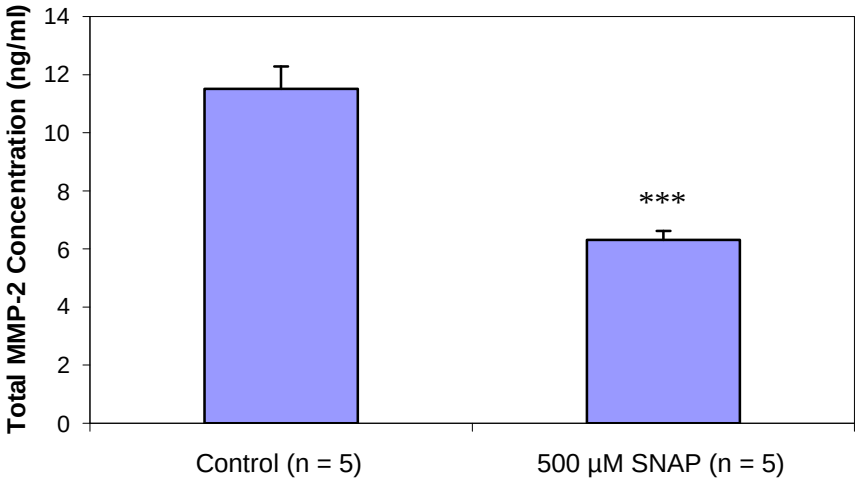

Figure 3-13: Effect of NO donor (SNAP) on SMC total MMP-2 levels. Conditioned media was obtained from cells exposed to either 500 μM SNAP or control conditions and SMC total MMP-2 levels were quantified via ELISA. n represents the number of times each experimental condition was completed. Data are presented as mean ± SEM. *** $P < 0.001$ compared to control (no SNAP exposure).

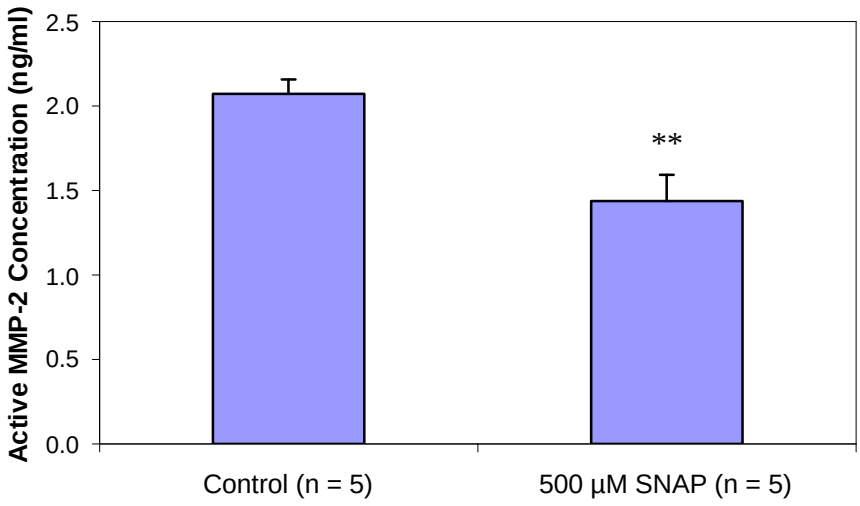

Figure 3-14: Effect of NO donor (SNAP) on SMC active MMP-2 levels. Conditioned media was obtained from cells exposed to either 500 μM SNAP or control conditions and SMC active MMP-2 levels were quantified via ELISA. n represents the number of times each experimental condition was completed. Data are presented as mean ± SEM. ** $P < 0.01$ compared to control (no SNAP exposure).

L-NAME (100 μM), a NOS inhibitor, was shown to abolish the shear-mediated inhibition of SMC migration (Fig. 3-9). Therefore, its effect on the shear-mediated downregulation of SMC MMP-2 activation (Fig. 3-11 and Fig. 3-12) was also evaluated. Conditioned media collected from control cells (no L-NAME or shear exposure) contained 27.77 ± 1.50 ng/ml total MMP-2 (n = 4) and cells incubated with L-NAME prior to exposure to 4 h of 20 dyn/cm^2 SS contained 28.82 ± 1.72 ng/ml total MMP-2 (n = 4; $P > 0.05$ with respect to control). Media from control cells contained 7.43 ± 0.34 ng/ml active MMP-2 (n = 4) and media from cells incubated with L-NAME prior to shear exposure contained 7.40 ± 0.71 ng/ml active MMP-2 (n = 4). SS had no significant effect

on SMC active MMP-2 levels (Fig. 3-15) when cells were incubated with L-NAME prior to shear exposure ($P > 0.05$ in each case).

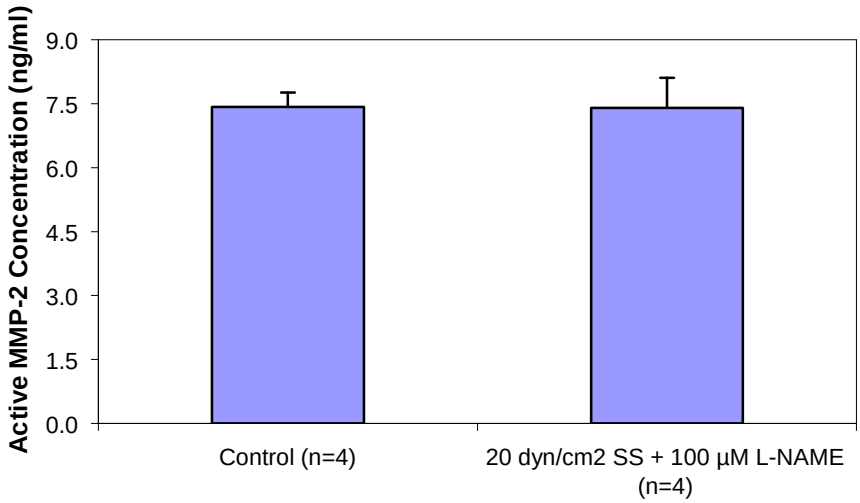

Figure 3-15: Effect of L-NAME on shear-induced downregulation of SMC MMP-2 activity. SMCs were seeded on cell culture inserts, incubated with 100 µM L-NAME, and exposed to 4 h of 20 dyn/cm^2 SS. Control conditions were those in which L-NAME was not added to inserts and the shear rod was in place but remained stationary throughout the experiment. Conditioned media from control and L-NAME + shear inserts were collected and assayed for active MMP-2 levels. n represents the number of times each experimental condition was completed. Data are presented as mean ± SEM. L-NAME abolished the shear-mediated reduction in SMC active MMP-2 levels.

3.7 Effect of changes in MMP-2 levels on SMC migration

To further test the hypothesis that SMCs respond to changes in MMP-2 levels by modulating their migratory activity, two sets of experiments were conducted. Either exogenous active MMP-2 was added to selected inserts to elevate MMP-2 activity or a

MMP-2 inhibitor was added to selected inserts to suppress MMP-2 activity. In the first set of experiments, 50 ng/ml active MMP-2 was added to inserts in the same manner as described earlier for SNAP experiments (Section 3.4). Total experiment time was 10-11 hours (6-7 h initial incubation followed by 4 h incubation in the presence of active MMP-2). The addition of MMP-2 to inserts significantly elevated SMC migration levels ($P < 0.05$; Fig. 3-16) as 41.93 ± 6.93 cells per 100x field migrated in control inserts ($n = 7$) and 73.01 ± 10.67 cells/field migrated in inserts exposed to exogenous MMP-2 ($n = 11$).

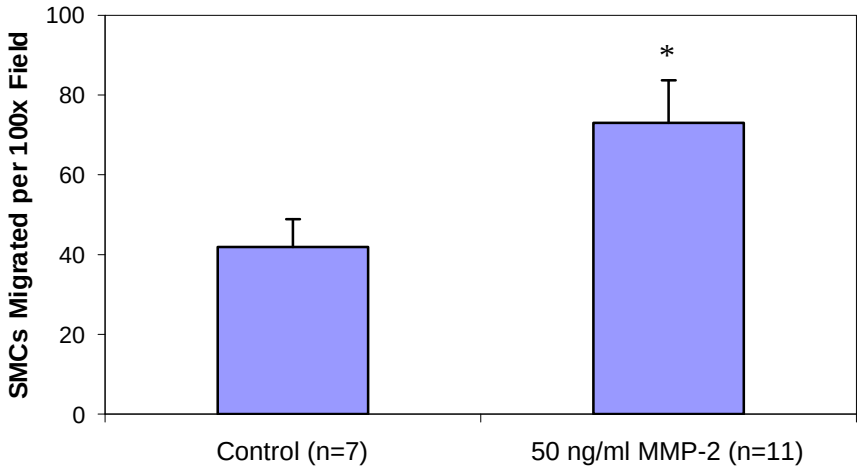

Figure 3-16: Effect of 50 ng/ml exogenous MMP-2 on SMC migration. SMCs were seeded onto Matrigel-coated cell culture inserts and incubated for 6-7 h. Exogenous MMP-2 was then added to selected inserts. Under control conditions, an equal volume of media was removed as in MMP-2 inserts, but was replaced with fresh media not containing MMP-2. All inserts were incubated for 4 additional h and SMC migration levels were then quantified. n represents the total number of inserts examined in each data set. Data are presented as mean ± SEM. * $P < 0.05$ compared to control (no MMP-2 exposure).

In a separate set of experiments, a MMP-2 inhibitor (10 μM; soluble in DMSO) was added to selected inserts as described earlier (Section 3.4). Addition of the inhibitor significantly attenuated SMC migration ($P < 0.05$; Fig. 3-17) as 76.95 ± 7.49 cells per 100x field migrated in control inserts ($n = 7$) and 31.38 ± 11.86 cells/field migrated in the presence of the inhibitor ($n = 6$). The effect of DMSO alone on SMC migration levels was also determined. In inserts in which DMSO was added, 59.85 ± 19.32 cells/field migrated ($n = 6$) and these migration levels were not significantly different from control levels (no DMSO or inhibitor added; $P > 0.05$). It is also of note that although control conditions maintained in experiments presented in Fig. 3-8 (Effect of SNAP on SMC migration), Fig. 3-16 (Effect of exogenous MMP-2 on SMC migration), and Fig. 3-17 (Effect of MMP-2 inhibitor on SMC migratory activity) were identical (10-11 h total incubation time with no exogenous chemical added), the number of cells migrated per 100x field in control inserts in Fig. 3-17 (76.95 ± 7.49; $n = 7$) was greater than that observed in control inserts in Fig. 3-8 (41.11 ± 5.43; $n = 9$) and Fig. 3-16 (41.93 ± 6.93; $n = 7$). The difference in migration levels under similar control conditions may be attributed to the fact that SMCs obtained from different primary cultures as well as different lots of experimental materials (GFR Matrigel and PDGF-BB) were utilized in the three sets of experiments.

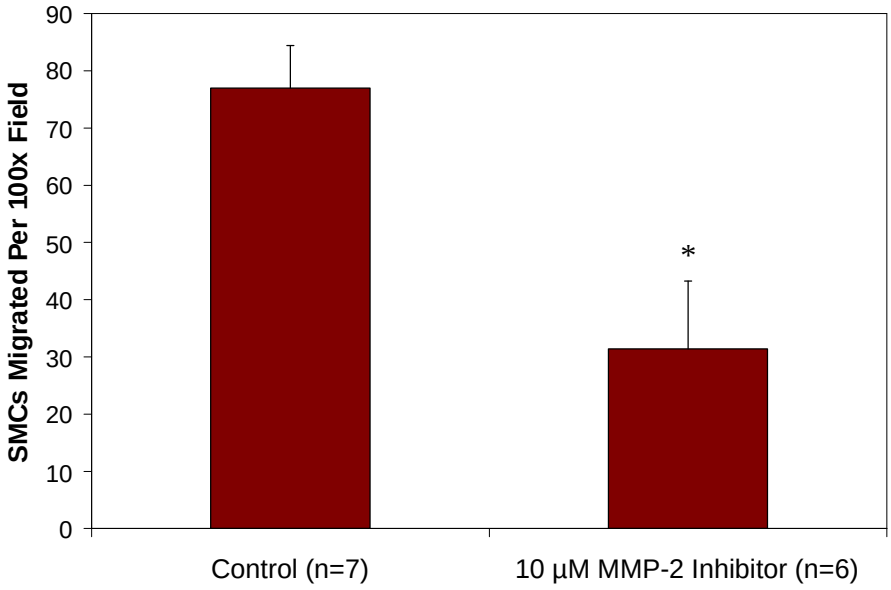

Figure 3-17: Effect of 10 µM MMP-2 inhibitor on SMC migratory activity. SMCs were seeded on Matrigel-coated cell culture inserts and incubated for 6-7 h. MMP-2 inhibitor was then added to selected inserts. Under control conditions, an equal volume of media was removed as in inhibitor inserts, but was replaced with fresh media not containing the inhibitor. Inserts were then incubated for 4 additional h following which migration levels were quantified. n represents the total number of inserts examined for each experimental condition. Data are presented as mean ± SEM. * $P < 0.05$ compared to control (no MMP-2 inhibitor present).

3.8 Effect of fluid shear stress on smooth muscle cell PDGF-AA production

While PDGF-BB is a widely accepted chemoattractant for SMCs, PDGF-AA has no chemoattractive properties of its own (58) and suppresses SMC migratory activity when used together with PDGF-BB (57). Before evaluating the role of SS on SMC production of PDGF-AA, experiments were first conducted to verify the lack of

chemoattractive activity for PDGF-AA. SMCs were seeded on Matrigel-coated inserts with either DMEM/F12 only (control), 100 ng/ml PDGF-AA, or 100 ng/ml PDGF-BB serving as the chemoattractant. Inserts were incubated for 10-11 h and migration levels were then quantified. As shown in Fig. 3-18, 4.33 ± 1.96 cells/field migrated in response to DMEM/F12, 6.8 ± 1.07 cells/field migrated in response to PDGF-AA, and 90.0 ± 7.62 cells/field migrated when PDGF-BB served as the chemoattractant. SMC migration in response to PDGF-BB was significantly greater than that in response to either DMEM/F12 or PDGF-AA ($P < 0.001$ in each case). Migration levels between inserts exposed to DMEM/F12 and PDGF-AA were not statistically different ($P > 0.05$).

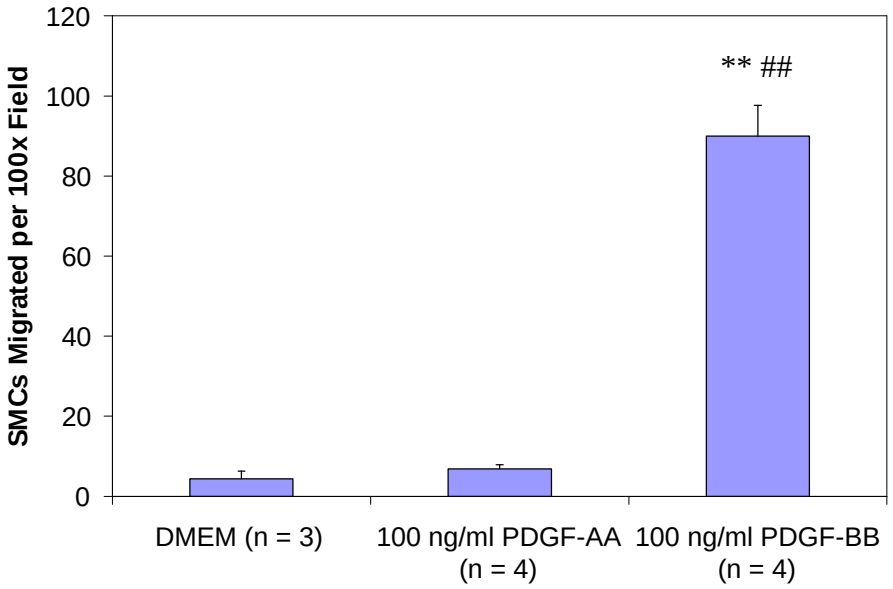

Figure 3-18: Effect of DMEM/F12, PDGF-AA, and PDGF-BB on SMC migration. Cells were seeded on Matrigel-coated cell culture inserts with DMEM/F12, 100 ng/ml PDGF-AA, or 100 ng/ml PDGF-BB serving as the chemoattractant. Inserts were incubated for 10-11 h and migratory activity was then quantified. n represents the number of times each experimental condition was completed. Data are presented as mean ± SEM. ** $P < 0.001$ compared to DMEM/F12; ## $P < 0.001$ compared to PDGF-AA.

Experiments were conducted to determine the role of SS on SMC production of PDGF-AA. SMCs were seeded on Matrigel-coated cell culture inserts and exposed to 4 h of 20 dyn/cm^2 SS or control conditions (rotating disk in place but stationary throughout experimental completion). Cells were lysed after shear exposure and samples were used in Western blotting procedures. A representative blot is shown in Fig. 3-19. SS had no significant effect on SMC PDGF-AA production as the PDGF-AA content in cells subjected to SS was 95% of that in control cells ($n = 3$; $P > 0.05$; Fig. 3-20). SMCs were also plated on glass slides without Matrigel to ensure that Matrigel had no effect on Western blotting results. Cells were exposed to 4 h of 20 dyn/cm^2 SS as described above and lysates from both control and sheared cells were run in Western blots. There was no effect of SS on SMC production of PDGF-AA in the absence of Matrigel as sheared cells contained 97% of the PDGF-AA content of control cells ($n = 3$; $P > 0.05$; Fig. 3-21).

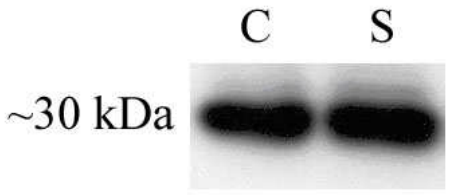

Figure 3-19: A representative Western blot for PDGF-AA (MW ~ 30 kDa). SMCs were seeded on Matrigel-coated cell culture inserts and exposed to 4 h of 20 dyn/cm^2 SS. Cells were then lysed and lysate was used in Western blotting procedures. C: control (no shear); S: shear stress.

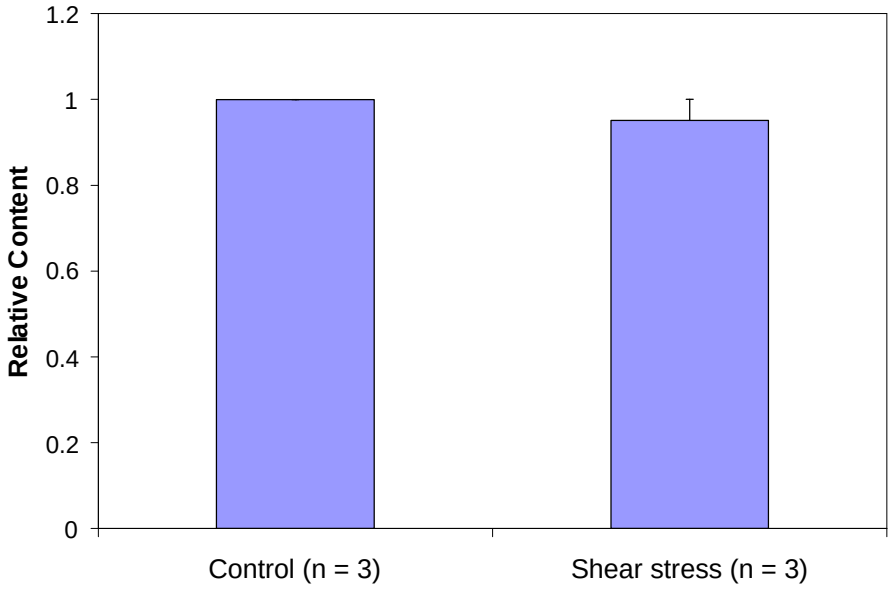

Figure 3-20: Relative PDGF-AA content in control and shear stress (4 h 20 dyn/cm^2) samples from SMCs seeded on Matrigel-coated cell culture inserts. n represents the number of times each experimental condition was completed. Data are presented as mean ± SEM. SS had no effect on PDGF-AA production by SMCs seeded on Matrigel-coated inserts.

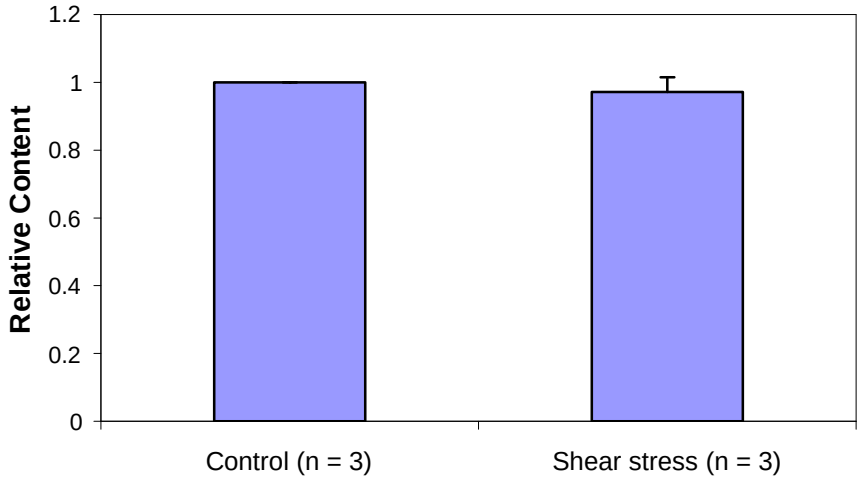

Figure 3-21: Relative PDGF-AA content in control and shear stress (4 h 20 dyn/cm^2) samples from SMCs seeded on glass slides with no Matrigel present. n represents the number of times each experimental condition was completed. Data are presented as mean ± SEM. SS had no effect on PDGF-AA production by SMCs seeded on glass slides.

Chapter 4

DISCUSSION (PART 1): THE ROLE OF FLUID SHEAR STRESS IN VASCULAR SMOOTH MUSCLE CELL MIGRATION

The primary findings of the first part of this thesis were that (1) 4 h of either 10 or 20 dyn/cm^2 fluid SS applied directly to rat aortic SMCs seeded on Matrigel-coated cell culture inserts inhibits their migration toward a known chemoattractant (PDGF-BB; Fig. 3-3); (2) this shear-induced inhibition is controlled by the NO-mediated downregulation of MMP-2 activity (Fig. 3-7 through Fig. 3-15); (3) increases or decreases in active MMP-2 levels result in respective increases or decreases in SMC migration levels (Fig. 3-16 and Fig. 3-17); and (4) 4 h of 20 dyn/cm^2 SS does not affect SMC production of PDGF-AA (Fig. 3-19 through Fig. 3-21). One other study examined the effect of SS on SMC migration indirectly by exposing cells to shear in culture and then transferring them to a migration assay (83), and another subjected SMCs to pulsatile SS and examined their spreading activity, which takes into account both migration and proliferation (113). The present work is, to our knowledge, the first to apply shear directly to SMCs while they were migrating in a quantifiable assay.

Abnormally high SMC proliferation in the media and subsequent migration to the intima are recognized as hallmark processes in intimal thickening. It has been well-documented that IH is reduced in regions of elevated blood flow SS *in vivo* (9, 55, 56, 60) and the data presented here are consistent with those observations (Fig. 3-3 and Fig. 3-4). Elevated flow has been shown to attenuate IH both in common carotid arteries (CCAs)

denuded of their endothelium by balloon catheter injury (SMCs directly exposed to blood flow (55)) and in endothelialized vascular grafts (9, 56, 60). Enhancement of intimal thickening following the placement of a silicone collar around rabbit CCAs suggests a role for interstitial flow SS in the control of IH (26). Elevated IH levels were proposed to be due to the inhibition of metabolite transport due to the reduction in interstitial flow caused by the collar. Another interpretation of these data is that the reduction in interstitial flow decreased interstitial flow SS levels experienced by underlying SMCs, leading to increased levels of both their migration and proliferation.

The observation that SS inhibits SMC migration both in the central area of inserts where there is relatively little shear (Fig. 3-5) and in the perimeter of inserts where shear is maximum (Fig. 3-6) suggests that a soluble factor is released by SMCs in response to SS and is communicated between cells to inhibit SMC migratory activity. Our working hypothesis was that SS enhances SMC production of NO, which in turn inhibits migration by suppressing MMP-2 levels. Support for this hypothesis was provided through the use of a NOS inhibitor, 100 μM L-NAME, which suppressed SMC NO production (Fig. 3-7), reversed the shear-mediated inhibition of SMC migration (Fig. 3-9), and abolished the shear-mediated downregulation of MMP-2 activity. A NO donor, 500 μM SNAP, significantly inhibited SMC migratory activity when added to inserts (Fig. 3-8). SNAP has been used by others in SMC migration experiments and a drastic decrease in migratory activity was also observed (35).

Other work supports a role for NO in the suppression of SMC migration. Sarkar et al. (102) used a razor blade to wound a confluent culture of SMCs and observed their subsequent migration in the presence of three NO donors. Each NO donor inhibited the

number of cells migrating and their maximal distance from the wound edge. In another study, a silicone collar was used to induce intimal thickening in rabbit CCAs (71). Increased flow conditions suppressed the IH caused by the collar, and this reduction was attributed to increased SMC production of NO in response to elevated flow (and subsequent interstitial SS). It is also plausible that, in studies in which IH was attenuated under elevated flow conditions in endothelialized vascular grafts (9, 56, 60), increased flow led to elevated EC production of NO, which in turn diffused to the underlying SMC and suppressed their migratory activity. Although it is possible that these elevated NO levels inhibited SMC proliferation, it is also likely that NO reduced SMC migratory activity, leading to the reduction in intimal thickening.

The effect of elevated NO levels on MMP activity is controversial. MMP-2 was specifically evaluated in this thesis because it has been shown to be required for rat aortic SMC migration (90). Addition of SNAP to the upper well of inserts for 4 h significantly downregulated both total and active MMP-2 levels in SMC conditioned media (Fig. 3-13 and Fig. 3-14). The reduction in total MMP-2 concentration following SNAP administration appears to have no effect on SMC migratory activity alone and is likely due to the larger dose used in the present work (500 μM; (15)) compared to other studies of SMC migration (10 μM; (35)). In another study, MMP-2 levels were examined three days after placing elevated flow through rabbit left CCAs (136). Active MMP-2 levels were significantly increased upon exposure to elevated flow (and elevated NO produced by EC), and when L-NAME was used to inhibit NO synthesis, MMP levels fell. In other work, the endothelial NOS (eNOS) gene was transferred to SMCs and its role in SMC migration and MMP-2 levels was determined (42). eNOS gene transfer inhibited SMC

migration but, in contrast to the study discussed above, it also suppressed MMP-2 activity in conditioned media. Addition of a NO donor (DETA NONOate) or 8-bromo-cGMP to media also reduced MMP-2 activity, suggesting a role for the NO/cGMP pathway in the inhibition of MMP-2 activity. eNOS gene transfer resulted in an increase in tissue inhibitor of MMPs (TIMP)-2 secretion by SMCs, indicating that alterations in the ratio of MMPs to their endogenous inhibitors (TIMPs) also participated in the eNOS-mediated regulation of MMP-2 activity. Considering these studies together, it seems that NO has multiple effects on SMC production and/or activation of MMP-2, the balance of which is likely determined by the physiological and/or pathological state of the vessel.

MMP-2 expression has also been shown to be sensitive to altered flow conditions (6, 52). Others have also reported that 15 h of 12 dyn/cm^2 SS reduced MMP-2 levels but did not affect MMP-9 in bovine aortic SMCs (83). In this work, 4 h of 10 or 20 dyn/cm^2 SS did not affect SMC total (proenzyme + active) MMP-2 levels, but did significantly decrease active MMP-2 levels (Fig. 3-11 and Fig. 3-12). Palumbo et al. (83) reported significant inhibition of both proenzyme and active MMP-2 levels in response to 15 h of 12 dyn/cm^2 SS, and therefore it seems that the shear-mediated inhibition of pro-MMP-2 occurs on a longer timescale (> 4 h) that inhibition of active MMP-2 (4 h or less). Reductions in mRNA and protein for MT-MMP, which activates pro-MMP-2 on the cell surface, were also reported after 15 h of shear but not after 3 h (83). It seems plausible that this inhibition of MT-MMP occurs on a timescale of approximately 4 h (the time point measured in this work) and that it is responsible for the decrease in MMP-2 activity reported here. Considering these data together, it appears that decreases in active MMP-2 levels are involved in the shear/NO-mediated inhibition of SMC migration.

Experiments were also conducted to evaluate the effect of SS on SMC production of PDGF-AA. PDGF-AA has been shown to have virtually no chemotactic activity on its own (21) and to inhibit PDGF-BB-mediated SMC migration when used in a modification of the Boyden chamber assay (57). SMC PDGF-AA mRNA expression has also been shown to be elevated under both high- (137) and low- (59) flow conditions. We thereby hypothesized that SMCs might produce more PDGF-AA upon exposure to elevated SS and this would inhibit their migration in an autocrine fashion. Initial experiments were conducted to validate the lack of PDGF-AA chemotactic activity in the model used here (Fig. 3-18) and the effect of 4 h of 20 dyn/cm^2 SS on SMC PDGF-AA production was then evaluated. Results showed no role of SS on SMC PDGF-AA protein levels as evaluated by Western blotting (Fig. 3-19 through Fig. 3-21). This is likely because SS was applied on a shorter time frame in this study (4 h) than in other studies (137) that reported SMC PDGF-AA expression in response to increased flow (a minimum of 24-h exposure to modified flow conditions). Thus it is possible that SMCs produce PDGF-AA upon exposure to enhanced SS, which effectively inhibits their migration, but this autocrine mechanism operates on a longer time frame than was tested in this study.

In summary, we have shown, for the first time, that SS applied directly to SMCs acts to inhibit their migratory activity. The biomolecular mechanism of inhibition involves the NO-mediated downregulation of MMP-2 levels. PDGF-AA does not appear to participate in the shear-induced inhibition of SMC migration on the time frame tested in this study. These results agree well with animal injury (balloon angioplasty) models that have reported less intimal lesion progression in regions of elevated blood flow and

suggest that the shear-mediated inhibition of SMC migration is involved in this phenomenon.

Chapter 5

RESULTS (PART 2): CHARACTERIZATION OF TWO DISTINCT POPULATIONS OF ADVENTITIAL FIBROBLASTS

5.1 Subconfluent and confluent fibroblast expression of smooth muscle α-actin and myosin heavy chain

Immunofluorescence experiments were conducted on FBs maintained at both subconfluent and confluent culture conditions to evaluate their expression of two phenotypic markers: SM α-actin, one of the proteins expressed earliest during SMC differentiation, and SM-MHC, a marker of fully differentiated, mature SMCs. Results of these experiments are summarized in Table 5-1. 29.5% of subconfluent cells evaluated expressed SM α-actin and 0.4% expressed SM-MHC. 93.9% of confluent cells evaluated expressed SM α-actin and 8.2% expressed SM-MHC. Serum-starving elevated subconfluent FB SM α-actin expression to 70.2% of total cells examined (a 2.4-fold increase over non-starved subconfluent FBs) and elevated SM-MHC expression to 28.5% (a 66.9-fold increase over non-starved subconfluent FBs). Serum-starving had little effect on confluent FB SM α-actin expression (96.4% of cells examined expressed the protein, a 1.03-fold increase over non-starved confluent FBs), but did elevate their expression of SM-MHC as 23.8% of serum-starved confluent FBs expressed this marker, a 2.9-fold increase compared to non-starved confluent FBs. Due to their low expression of both phenotypic markers in the non-starved state, subconfluent cells were labeled

"fibroblasts (FBs)" based on literature convention (103). Based on their overwhelming expression of SM α-actin and modest expression of SM-MHC in the non-starved state, confluent cells were labeled "myofibroblasts (myoFBs)" according to literature convention (103).

Table 5-1: Subconfluent and confluent fibroblast SM α-actin and SM-MHC expression.

Cell Type	Serum-starved?	Phenotype Marker	Stained Cells Counted	Total Cells Counted	Percent Stained
Subconfluent	No	SM α-actin	458	1551	29.5
Subconfluent	Yes	SM α-actin	1061	1511	70.2
Subconfluent	No	SM-MHC	7	1643	0.4
Subconfluent	Yes	SM-MHC	208	730	28.5
Confluent	No	SM α-actin	5521	5881	93.9
Confluent	Yes	SM α-actin	4515	4682	96.4
Confluent	No	SM-MHC	198	2420	8.2
Confluent	Yes	SM-MHC	948	3982	23.8

5.2 Effect of fluid shear stress on fibroblast and myofibroblast migration

FBs were seeded on Matrigel-coated cell culture inserts, incubated for 7 h, and then exposed to 4 h of 20 dyn/cm^2 SS in a similar manner to the SS/SMC migratory study presented earlier (Section 3.2). SS significantly enhanced FB migration to two doses of PDGF-BB (10 and 100 ng/ml; $P < 0.05$ in each case; Fig. 5-1). Migration levels in inserts exposed to SS were 2.05 ± 0.32 times greater than in control (no shear) inserts (normalized to 1) in the presence of 10 ng/ml PDGF-BB ($n = 7$) and 1.54 ± 0.14 times greater than in control inserts in the presence of 100 ng/ml PDGF-BB ($n = 6$).

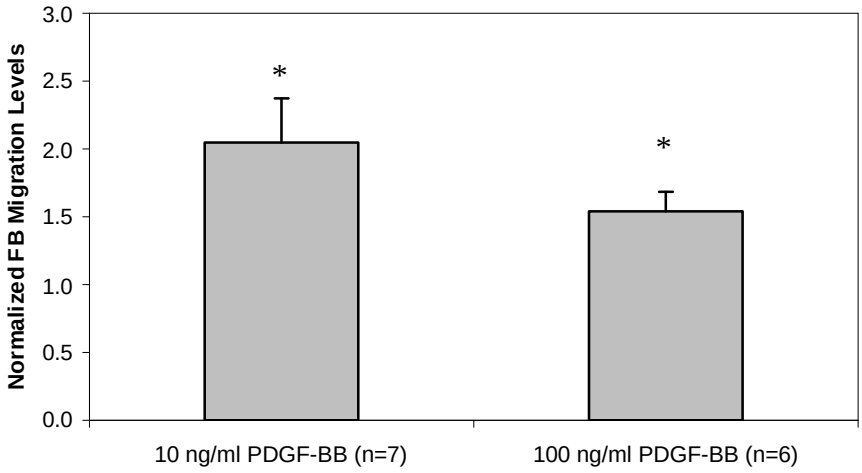

Figure 5-1: Effect of shear stress on fibroblast migration. FBs were seeded on Matrigel-coated cell culture inserts, incubated for 7 h, and then exposed to 4 h of 20 dyn/cm^2 SS in the presence of either 10 or 100 ng/ml PDGF-BB. Migration levels were quantified following shear exposure. FB migration levels in response to SS were normalized by those measured under control conditions (shear rod in place but stationary throughout experimental completion). n represents the number of times each experimental condition was completed. Data are presented as mean ± SEM. * $P < 0.05$ compared to companion control (no shear exposure).

SS significantly elevated FB migration levels in the central area of inserts, where shear is relatively small, in response to both 10 and 100 ng/ml PDGF-BB. Normalized migration levels were 2.10 ± 0.41 in the center of sheared inserts when 10 ng/ml PDGF-BB served as the chemoattractant ($n = 7$; $P < 0.05$ compared to control; Fig. 5-2) and 1.63 ± 0.16 when 100 ng/ml PDGF-BB acted as the chemoattractant ($n = 6$; $P < 0.05$ compared to control; Fig. 5-2). Shear significantly enhanced FB migration in the perimeter of inserts, where shear is maximum, in response to 10 ng/ml PDGF-BB, but not 100 ng/ml PDGF-BB. Normalized migration levels were 2.01 ± 0.36 in the perimeter of inserts subjected to SS in the presence of 10 ng/ml PDGF-BB ($n = 7$; $P < 0.05$ compared

to control; Fig. 5-3) and 1.32 ± 0.21 in the perimeter of sheared inserts in the presence of 100 ng/ml PDGF-BB (n = 6; P > 0.05; Fig. 5-3).

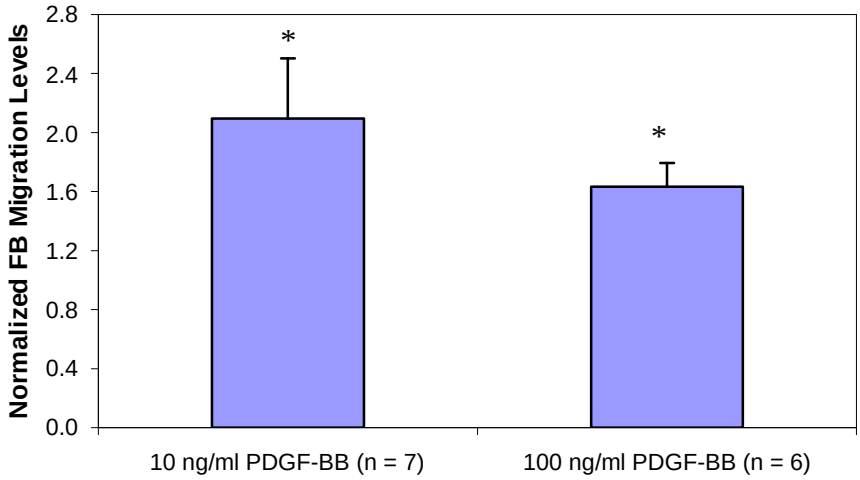

Figure 5-2: Effect of shear stress on FB migration in the central area of inserts. FB migration levels were quantified in only the central area of inserts exposed to shear in Fig. 5-1 and were normalized by companion control (no shear) levels. n represents the number of times each experimental condition was completed. Data are presented as mean ± SEM. * P < 0.05 compared to companion control.

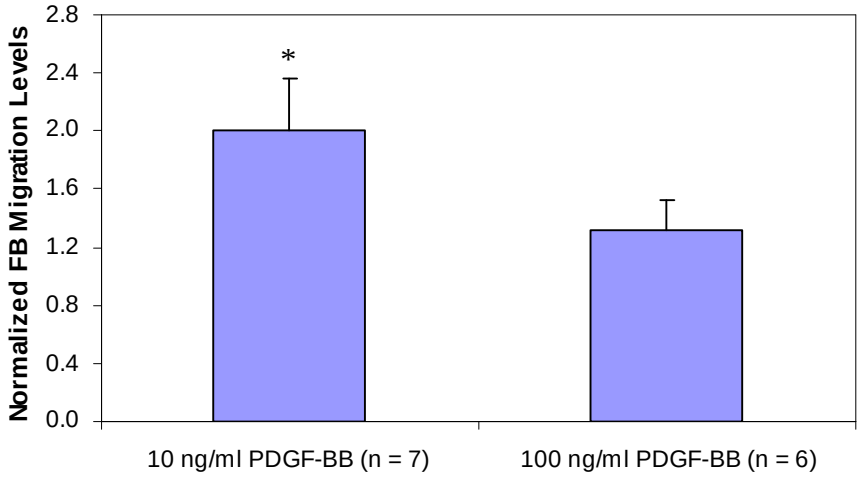

Figure 5-3: Effect of shear stress on FB migration in the perimeter of inserts. FB migration levels were quantified in only the perimeter fields of inserts exposed to shear in Fig. 5-1 and were normalized by companion control (no shear) levels. n represents the number of times each experimental condition was completed. Data are presented as mean ± SEM. * $P < 0.05$ compared to companion control.

Similar experiments were conducted to determine the role of SS on myoFB migratory activity, and, in contrast to the response observed for FBs (Fig. 5-1), SS significantly inhibited myoFB migration to both 10 and 100 ng/ml PDGF-BB ($P < 0.01$ in both cases; Fig. 5-4). Normalized migration levels were 0.62 ± 0.03 in sheared inserts relative to companion control when 10 ng/ml PDGF-BB served as the chemoattractant ($n = 4$) and 0.47 ± 0.05 in sheared inserts when 100 ng/ml PDGF-BB acted as the chemoattractant ($n = 11$). It is of note that in all SMC migration work presented earlier (Chapter 3), migration levels were reported as SMCs migrated per 100x field whereas now FB and myoFB migration levels in the presence of SS are normalized by companion control (no SS) levels. This was done to account for the fact that although the effect of

SS on FB (elevated compared to companion control) or myoFB (suppressed compared to companion control) migratory activity reported in Fig. 5-1 and Fig. 5-4, respectively, was observed in all individual experiments, the number of cells migrated per 100x field under both control and SS conditions varied between experiments. Migratory activity (cells migrated per 100x field) in the presence of SS was therefore normalized by control migratory activity for each experiment to highlight the role of SS on FB and myoFB migration.

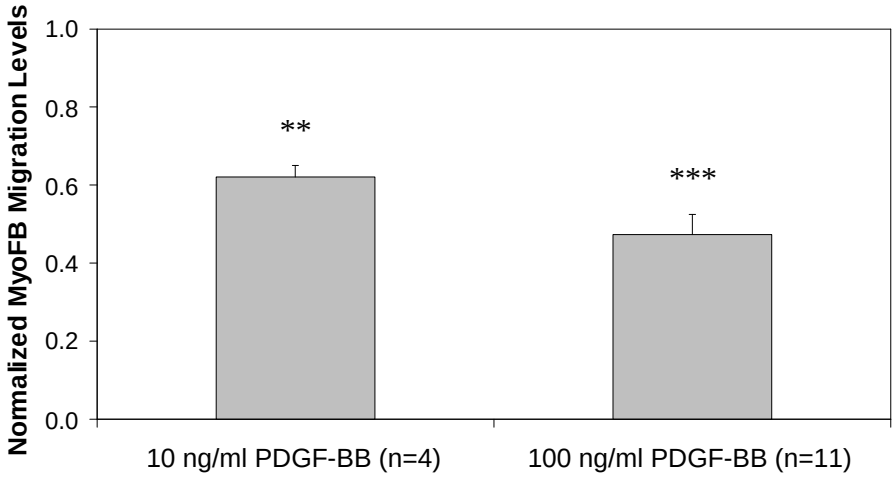

Figure 5-4: Effect of shear stress on myoFB migration levels. MyoFBs were seeded on Matrigel-coated cell culture inserts and exposed to 4 h of 20 dyn/cm^2 SS following an initial 7 h incubation. Either 10 or 100 ng/ml PDGF-BB acted as the chemoattractant. Migration levels were then quantified and migratory activity in inserts subjected to SS was normalized by that in inserts exposed to control conditions (shear rod in place but stationary throughout duration of the experiment). n represents the number of times each experimental case was completed. Data are presented as mean ± SEM. ** $P < 0.01$ compared to companion control.

Shear significantly reduced myoFB migration in the central area of inserts in the presence of either 10 (n = 4; normalized migration level of 0.68 ± 0.09; $P < 0.05$ relative to companion control; Fig. 5-5) or 100 ng/ml PDGF-BB (n = 11; normalized migration level of 0.45 ± 0.06; $P < 0.001$ relative to companion control; Fig. 5-5). SS also significantly inhibited myoFB migratory activity in the perimeter of inserts in the presence of either 10 ($P < 0.05$; Fig. 5-6) or 100 ng/ml PDGF-BB ($P < 0.001$; Fig. 5-6). Normalized migration levels were 0.44 ± 0.13 in the perimeter of sheared inserts in the presence of 10 ng/ml PDGF-BB (n = 4) and 0.55 ± 0.05 in the perimeter of inserts subjected to SS in the presence of 100 ng/ml PDGF-BB (n = 11).

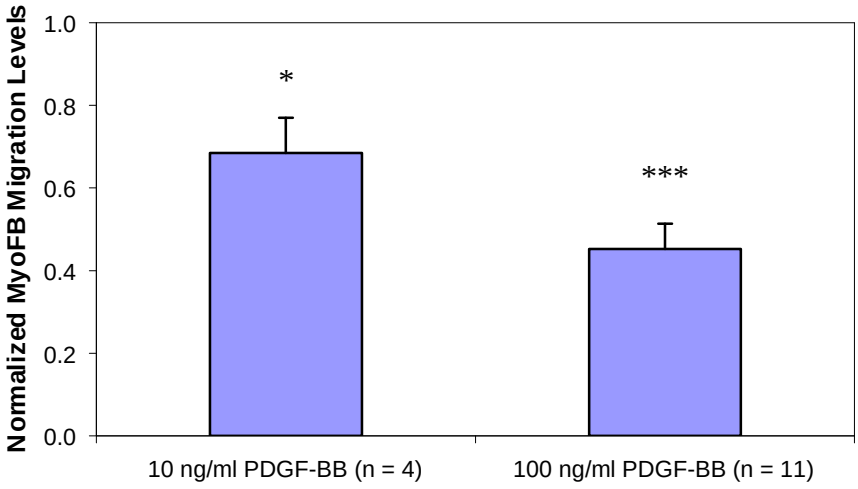

Figure 5-5: Effect of shear stress on myoFB migration levels in the central area of inserts. MyoFB migratory activity was quantified in only the central fields of inserts exposed to SS in Fig. 5-4 and was normalized by companion control (no shear exposure) levels. n represents the number of times each experimental case was completed. Data are presented as mean ± SEM. * $P < 0.05$ compared to companion control; *** $P < 0.001$ compared to companion control.

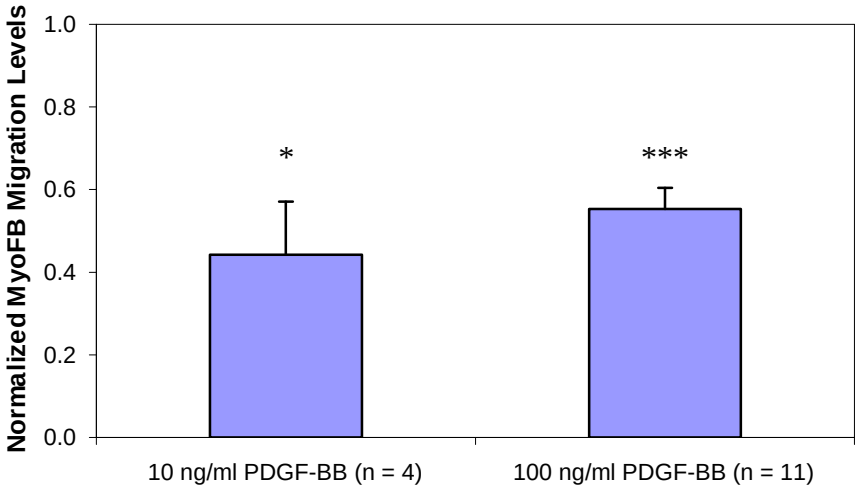

Figure 5-6: Effect of shear stress on myoFB migration levels in the perimeter of inserts. MyoFB migratory activity was quantified in only the perimeter fields of inserts exposed to SS in Fig. 5-4 and was normalized by companion control (no shear exposure) levels. n represents the number of times each experimental condition was completed. Data are presented as mean ± SEM. * $P < 0.05$ compared to companion control; *** $P < 0.001$ compared to companion control.

5.3 Effect of serum on fibroblast and myofibroblast contraction

The 60-minute contraction response of serum-starved FBs upon re-exposure to 2% serum is shown in Fig. 5-7. FBs that had been serum-starved for 4 days did not contract significantly when exposed to fresh DMEM/F12 + 1% P/S containing 2% FBS at any time point examined compared to companion time controls (exposure to fresh culture media not containing FBS; $P > 0.90$ at each time point). The normalized cell area of serum-starved FBs subjected to serum was 0.621 ± 0.049 at t = 60 min (n = 35 cells) and the normalized area of serum-starved FBs exposed to media containing no serum was

0.735 ± 0.040 at t = 60 min (n = 33 cells). In addition, FBs that were not serum-starved did not contract significantly upon exposure to culture media containing 2% FBS (P = 1.0 at all time points compared to companion time controls; Fig. 5-8). The normalized cell area of non-starved FBs exposed to culture media containing 2% serum was 0.959 ± 0.063 at t = 60 min (n = 27 cells) and the normalized area of non-starved FBs subjected to media without serum was 0.940 ± 0.062 at t = 60 min (n = 23 cells).

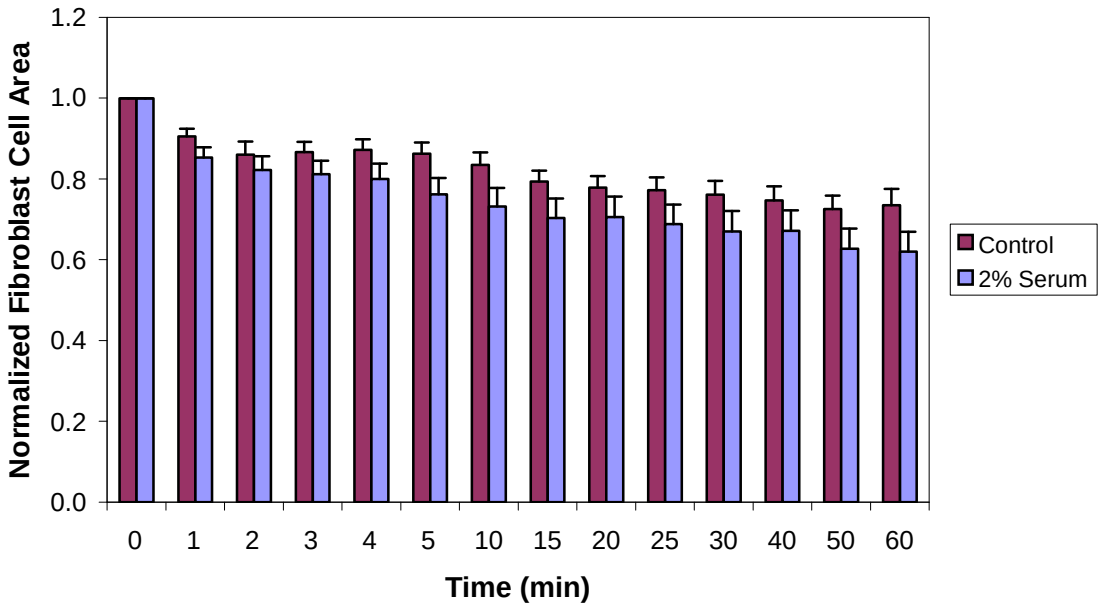

Figure 5-7: Change in normalized cell area of serum-starved FBs in response to 2% serum. Fresh DMEM/F12 + 1% P/S supplemented with 2% serum was added to glass slides containing FBs and changes in normalized cell area were quantified at designated time points up to 60 min. Under control conditions, fresh DMEM/F12 + 1% P/S without serum was added to slides containing FBs. n = 35 cells were examined at each time point for the 2% serum case and n = 33 cells were analyzed at each time point for the Control case. Data are presented as mean ± SEM. Normalized FB area in the 2% serum case was not statistically different from the companion time control normalized area at any time point examined.

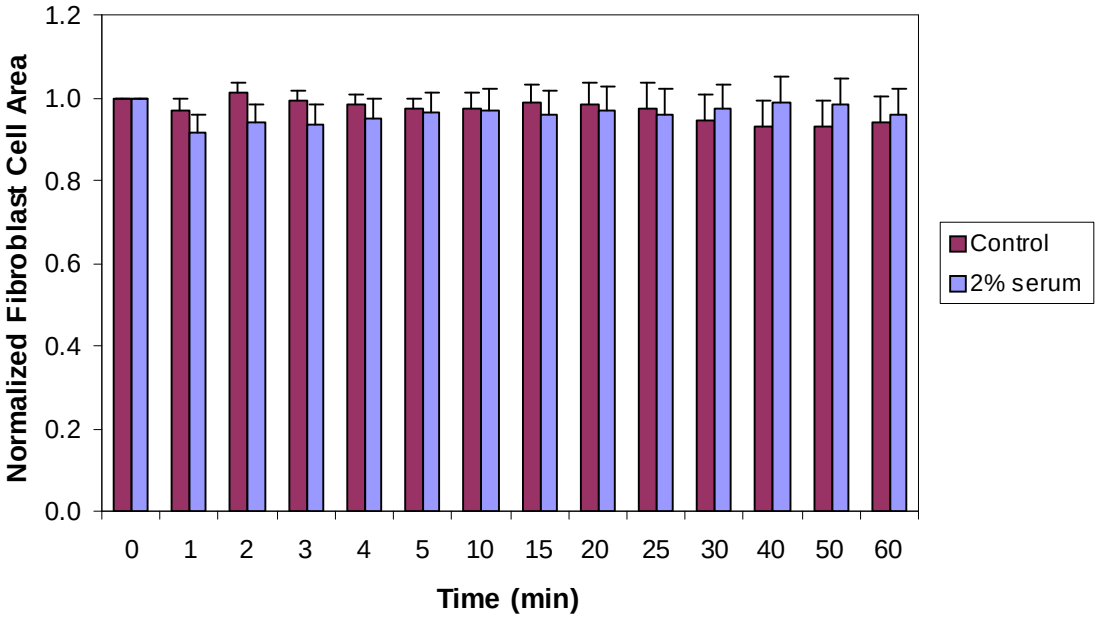

Figure 5-8: Change in normalized cell area of non-starved FBs in response to 2% serum. Fresh culture media containing either 2% serum or no serum (Control) was added to non-starved FBs plated on glass slides. Changes in normalized cell area were quantified at designated time points up to 60 min. n = 27 cells were analyzed at each time point for the 2% serum case and n = 23 cells were examined at each time point for the Control case. Data are presented as mean ± SEM. Normalized non-starved FB area in the 2% serum case was not statistically different from the companion time control normalized area at any time point examined.

The 60-minute contraction response to 2% serum was also quantified for serum-starved myoFBs and is displayed in Fig. 5-9. Serum-starved myoFBs contracted significantly to culture media containing 2% FBS 2 min following exposure ($P < 0.01$ with respect to companion time control; n = 35 cells) and this contraction remained significant at each subsequent time point evaluated up to and including t = 60 min ($P < 0.001$ in each case). The normalized cell area of serum-starved myoFBs subjected to media supplemented with 2% FBS was 0.446 ± 0.056 at t = 60 min (n = 22 cells). The

normalized area of serum-starved myoFBs subjected to DMEM/F12 + 1% P/S without serum was 0.899 ± 0.034 at t = 60 min (n = 24 cells). Non-starved myoFBs did not contract significantly upon exposure to 2% serum ($P > 0.34$ compared to companion time control at each time point; Fig. 5-10). The normalized cell area of non-starved myoFBs 60 min following exposure to DMEM/F12 + 2% FBS + 1% P/S was 1.045 ± 0.018 (n = 35 cells) and the normalized area of non-starved myoFBs exposed to culture media not containing serum was 0.955 ± 0.031 at t = 60 min (n = 31 cells).

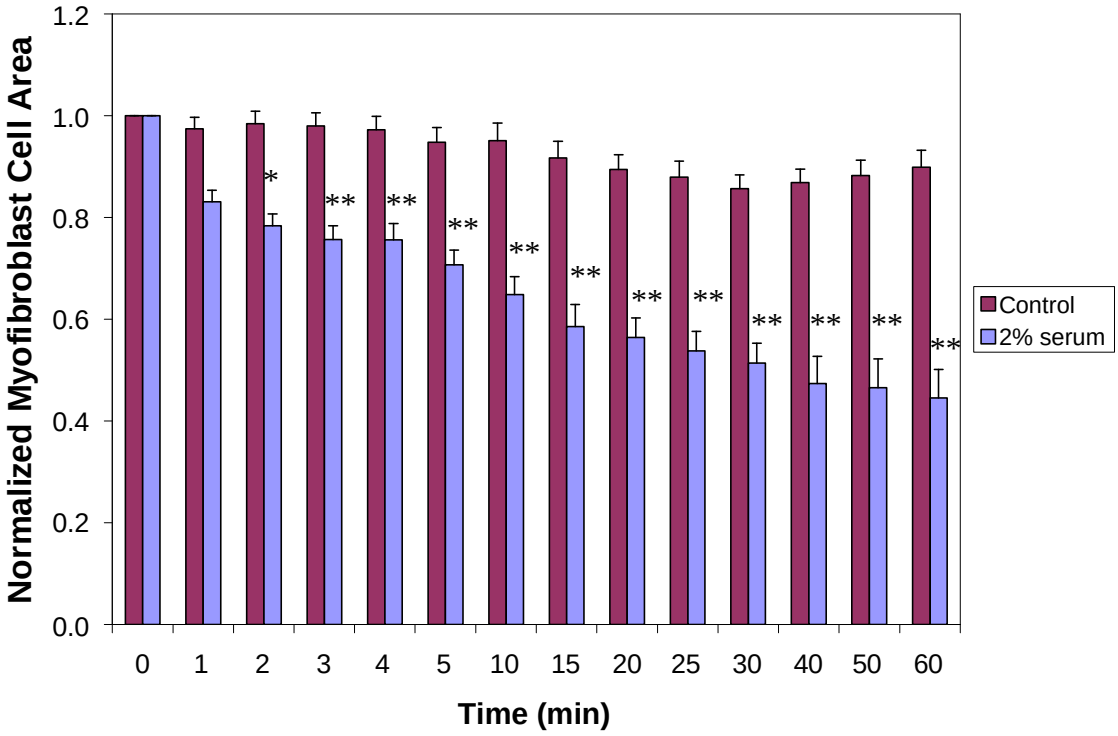

Figure 5-9: Change in normalized cell area of serum-starved myoFBs upon exposure to 2% serum. Fresh culture media supplemented with 2% serum was added to myoFBs plated on glass slides. Changes in normalized cell area were determined at designated time points up to and including 60 min. Control conditions were those in which fresh culture media containing no serum was added to slides containing myoFBs. For the 2% serum case, n = 35 cells were examined at the 0-10, 20, 25, and 30 min time points, n = 28 cells were analyzed at t = 15 min, and n = 22 cells were examined at t = 40, 50, and 60 min. For the control condition, n = 29 cells were analyzed from 0-30 min and n = 24 cells were analyzed at t = 40, 50, and 60 min. Data are presented as mean ± SEM. * $P < 0.01$ compared to companion time control; ** $P < 0.001$ compared to companion time control.

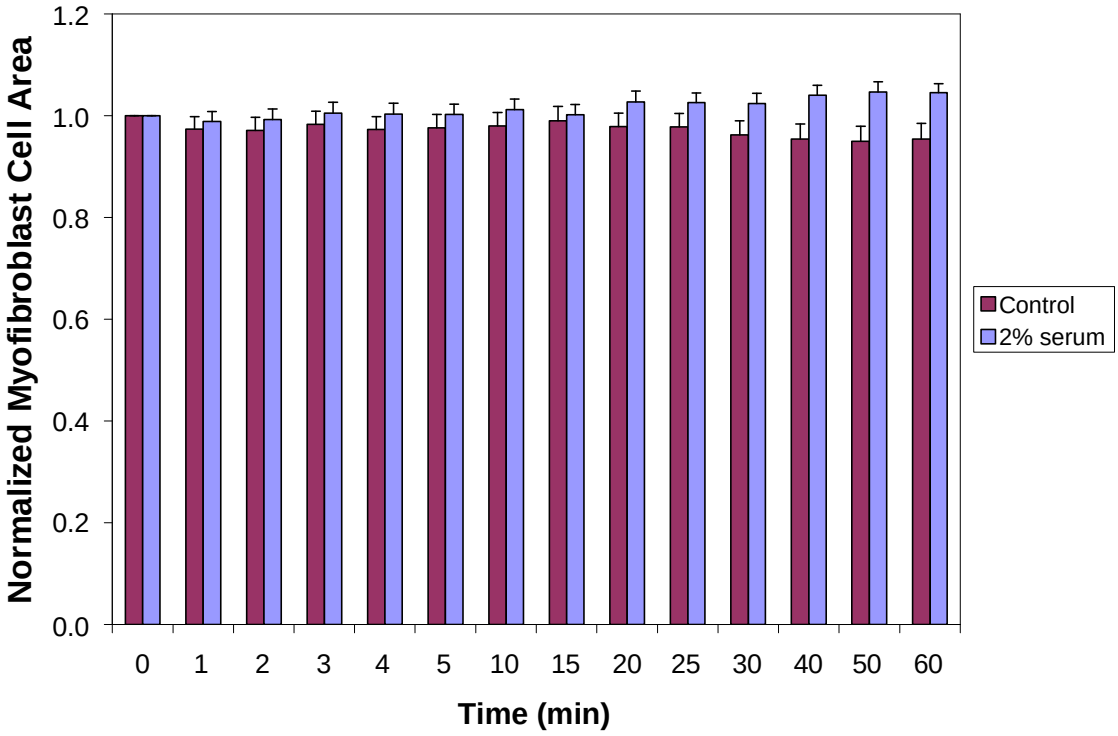

Figure 5-10: Change in normalized cell area of non-starved myoFBs in response to 2% serum. Fresh DMEM/F12 + 1% P/S with 2% FBS was added to myoFBs plated on glass slides and changes in normalized cell area were quantified at designated time points up to and including 60 min. Under control conditions, fresh DMEM/F12 + 1% P/S without FBS was added to myoFBs plated on glass slides. n = 35 cells were analyzed at each time point in the 2% FBS case and n = 31 cells were analyzed at each time point in the control case. Data are presented as mean ± SEM. Normalized non-starved myoFB cell area in the 2% serum case was not statistically different from the companion time control normalized area at any time point evaluated.

FB and myoFB subpopulations were also characterized by the percentage of serum-starved cells that contracted upon exposure to serum. A cell was considered to have "contracted" if its normalized area at t = 60 min was less than the normalized area for the respective control population (exposure to fresh culture media without serum) at t = 60 min. Using this criterion, 54% (19 of 35 cells) of the serum-starved FBs contracted

and 82% (18 of 22 cells) of the serum-starved myoFBs contracted (Fig. 5-11). There was no significant difference in normalized area between the two subpopulations at any time point analyzed for these contracting cells ($P > 0.05$ in each case).

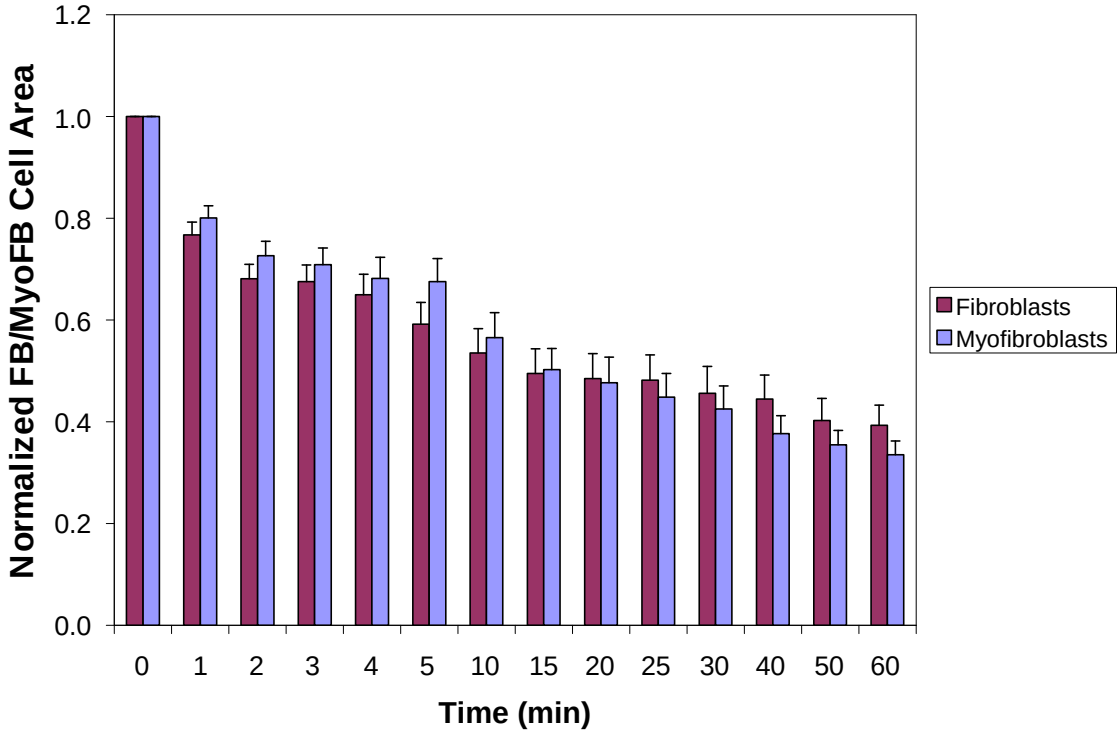

Figure 5-11: Change in normalized cell area of "contracting" serum-starved FBs and myoFBs in response to 2% serum. Cells were considered to have contracted if their normalized area at t = 60 min was less than the 60 min normalized area for the respective control condition (exposure to fresh culture media not containing serum). Based on this criterion, 54% of FBs contracted while 82% of myoFBs contracted. Data are presented as mean ± SEM. Normalized cell areas of the two contracting cell populations were not statistically different at any time point analyzed.

Chapter 6

DISCUSSION (PART 2): CHARACTERIZATION OF TWO DISTINCT POPULATIONS OF ADVENTITIAL FIBROBLASTS

The results of the second part of this thesis suggest that two subpopulations of adventitial fibroblasts, one maintained at subconfluent culture conditions (FBs) and the other maintained at confluent culture conditions (myoFBs), display marked differences in their phenotype marker expression as well as their responses to mechanical and chemical stimulation. FBs in culture express a modest amount of SM-specific α-actin and virtually no SM-MHC (Table 5-1), enhance their migratory activity in response to two doses of PDGF-BB upon exposure to 4 h of 20 dyn/cm^2 SS (Fig. 5-1), and do not contract significantly when serum-starved and subjected to culture media containing 2% serum (Fig. 5-7). Myofibroblasts, on the other hand, express abundant SM-specific α-actin and a minimal amount of SM-MHC in culture (Table 5-1), reduce their migration levels in response to SS (Fig. 5-4), and contract significantly when serum-starved and exposed to culture media supplemented with 2% serum (Fig. 5-9). The migratory response to SS and contractile response to 2% serum displayed by myoFBs are similar to behavior reported previously in rat aortic SMCs (1, 33). The present work is, to our knowledge, the first to characterize the effects of shear stress on adventitial fibroblast function (migration), the first to characterize adventitial fibroblast contraction in response to stimulation by serum, and the first to demonstrate fibroblast differentiation induced by state of confluence in culture.

It has been hypothesized that FBs, myoFBs, and SMCs all derive from a common progenitor cell and that these cell populations are distinguishable through the varied expression of phenotypic markers. Among these markers are SM α-actin, one of the proteins expressed earliest during SMC differentiation, and SM-MHC, which is only expressed by mature SMCs (81). FBs express neither SM α-actin nor SM-MHC, myoFBs express SM α-actin but not SM-MHC, and fully differentiated SMCs express both SM α-actin and SM-MHC (103). These established conventions were used to label the cells maintained at subconfluent culture conditions "fibroblasts" and those maintained at confluent culture conditions "myofibroblasts" (see Table 5-1). It should be noted that both cell populations used in this work were obtained from the same primary culture, the only difference between them being the degree of confluence they were maintained at during expansion in culture. A 3-fold increase in SM α-actin expression in myoFBs relative to FBs indicates variation in phenotype between the two cell populations and suggests a novel cell culture technique that allows for examination of two distinct cell populations from the same initial primary culture.

Serum-starving, a cell culture technique used to transform SMCs from a proliferative, synthetic phenotype to a quiescent, contractile phenotype *in vitro* (1, 2, 18), enhanced myoFB SM-MHC expression by a factor of 2.9 (Table 5-1). A majority (93.9%) of non-starved myoFBs expressed SM α-actin and serum-starving therefore had a negligible effect on further expression. Serum-starving elevated FB SM α-actin expression by a factor of 2.4 compared to non-starved FBs and enhanced FB SM-MHC expression to 28.5% of cells examined, a 66.9-fold increase compared to non-starved FBs. Because serum-starving increased both FB and myoFB phenotypic marker

expression, the contractile response of both cell populations upon re-exposure to 2% serum following serum-starvation was quantified. Similar experiments conducted on serum-starved SMCs showed that 2% serum elicited significant contraction within 5 mins of exposure that remained significant after 30 mins (1). Data presented here indicate that exposure to serum results in a similar response in serum-starved myoFBs. Serum induced significant contraction in serum-starved myoFBs following 2 mins of exposure and this contraction remained significant at each time point examined up to 60 mins (Fig. 5-9). The normalized cell area for serum-starved myoFBs following 30 mins of exposure to 2% serum (0.514 ± 0.039; Fig. 5-9) was virtually identical to that reported previously for serum-starved SMCs (0.519 ± 0.063) (1). As was the case with non-starved SMCs (1), non-starved myoFBs did not contract when subjected to 2% serum at any time point (Fig. 5-10), indicating our ability to manipulate cell phenotype through serum-starvation. Although serum-starving elevated FB expression of SM α-actin to a level near that expressed by serum-starved myoFBs and FB SM-MHC expression to a level greater than that expressed by serum-starved myoFBs (Table 5-1), serum-starved FBs did not contract to serum at any time point examined (Fig. 5-7).

The difference in the contraction response to serum between serum-starved FBs and myoFBs, although they express similar levels of SM α-actin and SM-MHC (Table 5-1), may be attributed to the fact that the expression of only one isoform of actin and one isoform of MHC was quantified in this study. It is likely that myoFB expression of non-muscle (NM) myosin is greater than that of FBs, providing them with the additional microfilamentous apparatus necessary for contraction (103). Others have suggested that FBs *in vivo* lack the contractile apparatus characteristic of myoFBs (30). The fractions of

the FB (54% of cells analyzed) and myoFB (82% of cells analyzed) populations that "contracted" showed very similar dynamic contractile responses to 2% serum (Fig. 5-11).

Li et al. (66) provided evidence that adventitial fibroblasts respond to mechanical stimulation by showing that conditioned media obtained from FBs subjected to mechanical stretch *in vitro* induced significant FB migration in a Boyden chamber assay. This, coupled with studies that have shown that SMC migration levels are attenuated by SS (33, 83), motivated the present study into the role of SS on FB and myoFB migration. The results indicate that, as was the case with chemical stimulation (contraction to serum), FBs and myoFBs have distinct responses to mechanical stimulation. In experiments conducted in a similar manner to those reported previously by Garanich et al. for SMCs (33), FB migratory activity was enhanced in response to 4 h of 20 dyn/cm^2 SS (Fig. 5-1), whereas the same SS levels downregulated myoFB migration levels (Fig. 5-4). The inhibition of migration observed for myoFBs in this study (approximately 53%) was not as drastic as the inhibition of SMC migration in response to 4 h of 20 dyn/cm^2 SS reported earlier (approximately 88%; Fig. 3-3). This is in contrast to the serum-starved myoFB contraction response to re-exposure to 2% serum (Fig. 5-9), which was very similar to the SMC response reported by Ainslie et al. (1). It appears that although myoFBs are "SMC-like" and display various SMC properties, they are not fully differentiated SMCs and therefore do not display responses to all stimuli that are entirely characteristic of SMCs.

6.1 Implications for intimal hyperplasia

The primary finding of this portion of the thesis, that FBs and myoFBs respond differently to both chemical and mechanical stimulation, has implications for vascular cell involvement in intimal thickening. FBs have been shown to participate in intimal lesions (63, 105, 110, 117) and shear-induced FB migration likely contributes to this pathological process as follows. When a vessel is injured (endothelial damage), transvascular interstitial flow increases (doubles in a medium-sized artery) which results in increased SS on adventitial FBs, stimulating their migration to the intima. Under the same injury conditions, damage to the internal elastic lamina removes the funneling mechanism responsible for exposing the superficial layer of SMCs to elevated SS levels (131) (and inhibiting their migration) and results in increased SMC migration and their contribution to intimal lesion formation.

6.2 Implications for capillary arterialization

The distinct FB and myoFB migratory responses to SS revealed in the present study also allow for a new interpretation of the role of mechanical stresses in the capillary arterialization process proposed by others (Fig. 6-1) (92-96, 118, 119). Price and colleagues have provided evidence that capillaries connecting two high-pressure arteriolar trees are exposed to elevated luminal pressures and therefore elevated circumferential wall stresses compared to neighboring capillaries in processes such as wound healing and exercise hypertrophy (92-96, 118, 119). They hypothesize that elevated wall stresses recruit SM-like cells to the arterializing vessel by enhancing EC

growth factor release. Another view of this process is that elevated luminal pressure drives elevated interstitial flow (shown in red in Fig. 6-1) through the capillary wall and into the interstitial space surrounding the vessel. FBs located adjacent to the arterioles are thereby exposed to elevated levels of interstitial flow SS, which in conjunction with EC-derived growth factor production, recruits FBs to the arterializing vessel. As these cells near the vessel and come into closer contact with neighboring cells, they differentiate to a SM-like (myoFB) phenotype, their migration is suppressed, and they integrate into the vessel wall.

In summary, the work conducted in this part of the thesis showed that two populations of rat adventitial FBs derived from the same primary culture, differing only in their treatment in culture (subconfluent FBs and confluent myoFBs), exhibited marked differences in their responses to both mechanical (shear stress) and chemical (serum) stimulation. These results allow for new views of FB participation in physiologic and pathologic processes on both the macrocirculatory and microcirculatory levels.

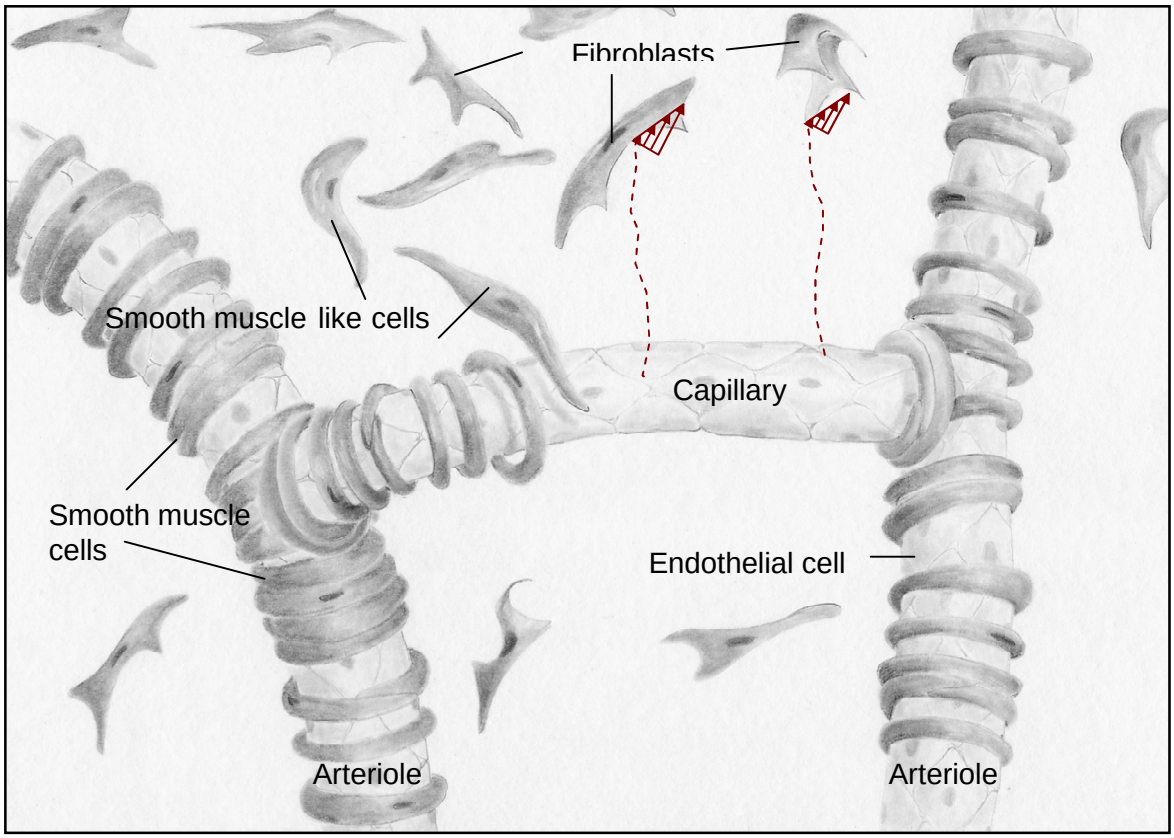

Figure 6-1: Schematic of proposed capillary arterialization process. Here, a capillary connecting two high-pressure arteriolar trees has begun to arterialize. Interstitial flow (shown in red) is enhanced due to elevated a higher capillary luminal pressure with respect to other capillaries. This elevated pressure results in: (1) elevated interstitial flow SS experienced by FBs located adjacent to the arterioles and (2) elevations in circumferential wall stress which increase endothelial cell production of growth factors such as PDGF. These processes work together to recruit FBs to the arterializing capillary. As they approach the vessel, FBs come into closer contact with neighboring cells and differentiate to a SM-like, myofibroblast phenotype as they attach to the abluminal side of the capillary wall. This hypothesis is based on previous work that elucidated the role of mechanical stresses on capillary arterialization (92-96, 118, 119).

Chapter 7

FUTURE WORK

The results of the initial study in this thesis (Chapter 3) provided the first direct evidence that fluid SS acts to inhibit SMC migration via the NO-mediated downregulation of SMC MMP-2 activity. Although this 2-dimensional study broadened our understanding of the role of SS in SMC migration, more physiologic 3-dimensional experiments are now required for improved understanding. Our lab (142) and others (121) have reported that SMCs respond quite differently to both mechanical and chemical stimulation when cultured on a 2-dimensional surface compared with a 3-dimensional gel. Therefore, it is of great importance to conduct experiments in which SMCs are suspended in gels representing the extracellular matrix *in vivo* (e.g. type I collagen) and are subjected to realistic levels of transmural interstitial flow (SS). In this manner, the role of SS on SMC migration and contraction can be evaluated. The biochemical mechanisms underlying these responses can also be determined using molecular biology approaches (Western blotting and ELISA) similar to the 2-dimensional studies. Co-culture experiments in which a monolayer of ECs is plated on a gel seeded with SMCs would shed light on the role of EC-SMC communication on the effect of physiological levels of transmural interstitial flow on EC transport properties as well as SMC migration and contraction.

The data presented in Chapter 5 in which two distinct populations of adventitial fibroblasts were characterized (FBs and myoFBs) based on their expression of SM-

specific phenotypic markers as well as their responses to both mechanical (SS) and chemical (exposure to serum) stimulation represent a new research direction for our lab. These initial results provide the impetus for numerous future studies. In particular, the shear-mediated increase in FB migration represents a pathologic condition in which FBs are subjected to elevated levels of SS during arterial injury, which stimulates their migration to the intima and accelerates lesion formation. MMP-2 and MMP-9 have been shown to play a role in FB migration (111). Therefore, their role in the shear-mediated increase in FB migratory activity should be evaluated. Pharmacological agents able to suppress FB migration in response to SS should be tested. Both rapamycin (91) and paclitaxel (147), two compounds widely used in drug-eluting stents to prevent restenosis, have inhibited SMC migration *in vitro*, so it seems plausible that they will attenuate FB migration levels as well. Rapamycin was also reported to reduce IH in a rat model of balloon angioplasty while suppressing MMP-2 and MMP-9 levels (139).

The serum-starved myoFB contractile response to serum (Fig. 5-9) was similar in nature to that observed previously in serum-starved SMCs (1). Serum-starved SMCs have also been reported to contract significantly in response to SS (2, 18). Therefore, studies of the role of SS on serum-starved myoFB contraction should be conducted and could elucidate the involvement of myoFBs in physiologic processes such as the myogenic response.

FBs and myoFBs are exposed to interstitial SS as they migrate to an arterializing capillary. Accordingly, the effect of SS on FB expression of SM α-actin (differentiation to myoFBs) and myoFB expression of SM-MHC (differentiation to SMCs) should also be evaluated. These experiments could shed light on the role of interstitial flow SS on the

differentiation of FBs to a SM-like phenotype as they attach to the abluminal side of an arterializing capillary.

As is the case with SMCs, FBs and myoFBs reside in a 3-dimensional extracellular matrix *in vivo*. Therefore, upon completion of the 2-dimensional experiments proposed above, FBs and myoFBs should be seeded in 3-dimensional gels and subjected to physiologic levels of interstitial flow SS and its role in modulating their phenotype marker expression, contraction, and migration evaluated.

REFERENCES

1. **Ainslie K, Shi ZD, Garanich JS, and Tarbell JM.** Rat aortic smooth muscle cells contract in response to serum and its components in a calcium dependent manner. *Ann Biomed Eng* 32: 1667-1675, 2004.

2. **Ainslie KM, Garanich JS, Dull RO, and Tarbell JM.** Vascular smooth muscle cell glyocalyx influences shear stress-mediated contractile response. *J Appl Physiol* 98: 242-249, 2005.

3. **Alshihabi SN, Chang YS, Frangos JA, and Tarbell JM.** Shear stress-induced release of PGE_2 and PGI_2 by vascular smooth muscle cells. *Biochem Biophys Res Comm* 224: 808-824, 1996.

4. **Ambalavanan N, Mariani G, Bulger A, and III JBP.** Role of nitric oxide in regulating neonatal porcine pulmonary artery smooth muscle cell proliferation. *Biol Neonate* 76: 291-300, 1999.

5. **Barrett TB and Benditt EP.** Platelet-derived growth factor gene expression in human atherosclerotic plaques and normal artery wall. *Proc Natl Acad Sci USA* 85: 2810-2814, 1988.

6. **Bassiouny HS, Song RH, Hong XF, Singh A, Kocharyan H, and Glagov S.** Flow regulation of 72-kD collagenase IV (MMP-2) after experimental arterial injury. *Circulation* 98: 157-163, 1998.

7. **Bendeck MP, Irvin C, and Reidy MA.** Inhibition of matrix metalloproteinase activity inhibits smooth muscle cell migration but not neointimal thickening after arterial injury. *Circ Res* 78: 38-43, 1996.

8. **Bendeck MP, Zempo N, Clowes AW, Galardy RE, and Reidy MA.** Smooth muscle cell migration and matrix metalloproteinase expression after arterial injury in the rat. *Circ Res* 75: 539-545, 1994.

9. **Bercelli SA, Davies MG, Kenagy RD, and Clowes AW.** Flow-induced neointimal regression in baboon polytetrafluoroethylene grafts is associated with decreased cell proliferation and increased apoptosis. *J Vasc Surg* 36: 1248-1255, 2002.

10. **Bodin P, Richard S, Travo C, Berta P, Stoclet J, Papin S, and Travo P.** Responses of subcultured rat aortic smooth muscle myocytes to vasoactive agents and KCl depolariation. *Am J Physiol Cell Physiol* 260: C151-C158, 1991.

11. **Bogatcheva NV, Verin AD, Wang P, Birukova AA, Birukova KG, Mirzopoyazova T, Adyshev DM, Chiang ET, Crow MT, and Garcia JG.** Phorbol esters increase MLC phosphorylation and actin remodeling in bovine lung endothelium without increase contraction. *Am J Physiol Lung Cell Mol Physiol* 285: L415-L426, 2003.

12. **Bowen-Pope DF, Hart CE, and Seifert RA.** Sera and conditioned media contain different isoforms of platelet-derived growth factor (PDGF) which bind to different classes of PDGF receptor. *J Biol Chem* 264: 2502-2508, 1989.

13. **Brinkman HC.** A calculation of the viscous force exerted by a flowing fluid on a dense swarm of particles. *Appl Sci Res* A1: 27-34, 1947.

14. **Chang Y, Munn L, Hillsley M, Dull R, Yuan J, Lakshiminarayanan S, Gardner T, Jain R, and Tarbell JM.** Effect of vascular endothelial growth factor on cultured endothelial cell monolayer transport properties. *Microvasc Res* 59: 265-277, 2000.

15. **Chang YS, Yaccino JA, Lakshminarayanan S, Frangos JA, and Tarbell JM.** Shear-induced increase in hydraulic conductivity in endothelial cells is mediated by a nitric oxide-dependent mechanism. *Arterioscler Thromb Vasc Biol* 20: 35-42, 2000.

16. **Chen C, Hanson SR, Keefer LK, Saavedra JE, Davies KM, Hutsell TC, Hughes JD, Ku DN, and Lumsden AB.** Boundary layer infusion of nitric oxide reduces early smooth muscle cell proliferation in the endarterectomized canine artery. *J Surg Res* 67: 26-32, 1997.

17. **Chesler NC, Ku DN, and Galis ZS.** Transmural pressure induces matrix-degrading activity in porcine arteries ex vivo. *Am J Physiol* 277 (Heart Circ. Physiol. 46): H2002-H2009, 1999.

18. **Civelek M, Ainslie K, Garanich JS, and Tarbell JM.** Smooth muscle cells contract in response to fluid flow via a Ca^{2+} independent signaling mechanism. *J Appl Physiol* 93: 1907-1917, 2002.

19. **Clark JM and Glagov S.** Transmural organization of the arterial media. The lamellar unit revisited. *Arteriosclerosis* 5: 19-34, 1985.

20. **Clowes AW, Kirkman TR, and Clowes MM.** Mechanisms of arterial graft failure 4: Chronic endothelial and smooth muscle cell proliferation in healing polytetrafluoroethylene prostheses. *J Vasc Surg* 3: 877-884, 1986.

21. **Clunn GF, Refson JS, Lymn JS, and Hughes AD.** Platelet-derived growth factor beta-receptors can both promote and inhibit chemotaxis in human vascular smooth muscle cells. *Arterioscler Thromb Vasc Biol* 17: 2622-2629, 1997.

22. **Dai J, Losy F, Guinault AM, Pages C, Anegon I, Desgranges P, Becquemin JP, and Allaire E.** Overexpression of transforming growth factor-beta1 stabilizes already-formed aortic aneurysms: a first approach to induction of functional healing by endovascular gene therapy. *Circulation* 112: 1008-1015, 2005.

23. **Davies MG, Owens EL, Mason DP, Lea H, Tran PK, Vergel S, Hawkins SA, Hart CE, and Clowes AW.** Effect of platelet-derived growth factor receptor-alpha and -beta blockade on flow-induced neointimal formation in endothelialized baboon vascular grafts. *Circ Res* 86: 779-786, 2000.

24. **Davignon J and Ganz P.** Role of endothelial dysfunction in atherosclerosis. *Circulation* 109[suppl III]: III-27-III-32, 2004.

25. **DeMaio L, Chang YS, Gardner TW, Tarbell JM, and Antonetti DA.** Shear stress regulates occludin content and phosphorylation. *Am J Physiol Heart Circ Physiol* 281: H105-H113, 2001.

26. **DeMeyer GRY, Put DJMV, Kockx MM, Schil PV, Bosmans R, Bult H, Buyssens N, Vanmaele R, and Herman AG.** Possible mechanisms of collar-induced intimal thickening. *Arterioscler Thromb Vasc Biol* 17: 1924-1930, 1997.

27. **Dobrian A, Wade SS, and Prewitt RL.** PDGF-A expression correlates with blood pressure and remodeling in 1K1C hypertensive rat arteries. *Am J Physiol Heart Circ Physiol* 276: H2159-H2167, 1999.

28. **Fay F and Delise C.** Contraction of isolated smooth muscle cells - structural changes. *Proc Natl Acad Sci USA* 70: 641-645, 1973.

29. **Fredriksson L, Li H, and Eriksson U.** The PDGF family: four gene products from five dimeric isoforms. *Cytokine and Growth Factor Reviews* 15: 197-204, 2004.

30. **Gabbiani G.** The myofibroblast in wound healing and fibrocontractive diseases. *J Pathol* 200: 500-503, 2003.

31. **Galis ZS and Khatri JJ.** Matrix metalloproteinases in vascular remodeling. The good, the bad, and the ugly. *Circ Res* 90: 251-262, 2002.

32. **Ganong WF.** *Review of medical physiology.* Stamford, CT: Appleton & Lange, 1999.

33. **Garanich JS, Pahakis M, and Tarbell JM.** Shear stress inhibits smooth muscle cell migration via nitric oxide-mediated downregulation of matrix metalloproteinase-2 activity. *Am J Physiol Heart Circ Physiol* 288: 2244-2252, 2005.

34. **Geary RL, Kohler TR, Vergel S, Kirkman TR, and Clowes AW.** Time course of flow-induced smooth muscle cell proliferation and intimal thickening in endothelialized baboon vascular grafts. *Circ Res* 74: 14-23, 1993.

35. **Gorog P and Kovacs IB.** Inhibition of vascular smooth muscle cell migration by intact endothelium is nitric oxide-mediated: interference by oxidised low density lipoproteins. *J Vasc Res* 35: 165-169, 1998.

36. **Gosgnach W, Challah M, Coulet F, Michel JB, and Battle T.** Shear stress induces angiotensin converting enzyme expression in cultured smooth muscle cells: possible involvement of bFGF. *Cardiovasc Res* 45: 486-492, 2000.

37. **Gosgnach W, Messika-Zeitoun D, Gonzalez W, Philipe M, and Michel JB.** Shear stress induces iNOS expression in cultured smooth muscle cells: role of oxidative stress. *Am J Physiol Cell Physiol* 279: C1880-C1888, 2000.

38. **Grainger DJ, Weissberg PL, and Metcalfe JC.** Tamoxifen decreases the rate of proliferation of rat vascular smooth muscle cells in culture by inducing production of transforming growth factor beta. *Biochem J* 294, 1993.

39. **Grotendorst GR, Chang T, Seppa HEJ, Kleinman HK, and Martin GR.** Platelet-derived growth factor is a chemoattractant for vascular smooth muscle cells. *J Cell Physiol* 113: 261-266, 1982.

40. **Grotendorst GR, Seppa HEJ, Kleinman HK, and Martin GR.** Attachment of smooth muscle cells to collagen and their migration toward platelet-derived growth factor. *Proc Natl Acad Sci USA* 78: 3669-3672, 1981.

41. **Groves PH, Banning AP, Penny WJ, Newby AC, Cheadle HA, and Lewis MJ.** The effects of exogenous nitric oxide on smooth muscle cell proliferation following porcine carotid angioplasty. *Cardiovasc Res* 30: 87-96, 1995.

42. **Gurjar MV, Sharma RV, and Bhalla RC.** eNOS gene transfer inhibits smooth muscle cell migration and MMP-2 and MMP-9 activity. *Arterioscler Thromb Vasc Biol* 19: 2871-2877, 1999.

43. **Guyton AC, Scheel K, and Murphree D.** Interstitial fluid pressure. III. Its effect on resistance to tissue fluid mobility. *Circ Res* 19: 412-419, 1966.

44. **Halloran BG, Prorok GD, So BJ, and Baxter BT.** Transforming growth factor-beta 1 inhibits human arterial smooth muscle cell proliferation in a growth-rate-dependent manner. *Am J Surg* 170: 193-197, 1995.

45. **Heldin C-H and Westermark B.** Mechanism of action and in vivo role of platelet-derived growth factor. *Physiol Rev* 79: 1283-1316, 1999.

46. **Hosang M, Rouge M, Wipf B, Eggimann B, Kaufmann F, and Hunziker W.** Both homodimeric isoforms of PDGF (AA and BB) have mitogenic and chemotactic activity and stimulate phosphoinositol turnover. *J Cell Physiol* 140: 558-564, 1989.

47. **Huang Y, Rumschitzki D, Chien S, and Weinbaum S.** A fiber matrix model for the growth of macromolecular leakage spots in the arerial intima. *J Biomech Eng* 116: 430-445, 1994.

48. **Hughes AD, Clunn GF, Refson J, and Demoliou-Mason C.** Platelet-derived growth factor (PDGF): actions and mechanisms in vascular smooth muscle. *Gen Pharmac* 27: 1079-1089, 1996.

49. **Jawien A, Bowen-Pope DF, Lindner V, Schwartz SM, and Clowes AW.** Platelet-derived growth factor promotes smooth muscle cell migration and intimal thickening in a rat model of balloon angioplasty. *J Clin Invest* 89: 507-511, 1992.

50. **Jenkins GM, Crow MT, Bilato C, Gluzband Y, Ryu W-S, Li Z, Stetler-Stevenson W, Nater C, Froehlich JP, Lakatta EG, and Cheng L.** Increased expression of membrane-type matrix metalloproteinase and preferential localization of matrix metalloproteinase-2 to the neointima of balloon-injured rat carotid arteries. *Circulation* 97: 82-90, 1998.

51. **Kenagy RD and Clowes AW.** A possible role for MMP-2 and MMP-9 in the migration of primate arterial smooth muscle cells through native matrix. *Ann NY Acad Sci* 732: 462-465, 1994.

52. **Kenagy RD, Fischer JW, Davies MG, Berceli SA, Hawkins SM, Wight TN, and Clowes AW.** Increased plasmin and serine proteinase activity during flow-induced intimal atrophy in baboon PTFE grafts. *Arterioscler Thromb Vasc Biol* 22: 400-404, 2002.

53. **Kenagy RD, Hart CE, Stetler-Stevenson WG, and Clowes AW.** Primate smooth muscle cell migration from aortic explants is mediated by endogenous platelet-derived growth factor and basic fibroblast growth factor acting through matrix metalloproteinases 2 and 9. *Circulation* 96: 3555-3560, 1997.

54. **Kenagy RD, Vergel S, Mattsson E, Bendeck M, Reidy MA, and Clowes AW.** The role of plasminogen, plasminogen activators, and matrix metalloproteinases in primate arterial smooth muscle cell migration. *Arterioscler Thromb Vasc Biol* 16: 1373-1382, 1996.

55. **Kohler TR and Jawien A.** Flow affects development of intimal hyperplasia after arterial injury in rats. *Arterioscler Thromb* 12: 963-971, 1992.

56. **Kohler TR, Kirkman TR, Kraiss LW, Zierler BK, and Clowes AW.** Increased blood flow inhibits neointimal hyperplasia in endothelialized vascular grafts. *Circ Res* 69: 1557-1565, 1991.

57. **Koyama N, Hart CE, and Clowes AW.** Different functions of the platelet-derived growth factor-alpha and -beta receptors for the migration and proliferation of cultured baboon smooth muscle cells. *Circ Res* 75: 682-691, 1994.

58. **Koyama N, Morisaki N, Saito Y, and Yoshida S.** Regulatory effects of platelet-derived growth factor-AA homodimer on migration of vascular smooth muscle cells. *J Biol Chem* 267: 22806-22812, 1992.

59. **Kraiss LW, Geary RL, Mattsson EJR, Vergel S, Au YP, and Clowes AW.** Acute reductions in blood flow and shear stress induce platelet-derived growth factor-A expression in baboon prosthetic grafts. *Circ Res* 79: 45-53, 1996.

60. **Kraiss LW, Kirkman TR, Kohler TR, Zierler B, and Clowes AW.** Shear stress regulates smooth muscle cell proliferation and neointimal thickening in porous polytetrafluoroethylene grafts. *Arterioscler Thromb* 11: 1844-1852, 1991.

61. **Lahteenmaki T, Sievi E, and Vapaatalo H.** Inhibitory effects of mesoionic 3-aryl substituted oxatriazole-5-imine derivatives on vascular smooth muscle cell mitogenesis and proliferation in vitro. *Br J Pharmacol* 125: 402-408, 1998.

62. **Lever MJ, Tarbell JM, and Caro CG.** The effect of luminal flow in the carotid artery on transmural fluid transport. *Experimental Physiology* 77: 553-563, 1992.

63. **Li G, Chen S, Oparil S, Chen Y, and Thompson JA.** Direct in vivo evidence demonstrating neointimal migration of adventitial fibroblasts after balloon injury of rat carotid arteries. *Circulation* 101: 1362-1365, 2000.

64. **Li G, Chen Y, Greene GL, Oparil S, and Thompson JA.** Estrogen inhibits vascular smooth muscle cell-dependent adventitial fibroblast migration in vitro. *Circulation* 100: 1639-1645, 1999.

65. **Li G, Chen Y, Kelpke SS, Oparil S, and Thompson JA.** Estrogen attenuates integrin-beta$_3$-dependent adventitial fibroblast migration after inhibition of osteopontin production in vascular smooth muscle cells. *Circulation* 101: 2949-2955, 2000.

66. **Li L, Couse TL, DeLeon H, Xu CP, Wilcox JN, and Chaikof EL.** Regulation of syndecan-4 expression with mechanical stress during the development of angioplasty-induced intimal thickening. *J Vasc Surg* 36: 361-370, 2002.

67. **Lindner V, Giachelli CM, Schwartz SM, and Reidy MA.** A subpopulation of smooth muscle cells in injured rat arteries express platelet-derived growth factor-B chain mRNA. *Circ Res* 76: 951-957, 1995.

68. **Lipowsky H.** Shear stress in the circulation. In: *Flow-Dependent Regulation of Vascular Function*, edited by Bevan JA, Kaley G and Rubanyi GM. Bethesda, MD: Am. Physiol. Soc., 1995, p. 28-45.

69. **Liu G, Eskin SG, and Mikos AG.** Integrin alphavbeta3 is involved in stimulated migration of vascular adventitial fibroblasts by basic fibroblast growth factor but not platelet-derived growth factor. *J Cell Biochem* 83: 129-135, 2001.

70. **MacLeod DC, Strauss BH, DeJong M, Escaned J, Umans VA, Suylen Rv, Verkerk A, deFeyter PJ, and Serruys PW.** Proliferation and extracellular matrix synthesis of smooth muscle cells cultured from human coronary atherosclerotic and restenotic lesions. *J Am Coll Cardiol* 23: 59-65, 1994.

71. **Marano G, Palazzesi S, Vergari A, and Ferrari AU.** Protection by shear stress from collar-induced intimal thickening. *Arterioscler Thromb Vasc Biol* 19: 2609-2614, 1999.

72. **Mattsson EJR, Kohler TR, Vergel SM, and Clowes AW.** Increased blood flow induces regression of intimal hyperplasia. *Arterioscler Thromb Vasc Biol* 17: 2245-2249, 1997.

73. **Miller FJ.** Adventitial fibroblasts. Backstage journeymen. *Arterioscler Thromb Vasc Biol* 21: 722-723, 2001.

74. **Misko TP, Schilling RJ, Salvemini D, Moore WM, and Currie MG.** A fluorometric assay for the measurement of nitrite in biological samples. *Anal Biochem* 214: 11-16, 1993.

75. **Mooradian DL, Hutsell TC, and Keefer LK.** Nitric oxide (NO) donor molecules: effect of NO release on vascular smooth muscle cell proliferation in vitro. *J Cardiovasc Pharmacol* 25: 674-678, 1995.

76. **Murphy G, Stanton H, Cowell S, Butler G, Knauper V, Atkinson S, and Gavrilovic J.** Mechanisms for pro matrix metalloproteinase activation. *APMIS* 107: 38-44, 1999.

77. **Nabel EG, Yang Z, Liptay S, San H, Gordon D, Haudenschild CC, and Nabel GJ.** Recombinant platelet-deried growth factor B gene expression in porcine arteries induces intimal hyperplasia in vivo. *J Clin Invest* 91: 1822-1829, 1993.

78. **Nanjo H, Sho E, Komatsu M, Sho M, Zarins CK, and Masuda H.** Intermittent short-duration exposure to low wall shear stress induces intimal thickening in arteries exposed to chronic high shear stress. *Exp Mol Pathol*: Epub ahead of print., 2005.

79. **Osanai T, Akutsu N, Fujita N, Nakano T, Takahashi K, Guan W, and Okumura K.** Cross talk between prostacyclin and nitric oxide under shear in smooth muscle cell: role in monocyte adhesion. *Am J Physiol Heart Circ Physiol* 281: H177-H182, 2001.

80. **Owen N.** Prostacyclin can inhibit DNA synthesis in vascular smooth muscle cells. In: *Prostaglandins, kukotrienes, and lipoxins: biochemistry, mechanisms of action, and clinical applications.*, edited by Bailey J. New York, NY: Plenum Press, 1985.

81. **Owens GK.** Regulation of differentiation of vascular smooth muscle cells. *Physiol Rev* 75: 487-517, 1995.

82. **Palumbo R, Gaetano C, Antonini A, Pompilio G, Bracco E, Ronnstrand L, Heldin C-H, and Capogrossi MC.** Different effects of high and low shear stress on platelet-derived growth factor isoform release by endothelial cells. Consequences for smooth muscle cell migration. *Arterioscler Thromb Vasc Biol* 22: 405-411, 2002.

83. **Palumbo R, Gaetano C, Melillo G, Toschi E, Remuzzi A, and Capogrossi MC.** Shear stress downregulation of platelet-derived growth factor receptor-beta and matrix metalloproteinase-2 is associated with inhibition of smooth muscle cell invasion and migration. *Circulation* 102: 225-230, 2000.

84. **Papadaki M and Eskin SG.** Effects of fluid shear stress on gene regulation of vascular cells. *Biotechnol Prog* 13: 209-221, 1997.

85. **Papadaki M, McIntire LV, and Eskin SG.** Effects of shear stress on the growth kinetics of human aortic smooth muscle cells in vitro. *Biotech Bioeng* 50: 555-561, 1996.

86. **Papadaki M, Ruef J, Nguyen KT, Li F, Patterson C, Eskin SG, McIntire LV, and Runge MS.** Differential regulation of protease activated receptor-1 and tissue plasminogen activator expression by shear stress in vascular smooth muscle cells. *Circ Res* 83: 1027-1034, 1998.

87. **Papadaki M, Tilton RG, Eskin SG, and McIntire LV.** Nitric oxide production by cultured human aortic smooth muscle cells: stimulation by fluid flow. *Am J Physiol* 274 (Heart Circ. Physiol. 43): H616-H626, 1998.

88. **Pares-Herbute N, Fliche E, and Monnier L.** Involvement of nitric oxide in the inhibition of aortic smooth muscle cell proliferation by calcium dobesilate. *Int J Angiol* 8: 5-10, 1999.

89. **Patel S, Shi Y, Niculescu R, Chung EH, Martin JL, and Zalewski A.** Characteristics of coronary smooth muscle cells and adventitial fibroblasts. *Circulation* 101: 524-532, 2000.

90. **Pauly RR, Passaniti A, Bilato C, Monticone R, Cheng L, Papadopoulos N, Gluzband YA, Smith L, Weinstein C, Lakatta EG, and Crow MT.** Migration of cultured vascular smooth muscle cells through a basement membrane barrier requires type IV collagenase activity and is inhibited by cellular differentiation. *Circ Res* 75: 41-54, 1994.

91. **Poon M, Marx SO, Gallo R, Badimon JJ, Taubman MB, and Marks AR.** Rapamycin inhibits vascular smooth muscle cell migration. *J Clin Invest* 98: 2277-2283, 1996.

92. **Price RJ, Owens GK, and Skalak TC.** Immunohistochemical identification of arteriolar development using markers of smooth muscle differentiation. Evidence that capillary arterialization proceeds from terminal arterioles. *Circ Res* 75: 520-527, 1994.

93. **Price RJ and Skalak TC.** Chronic alpha-1 adrenergic blockade stimulates terminal and arcade arteriolar growth in skeletal muscle. *Am J Physiol* 271: H752-H759, 1996.

94. **Price RJ and Skalak TC.** A circumferential wall stress-growth rule predicts arcade arteriole formation in a network model. *Microcirculation* 2: 41-51, 1995.

95. **Price RJ and Skalak TC.** Circumferential wall stress as a mechanism for arteriolar rarefaction and proliferation in a network model. *Microvascular Research* 47: 188-202, 1994.

96. **Price RJ and Skalak TC.** Prazosin administration enhances proliferation of arteriolar adventitial fibroblasts. *Microvascular Research* 55: 138-145, 1998.

97. **Pross C, Farooq MM, Angle N, Lane JS, Cerveira JJ, Xavier AE, Freischlag JA, Law RE, and Gelabert HA.** Dexamethasone inhibits vascular smooth muscle cell migration via modulation of matrix metalloproteinase activity. *J Surg Res* 102: 57-62, 2002.

98. **Ravanti L and Kahari VM.** Matrix metalloproteinases in wound repair (review). *Int J Mol Med* 6: 391-407, 2000.

99. **Reddy KB and Howe PH.** Transforming growth factor beta 1-mediated inhibition of smooth muscle cell proliferation is associated with a late G1 cell cycle arrest. *J Cell Physiol* 156: 48-55, 1993.

100. **Saltis J, Agrotis A, Kanellakis P, and Bobik A.** Developmentally regulated transforming growth factor-beta 1 action on vascular smooth muscle cell growth in the SHR. *Clin Exp Pharmacol Physiol* 21: 149-152, 1994.

101. **Sarkar R, Gordon D, Stanley JC, and Webb RC.** Dual cell-cycle specific mechanisms mediate the antimitogenic effects of nitric oxide in vascular smooth muscle cells. *J Hypertens* 15: 275-283, 1997.

102. **Sarkar R, Meinberg EG, Stanley JC, Gordon D, and Webb RC.** Nitric oxide reversibly inhibits the migration of cultured vascular smooth muscle cells. *Circ Res* 78: 225-230, 1996.

103. **Sartore S, Chiavegato A, Faggin E, Franch R, Puato M, Ausoni S, and Pauletto P.** Contribution of adventitial fibroblasts to neointima formation and vascular remodeling. From innocent bystander to active participant. *Circ Res* 89: 1111-1121, 2001.

104. **Schwartz RS.** *Coronary restenosis.* Cambridge, MA: Blackwell Scientific, 1993.

105. **Scott NA, Cipolla GD, Ross CE, Dunn B, Martin FH, Simonet L, and Wilcox JN.** Identification of a potential role for the adventitia in vascular lesion formation after balloon overstretch injury of porcine coronary arteries. *Circulation* 93: 2178-2187, 1996.

106. **Seiki M.** Membrane-type matrix metalloproteinases. *APMIS* 107: 137-143, 1999.

107. **Seki J, Nishio M, Kato Y, Motoyama Y, and Yoshida K.** FK409, a new nitric oxide donor, suppresses smooth muscle cell proliferation in the rat model of balloon angioplasty. *Atherosclerosis* 117: 97-106, 1995.

108. **Seliktar D, Nerem RM, and Galis ZS.** The role of matrix metalloproteinase-2 in the remodeling of cell-seeded vascular constructs subjected to cyclic strain. *Ann Biomed Eng* 29: 923-934, 2001.

109. **Serini G and Gabbiani G.** Mechanisms of myofibroblast activity and phenotypic modulation. *Experimental Cell Research* 250: 273-283, 1999.

110. **Shi Y, O'Brien JE, Fard A, Mannion JD, Wang D, and Zalewski A.** Adventitial myofibroblasts contribute to neointimal formation in injured porcine coronary arteries. *Circulation* 94: 1655-1664, 1996.

111. **Shi Y, Patel S, Niculescu R, Chung W, Desrochers P, and Zalewski A.** Role of matrix metalloproteinases and their tissue inhibitors in the regulation of coronary cell migration. *Arterioscler Thromb Vasc Biol* 19: 1150-1155, 1999.

112. **Shi Y, Pieniek M, Fard A, O'Brien J, Mannion JD, and Zalewski A.** Adventitial remodeling after coronary arterial injury. *Circulation* 93: 340-348, 1996.

113. **Shigematsu K, Yasuhara H, Shigematsu H, and Muto T.** Direct and indirect effects of pulsatile shear stress on the smooth muscle cell. *Int Angiol* 19: 39-46, 2000.

114. **Sho M, Sho E, Singh TM, Komatsu M, Sugita A, Xu C, Nanjo H, Zarins CK, and Masuda H.** Subnormal shear stress-induced intimal thickening requires medial smooth muscle cell proliferation and migration. *Exp Mol Pathol* 72: 150-160, 2002.

115. **Shofuda K-I, Hasenstab D, Kenagy RD, Shofuda T, Li Z-Y, Lieber A, and Clowes AW.** Membrane-type matrix metalloproteinase-1 and -3 activity in primate smooth muscle cells. *FASEB J* 15: 2010-2012, 2001.

116. **Sill HW, Chang YS, Artman JR, Frangos JA, Hollis TM, and Tarbell JM.** Shear stress increases hydraulic conductivity of cultured endothelial monolayers. *Am J Physiol Heart Circ Physiol* 268: H535-H543, 1995.

117. **Siow RCM, Mallawaarachchi CM, and Weissberg PL.** Migration of adventitial myofibroblasts following vascular balloon injury: insights from in vivo gene transfer to rat carotid arteries. *Cardiovascular Research* 59: 212-221, 2003.

118. **Skalak TC and Price RJ.** The role of mechanical stresses in microvascular remodeling. *Microcirculation* 3: 143-165, 1996.

119. **Skalak TC, Price RJ, and Zeller PJ.** Where do new arterioles come from? Mechanical forces and microvessel adaptation. *Microcirculation* 5: 91-94, 1998.

120. **Song RH, Kocharyan HK, Fortunato JE, Glagov S, and Bassiouny HS.** Increased flow and shear stress enhance transforming growth factor-beta 1 after experimental arterial injury. *Arterioscler Thromb Vasc Biol* 20: 923-930, 2000.

121. **Stegemann JP and Nerem RM.** Altered response of vascular smooth muscle cells to exogenous biochemical stimulation in two- and three-dimensional culture. *Experimental Cell Research* 283: 146-155, 2003.

122. **Sterpetti AV, Cucina A, D'Angelo LS, Cardillo B, and Cavallaro A.** Response of arterial smooth muscle cells to laminar flow. *J Cardiovasc Surg* 33: 619-624, 1992.

123. **Sterpetti AV, Cucina A, Fragale A, Lepidi S, Cavallaro A, and Santoro-D'Angelo L.** Shear stress influences the release of platelet derived growth factor and basic fibroblast growth factor by arterial smooth muscle cells. *Eur J Vasc Surg* 8: 138-142, 1994.

124. **Sterpetti AV, Cucina A, Napoli F, Shafer H, Cavallaro A, and D'Angelo LS.** Growth factor release by smooth muscle cells is dependent on haemodynamic factors. *Eur J Vasc Surg* 6: 636-638, 1992.

125. **Sterpetti AV, Cucina A, Santoro-D'Angelo L, Cardillo B, and Cavallaro A.** Shear stress modulates the proliferation rate, protein synthesis, and mitogenic activity of arterial smooth muscle cells. *Surgery* 113: 691-699, 1993.

126. **Sterpetti AV, Cucina A, Santoro L, Cardillo B, and Cavallaro A.** Modulation of arterial smooth muscle cell growth by haemodynamic forces. *Eur J Vasc Surg* 6: 16-20, 1992.

127. **Strauss BH and Rabinovitch M.** Adventitial fibroblasts. Defining a role in vessel wall remodeling. *Am J Respir Cell Mol Biol* 22: 1-3, 2000.

128. **Stringa E, Knauper V, Murphy G, and Gavrilovic J.** Collagen degradation and platelet-derived growth factor stimulate the migration of vascular smooth muscle cells. *J Cell Science* 113: 2055-2064, 2000.

129. **Swabb EA, Wei J, and Gullino P.** Diffusion and convection in normal and neoplastic tissues. *Cancer Res* 34: 2814-2822, 1974.

130. **Tada S and Tarbell JM.** Fenestral pore size in the internal elastic lamina affects transmural flow distribution in the artery wall. *Annals of Biomedical Engineering* 29: 456-466, 2001.

131. **Tada S and Tarbell JM.** Flow through internal elastic lamina affects shear stress on smooth muscle cells (3D simulations). *Am J Physiol Heart Circ Physiol* 282: H576-H584, 2002.

132. **Tada S and Tarbell JM.** Interstitial flow through the internal elastic lamina affects shear stress on arterial smooth muscle cells. *Am J Physiol Heart Circ Physiol* 278: H1589-H1597, 2000.

133. **Tarbell JM, Civelek M, and Garanich JS.** Fluid shear stress control of vascular smooth muscle. In: *Molecular Basis for Microcirculatory Disorders*, edited by Schmid-Schönbein GW and Granger DN: Springer Verlag, 2003, p. 171-199.

134. **Thompson MM, Wills A, McDermott E, Crowther M, Brindle N, and Bell PRF.** An in vitro model of aneurysmal disease: effect of leukocyte infiltration and shear stress on MMP production within the arterial wall. *Ann NY Acad Sci* 800: 270-273, 1996.

135. **Tortora GJ.** *Principles of human anatomy.* New York, NY: HarperCollins Publishers, 1992.

136. **Tronc F, Mallat Z, Lehoux S, Wassef M, Esposito B, and Tedgui A.** Role of matrix metalloproteinases in blood flow-induced arterial enlargement: interaction with NO. *Arterioscler Thromb Vasc Biol* 20: E120-E126, 2000.

137. **Tulis DA and Prewitt RL.** Medial and endothelial platelet-derived growth factor A chain expression is regulated by in vivo exposure to elevated flow. *J Vasc Res* 35: 413-420, 1998.

138. **Ueba H, Kawakami M, and Yaginuma T.** Shear stress as an inhibitor of vascular smooth muscle cell proliferation: role of transforming growth factor-beta 1 and tissue-type plasminogen activator. *Arterioscler Thromb Vasc Biol* 17: 1512-1516, 1997.

139. **Waller JR, Brook NR, Bicknell GR, and Nicholson ML.** Differential effects of modern immunosuppressive agents on the development of intimal hyperplasia. *Transplant International* 17: 9-14, 2004.

140. **Wang DM and Tarbell JM.** Modeling interstitial flow in an artery wall allows estimation of wall shear stress on smooth muscle cells. *J Biomech Eng* 117: 358-363, 1995.

141. **Wang H and Keiser JA.** Expression of membrane-type matrix metalloproteinase in rabbit neointimal tissue and its correlation with matrix-metalloproteinase-2 activation. *J Vasc Res* 35: 45-54, 1998.

142. **Wang S and Tarbell JM.** Effect of fluid flow on smooth muscle cells in a 3-dimensional collagen gel model. *Arterioscler Thromb Vasc Biol* 20: 2220-2225, 2000.

143. **Ward MR, Tsao PS, Agrotis A, Dilley RJ, Jennings GL, and Bobik A.** Low blood flow after angioplasty augments mechanisms of restenosis. Inward vessel remodeling, cell migration, and activity of genes regulating migration. *Arterioscler Thromb Vasc Biol* 21: 208-213, 2001.

144. **Webb KE, Henney AM, Anglin S, Humphries SE, and McEwan JR.** Expression of matrix metalloproteinases and their inhibitor TIMP-1 in the rat carotid artery after balloon injury. *Arterioscler Thromb Vasc Biol* 17: 1837-1844, 1997.

145. **Wilcox JN and Scott NA.** Potential role of the adventitia in arteritis and atherosclerosis. *International Journal of Cardiology* 54 Suppl.: S21-S35, 1996.

146. **Williams DA.** Network assessment of capillary hydraulic conductivity after abrupt changes in fluid shear stress. *Microvascular Research* 57: 107-117, 1999.

147. **Wiskirchen J, Schober W, Schart N, Kehlbach R, Wersebe A, Tepe G, Claussen CD, and Duda SH.** The effects of paclitaxel on the three phases of restenosis. Smooth muscle cell proliferation, migration, and matrix formation: an in vitro study. *Invest Radiol* 39: 565-571, 2004.

148. **Yuan F, Chien S, and Weinbaum S.** A new view of convective-diffusive transport processes in the arterial intima. *Trans ASME J Biomech Eng* 113: 314-329, 1991.

149. **Zalewski A and Shi Y.** Vascular myofibroblasts. Lessons from coronary repair and remodeling. *Arterioscler Thromb Vasc Biol* 17: 417-422, 1997.

150. **Zalewski A, Shi Y, and Johnson AG.** Diverse origin of intimal cells. Smooth muscle cells, myofibroblasts, fibroblasts, and beyond? *Circ Res* 91: e13-e20, 2002.

151. **Zempo N, Kenagy RD, Au YP, Bendeck M, Clowes MM, Reidy MA, and Clowes AW.** Matrix metalloproteinases of vascuar wall cells are increased in balloon-injured rat carotid artery. *J Vasc Surg* 20: 209-217, 1994.

152. **Zempo N, Koyama N, Kenagy RD, Lea HJ, and Clowes AW.** Regulation of vascular smooth muscle cell migration and proliferation in vitro and in injured rat arteries

by a synthetic matrix metalloproteinase inhibitor. *Arterioscler Thromb Vasc Biol* 16: 28-33, 1996.

153. **Zhang H, Facemire CS, Banes AJ, and Faber JE.** Different alpha-adrenoceptors mediate migration of vascular smooth muscle cells and adventitial fibroblasts in vitro. *Am J Physiol Heart Circ Physiol* 282: H2364-H2370, 2002.

154. **Zheng F, Cornacchia F, Schulman I, Banerjee A, Cheng Q, Potier M, Plati AR, Berho M, Elliot SJ, Li J, Fornoni A, Zang Y-J, Zisman A, Striker LJ, and Striker GE.** Development of albuminuria and glomerular lesions in normoglycemic B6 recipients of *db/db* mice bone marrow. The role of mesangial cell progenitors. *Diabetes* 53: 2420-2427, 2004.

155. **Zhuang YJ, Singh TM, Zarins CK, and Masuda H.** Sequential increases and decreases in blood flow stimulates progressive intimal thickening. *Eur J Vasc Endovasc Surg* 16: 301-310, 1998.

VITA

Jeffrey Stock Garanich

EDUCATION

Ph.D. in Bioengineering (expected May 2006)
The Pennsylvania State University

B.S. in Mechanical Engineering (May 1999)
The Pennsylvania State University

PUBLICATIONS

Garanich J.S., R.A. Mathura, Z.D. Shi, and J.M. Tarbell. Characterization of two subpopulations of adventitial fibroblasts: implications for flow-mediated mechanisms of arterialization and intimal hyperplasia. J. Vasc. Res., in review.

Garanich J.S., M. Pahakis, and J.M. Tarbell. Shear stress inhibits smooth muscle cell migration via nitric oxide-mediated downregulation of matrix metalloproteinase-2 activity. Am. J. Physiol. Heart Circ. Physiol., 288(5): H2244-H2252, 2005.

Ainslie K.M., J.S. Garanich, R.O. Dull, and J.M. Tarbell. Vascular smooth muscle cell glycocalyx influences shear stress-mediated contractile response. J. Appl. Physiol., 98(1): 242-249, 2005.

Ainslie K.M., Z. Shi, J.S. Garanich, and J.M. Tarbell. Rat aortic smooth muscle cells contract in response to serum and its components in a calcium independent manner. Ann. Biomed. Eng., 32(12): 1667-1675, 2004.

Tarbell J.M., M. Civelek, and J.S. Garanich. Fluid shear stress control of vascular smooth muscle. Chapter in "Molecular Basis for Microcirculatory Disorders", eds. Schmid-Schönbein G.W., Granger D.N. 2003.

Civelek M., K. Ainslie, J.S. Garanich, and J.M. Tarbell. Smooth muscle cells contract in response to fluid flow via a Ca^{2+}-independent signaling mechanism. J. Appl. Physiol., 93: 1907-1917, 2002.